Fermi National Accelerator Laboratory

Research Associate Postdoc Position Interview

Position Applicant: Roberto Acciarri

- ✔ First Level Degree in Physics @ L'Aquila University on 2003
  Thesis: "Reconstruction and analysis of muon bundle events with ICARUS T600 detector"
- ✔ Master Degree in AstroParticle Physics @ L'Aquila University on 2006
  Thesis: "Study and optimization of Pulse Shape Discrimination Methods with the WArP detector"
- ✔ PhD degree @ L'Aquila University and LNGS on 2010
  Thesis: "Measurement of the scintillation time spectra and Pulse Shape Discrimination of low-energy electron and nuclear recoils in liquid Argon with the WArP 2.3 lt detector."
- ✔ Research grant (period 12/2009 - 11/2010) @ LNGS
  Project title: "Optimization of the collection systems of light and charge signals produced by ionizing particles in liquified and solidified high-purity noble gas detectors."

Outline

- First work with LAr: LAr TPC working principle, analysis of cosmic rays data acquired with the ICARUS T600 detector.

- Brief introduction on Dark Matter: why we think it is there, what we think it is, how we try to find it.

- Presentation of the main activity of my Master and PhD thesis: PSD in liquid Argon. Techniques investigated, optimization performed, results obtained.

- Presentation of the other major work that characterized my activity so far: optimization of the light collection in LAr detectors.

- Other activities as member of the WArP collaboration.

Outline

- First work with LAr: LAr TPC working principle, analysis of cosmic rays data acquired with the ICARUS T600 detector.

- Brief introduction on Dark Matter: why we think it is there, what we think it is, how we try to find it.

- Presentation of the main activity of my Master and PhD thesis: PSD in liquid Argon. Techniques investigated, optimization performed, results obtained.

- Presentation of the other major work that characterized my activity so far: optimization of the light collection in LAr detectors.

- Other activities as member of the WArP collaboration.

- ...signing the contract????

Liquid Argon Technology

Two major applications of Liquid Argon as target/sensitive material:

Double phase (LAr-GAr) detector for Dark Matter search

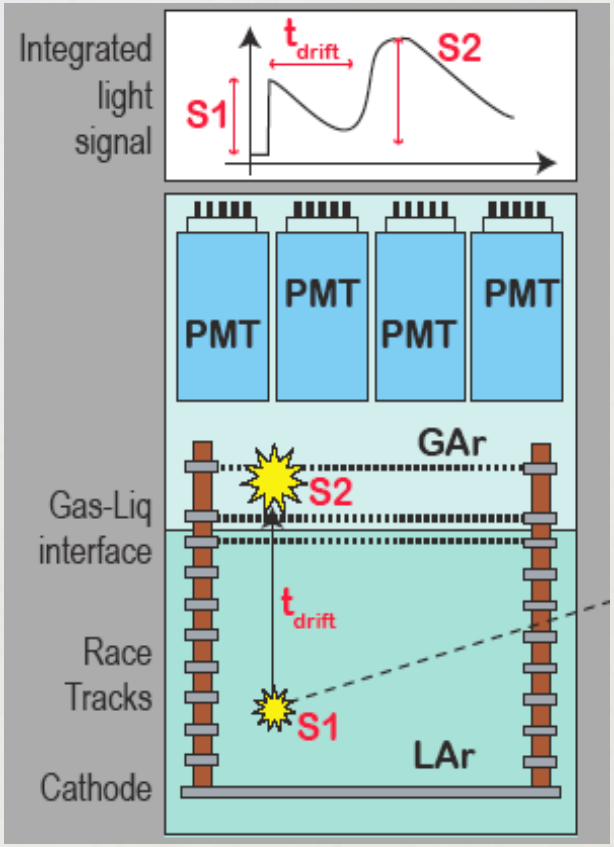

Make use of scintillation (and also ionization) in LAr

LAr TPC for neutrino physics

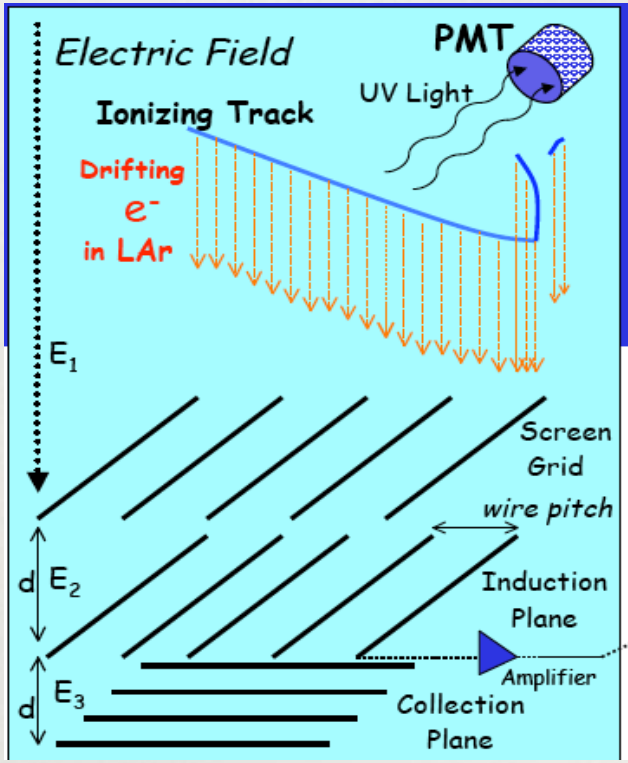

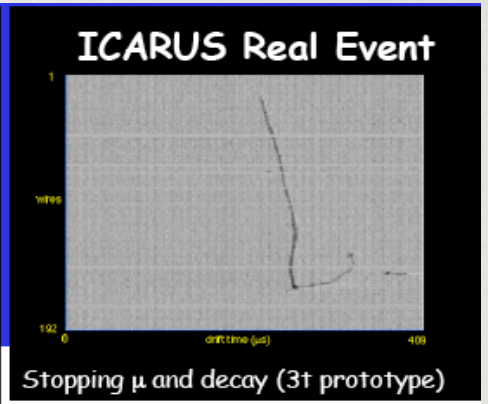

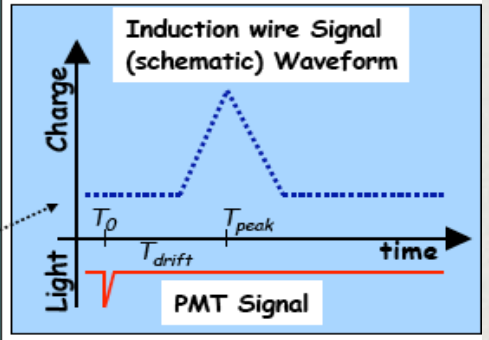

Make use of ionization in LAr (and also scintillation for triggering)

Reconstruction and analysis of cosmic ray muon bundle events with ICARUS T600 detector

Why cosmic ray muon bundles?

- Muon bundles are produced by interactions of high energy cosmic rays in the highest layers of the atmosphere.

- The rates of muon bundles of different multiplicities and the spatial separation between muons measured in deep underground experiments are sensitive to the chemical composition and energy spectra of the primary cosmic rays, above a threshold determined by the rock overburden (~50 TeV at LNGS).

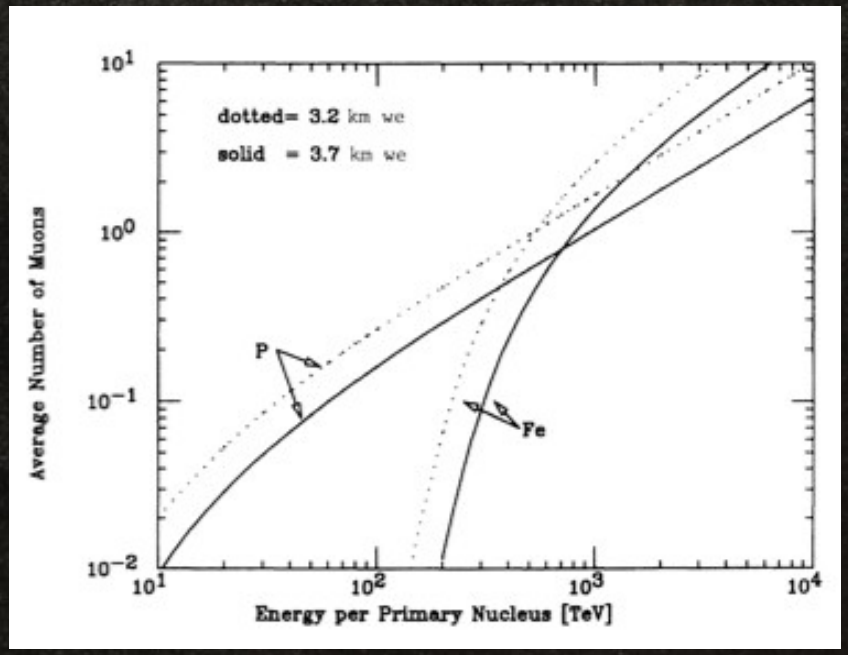

- Detection and analysis of muon bundle events is thus a way to study the characteristics (mass composition and energy spectrum) of very high energy (TeV–several thousand TeV) cosmic rays and their interactions in the upper part of the atmosphere through the comparison of data with predictions from different chemical composition and hadronic interaction models.

About my activity...

- My activity (first level degree) was to select, reconstruct and analyze muon "bundle events" in order to determine:
  - ✔ muon multiplicity;
  - ✔ angular distribution;
  - ✔ spatial separation between muons in the bundle.

- Data sample used for this analysis belongs to the data set acquired during a surface test run of ICARUS T600, a LAr TPC detector (600 ton of LAr) for neutrino physics.

- Main goal of the analysis: demonstrate the detector capability to achieve a good 2-track resolution and to perform a 3D reconstruction of large multiplicity events, in view of the underground (at LNGS) measurement of muon bundle events.

T600 detector

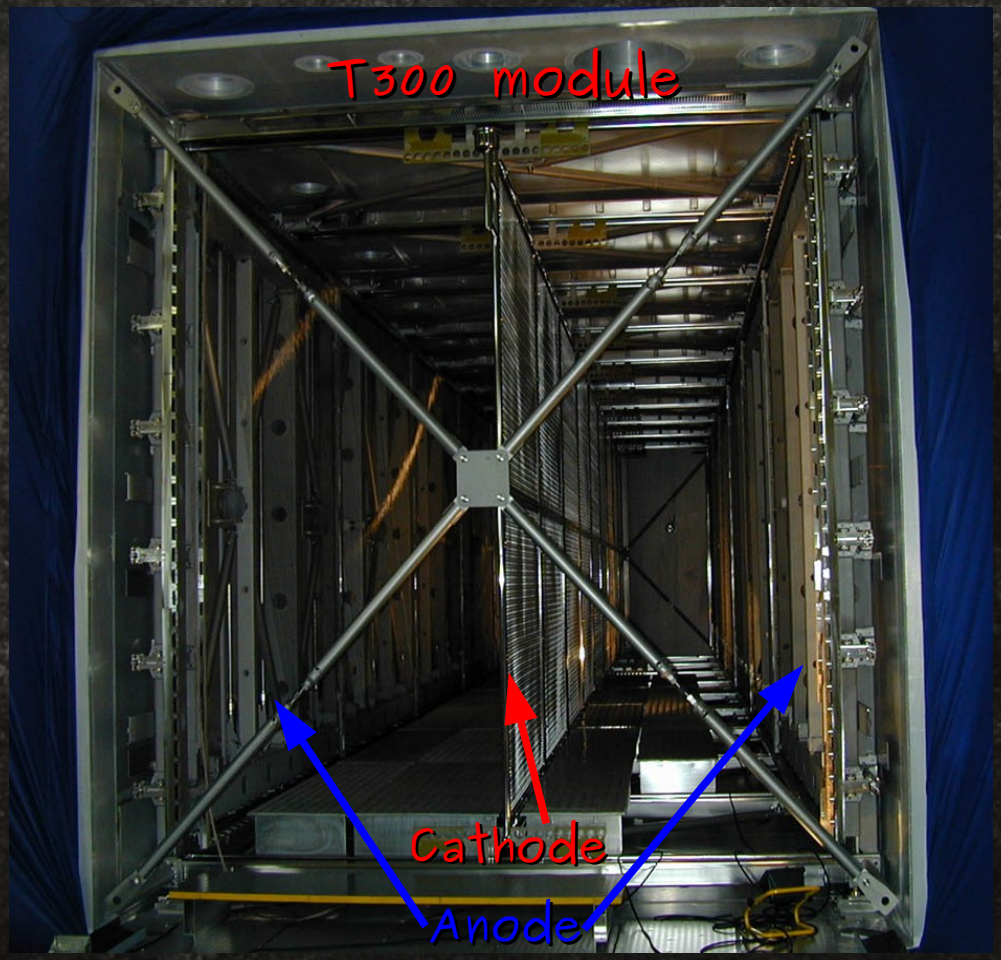

- ✔ Two indipendent modules of 300 ton each and 3.9X4.2X19.6 m^3
- ✔ Each module has a central cathode and two anodic wire planes on the lateral walls
- ✔ Each anode is formed by 3 wire planes oriented at 0°, ±60°: two induction and one collection plane
- ✔ A particle crossing the detector will leave e^-–ion pairs along its path. e^-, drifting parallel (little lateral diffusion) to the particle track, will induce a signal on the first two wire planes and be collected by the third one

Combining the signals from at least two wire planes and informations from the drift time of the electrons a *3-dimensional image of the event is obtained* with mm resolution (given by the wire pitch)

Event Reconstruction procedure in LAr TPC

Through the reconstruction procedure not only a complete 3D (imaging) but also a calorimetric picture of the event is obtained.

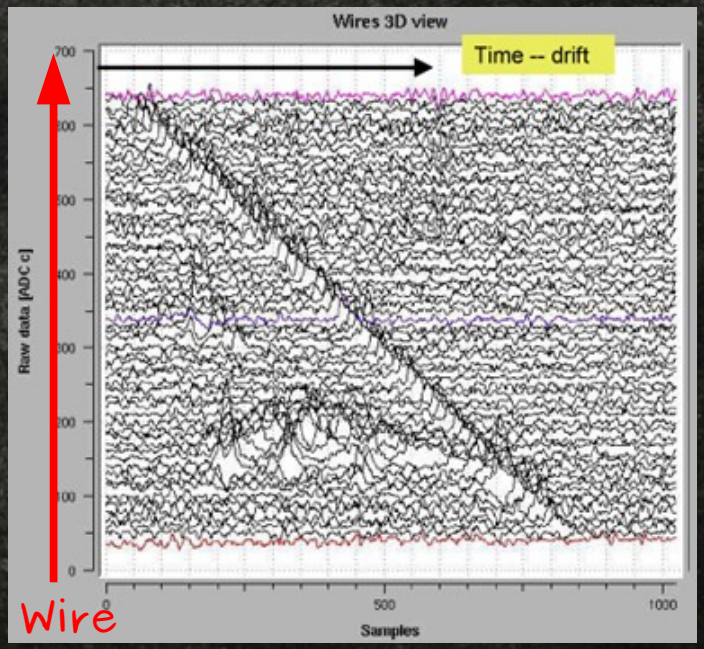

Offline reconstruction procedure consist of:

✔ Hit identification: hits are indipendently searched for in every wire as signal regions of a certain width above the baseline;

✔ Hit reconstruction: parameters defining the hit (position, height, area), which contain the physical information, are determined;

✔ Cluster reconstruction: hits are grouped based on their position in the wire/drift coordinate plane (2D reconstruction);

✔ 3D hit reconstruction: hit spatial coordinates are reconstructed by the association of hits from different views into common track segments;

✔ Calorimetric reconstruction: determination of energy release in LAr performed through charge to energy conversion accounting for charge loss due both to attachment to electronegative impurities and recombinations effects;

✔ Particle ID: with dE/dx measurement vs range.

Event selection and reconstruction

After visual scan of over 250 events (classified as multi-muon candidate from automatic reconstruction), I selected 91 multi-muon events according to the following characteristics:

- ✔ presence of at least two parallel muon tracks both in the Collection and Induction 2 view;
- ✔ absence of electromagnetic showers big enough to don't allow for muon track reconstruction.

Event selection and reconstruction

Run 313 Event 239 - Collection view

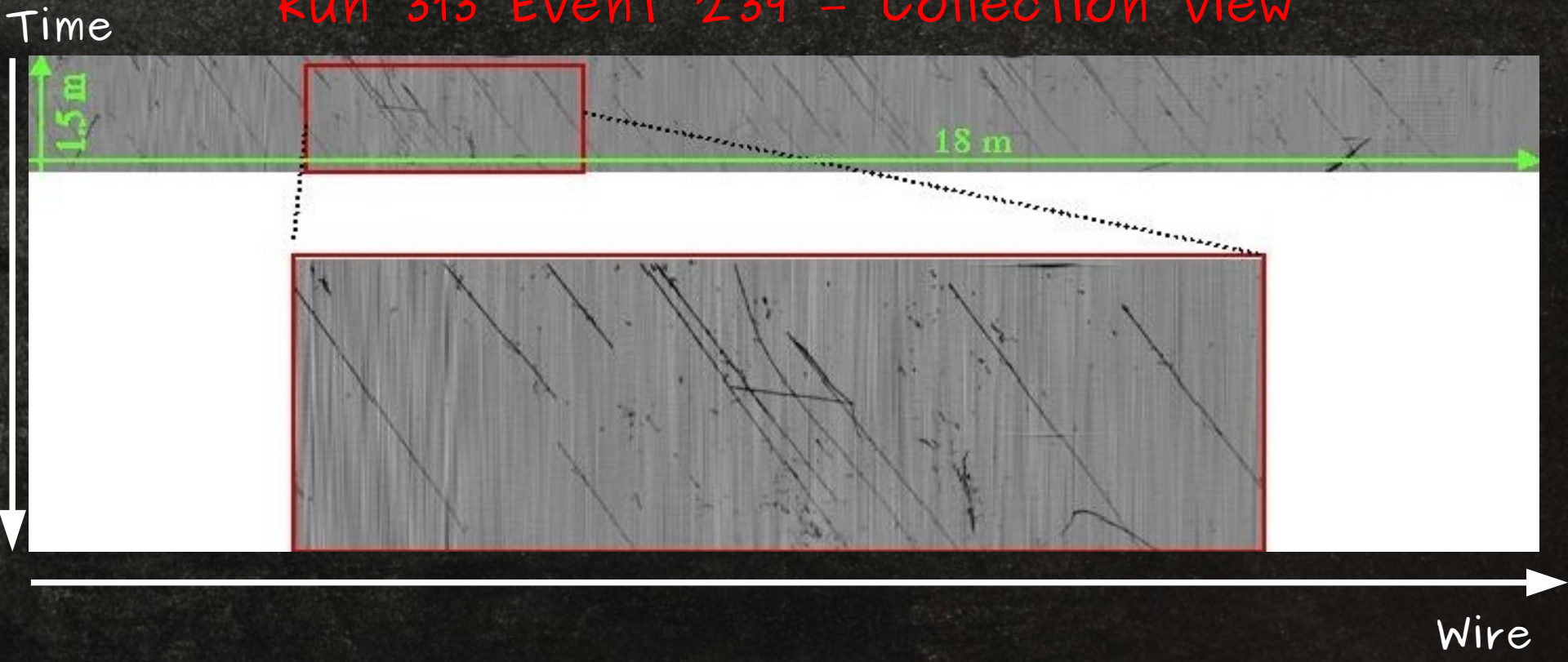

Event selection and reconstruction

- For each event and for each of the two views, a ROI (region of interest) containing the muon bundle is selected.
- Through a hit finding algorithm, hits in the ROI are selected.
- A clustering algorithm, searching for a set of subsequent points among the hits, is carried out and then a linear fit is performed, giving slope and intercept of each 2D track.
- Association of 2D projected tracks on the two view to reconstruct 3D tracks: from mean values (from gaussian fit) of the slopes for the two views, the zenith (ϑ) and azimuth (φ) angles in space of the bundle are inferred.

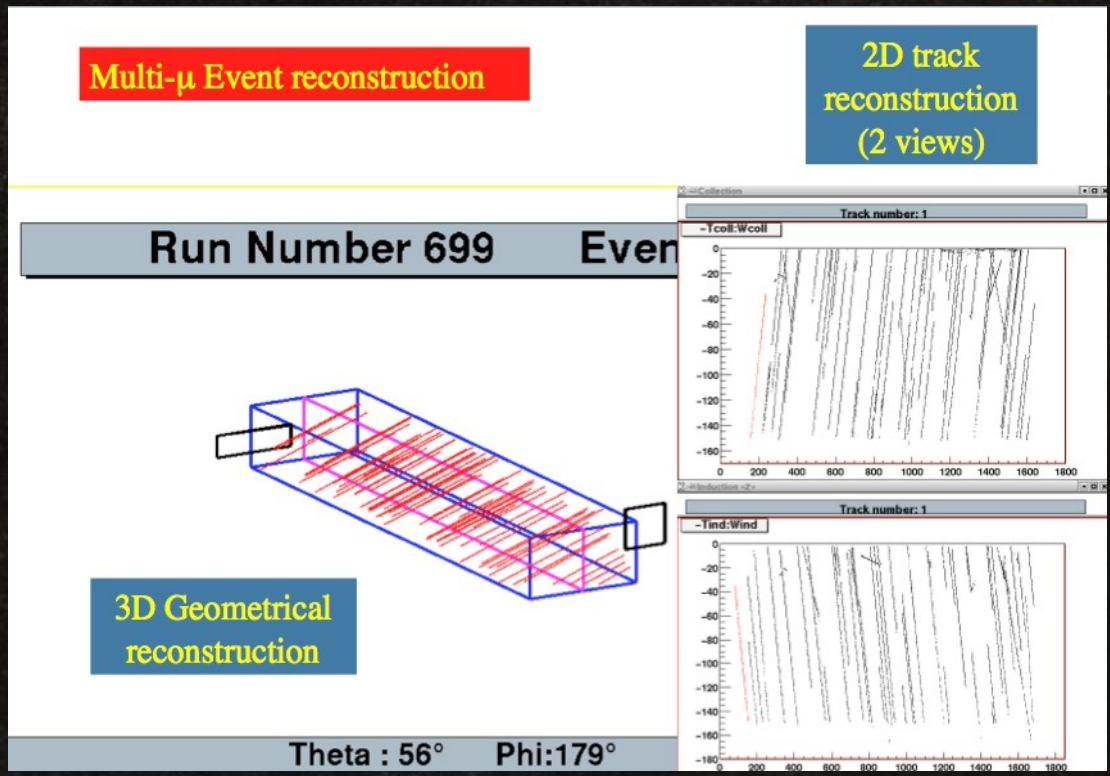

Analysis results

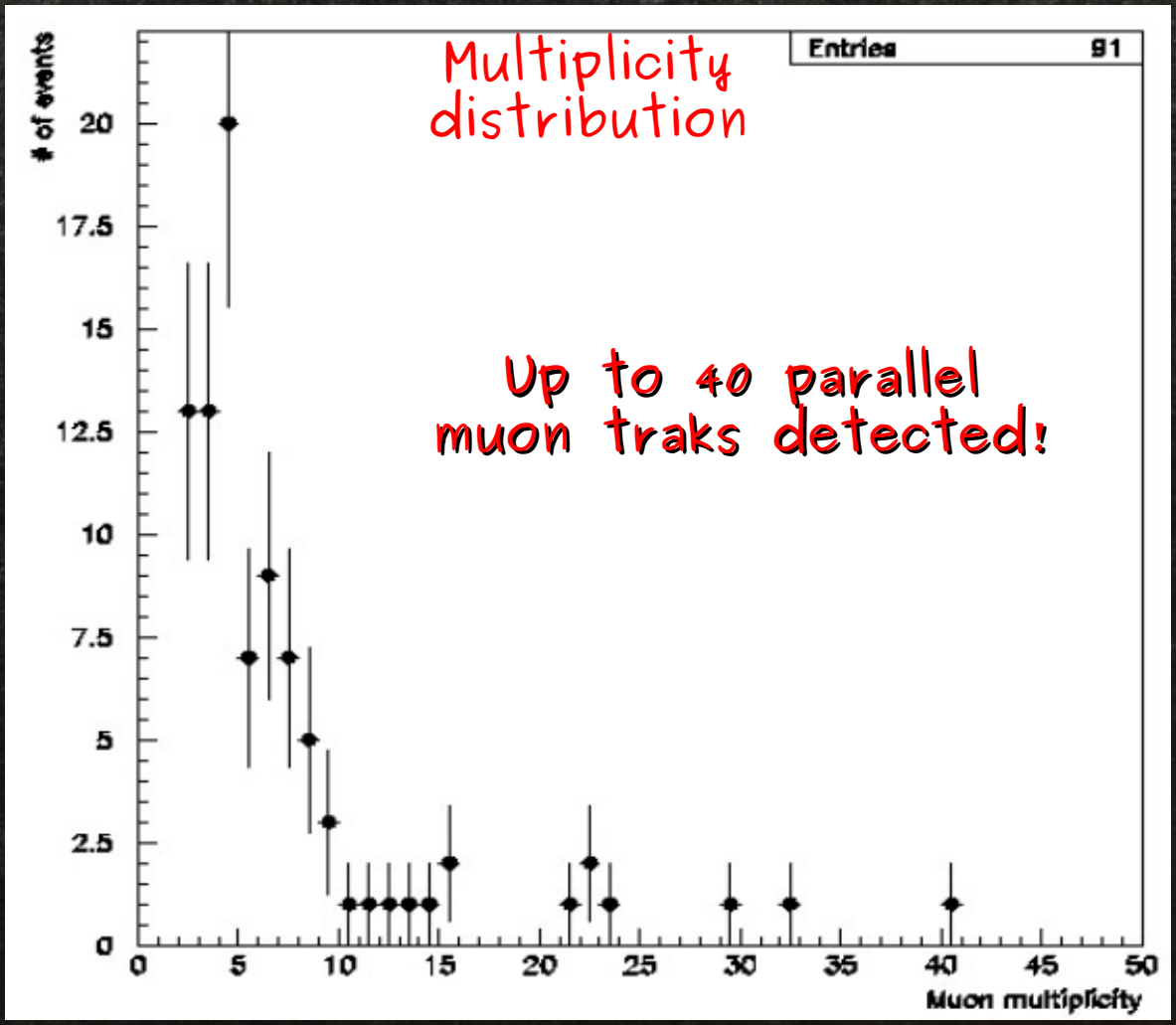

Muon multiplicity is mainly dependent on primary cosmic ray energy and composition.

Analysis results

The angular distribution $dN/d\cos(\theta)$ can be predicted starting from few considerations:

- ✔ For single muons $dN/d\cos(\theta) \propto$:
  $1/\cos(\theta)$ ($E_\mu \gg 100$ GeV) ;
  $\cos^2(\theta)$ ($E_\mu \sim 100$ GeV) ;
  $\cos^n(\theta)$ ($E_\mu \ll 100$ GeV and $n>2$).
- ✔ A muon bundle can be tought as a bunch of single muons.
- ✔ Muons from a bundle are generally less energetic than a single muon.

I expect $dN/d\cos(\theta) \propto \cos^n(\theta)$; $n>2$

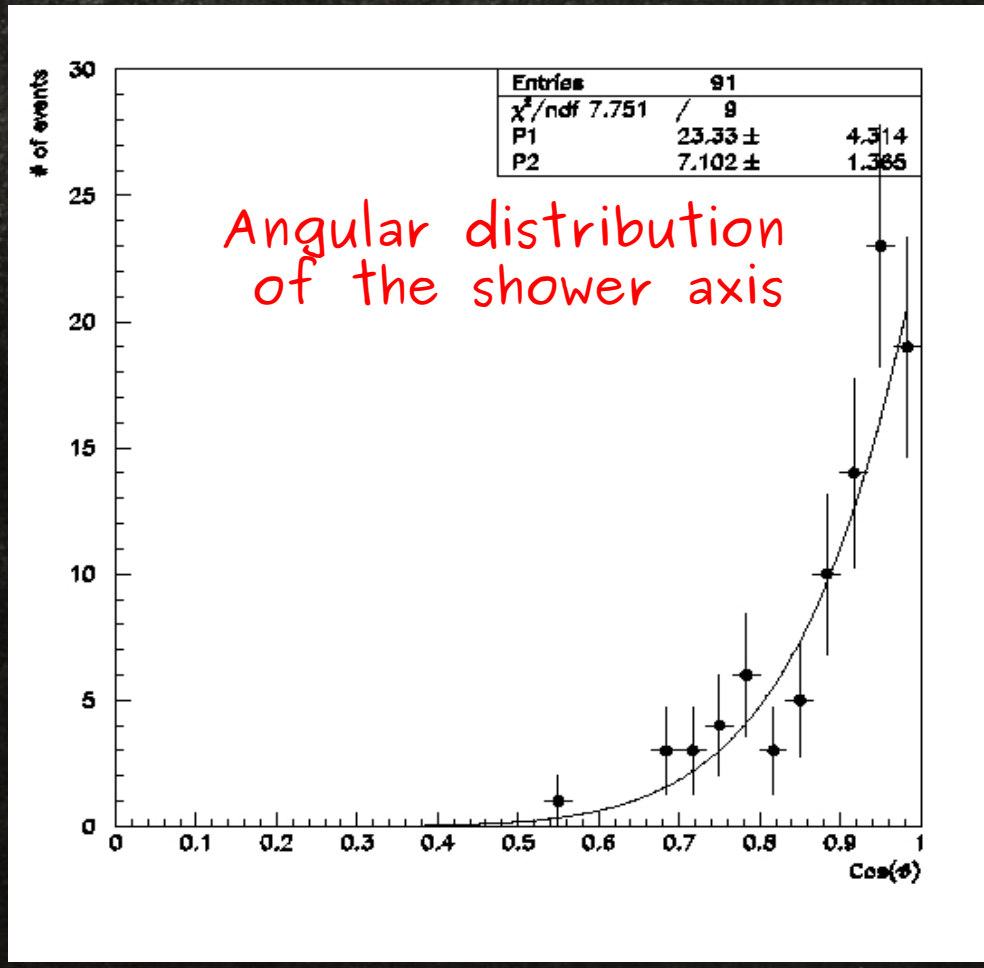

Fit of the distribution with the function $f(\theta)=P1\cdot\cos^{P2}(\theta)$ gives as result:
$P1 = 23\pm4$; $P2 = 7\pm1$; $\chi^2/np = 0.86$

Agreement with theoretical expectation with $n=7$

Light collection and Pulse Shape Discrimination in Liquid Argon Detectors for Dark Matter search

Roberto Acciarri

A bit of background...

✔ First evidence of Dark Matter dates back to 1933, when Zwicky, observing the galaxies of the COMA cluster, found out they were too fast to be bounded by the gravitational pull of only the luminous matter.

✔ Since then, many observation both in the astrophysical and cosmological field (galaxies rotation curve, hot inter-galaxy gas, strong and weak lensing, collision of galaxy clusters, Cosmic Microwave Background, Big Bang Nucleosynthesis, simulation of structure formation...) lead us to believe Dark Matter is there and hiding from us.

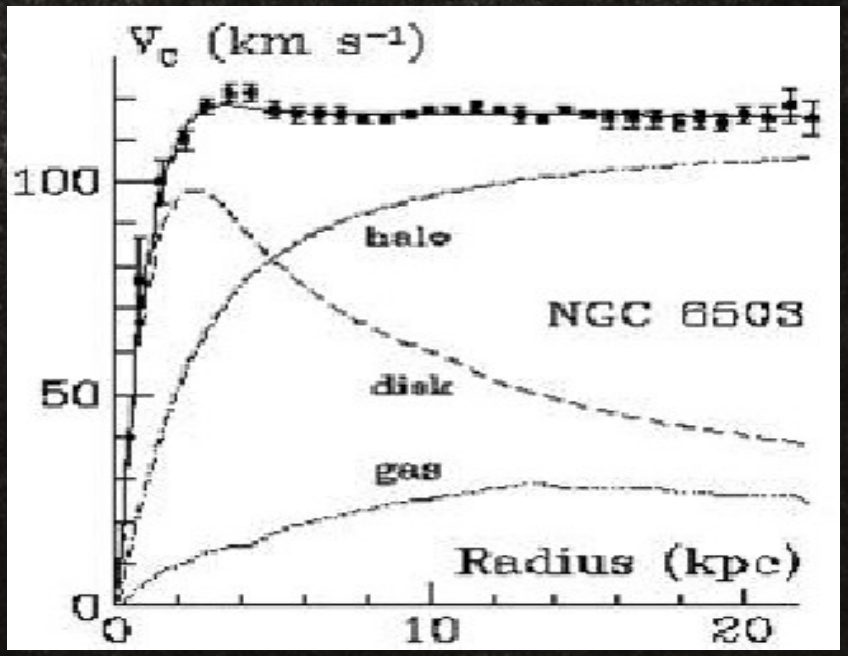

Galaxies rotation curve

In the '70s V. Rubin studies on many spiral galaxies pointed out that most stars in spiral galaxies orbit at roughly the same speed, even the ones far from the galactic bulge (where v is supposed to decrease): *a dark halo must sorround galaxies, extending much further and containing much more mass than the visible one.*

A bit of background...

Strong and weak lensing

Gravitational lensing occurs when the light from a very distant, bright source is bent around a massive object (cluster of galaxies) between the source object and the observer, producing

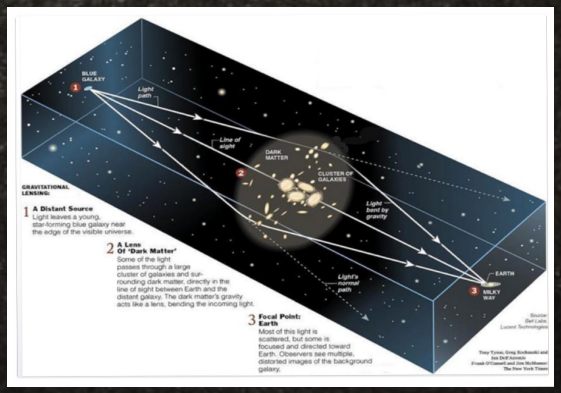

archs, rings (strong lensing) or distortions (weak lensing) of the background objects. From such deformations the mass of the lens cluster can be inferred. DM densities compatible with other observations have been found.

Bullet Cluster: the smoking gun

Merge of two cluster 150 My ago. In the merging process, galaxies and DM particles (blue halo) act like collisionless particles, moving away. Plasma (pink halo) from the two cluster will interact electromagnetically and will slow down. Mass determination of the merged cluster via weak lensing showed that most of the mass acts like collisionless particles. (Plasma counts for most of the visible mass of a cluster). *Strong evidence for the existence of Dark Matter.*

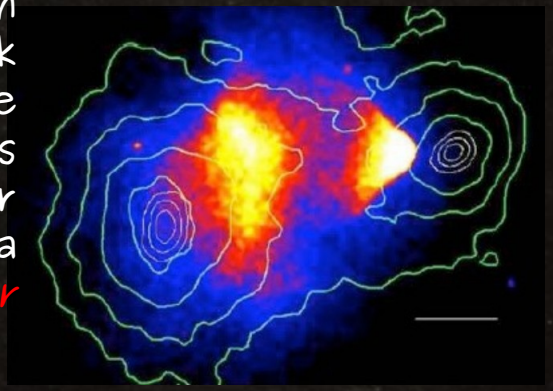

A bit of background...

Combining all the observations, some of the properties Dark Matter should have can be inferred:

✔ From the astrophysical evidences, DM must be only weakly interacting (otherwise we would have seen effects, other than the gravitational ones, of its interaction with other particles).

✔ From the power spectrum of CMB anisotropies + BBN + Galaxy structure formation, DM (at least most of it), must be non-barionic, cold (non relativistic when decoupled from radiation), massive (DM needs to decouple from radiation before the recombination time and be non relativistic, hence massive, to allow for the growth of the large structures we see today).

WIMP: Weakly Interacting Massive Particles

The study of the anisotropies of the CMB, together with study of the Supernovae 1A and Big Bang Nuclosynthesis, leads to the determination the composition of the Universe

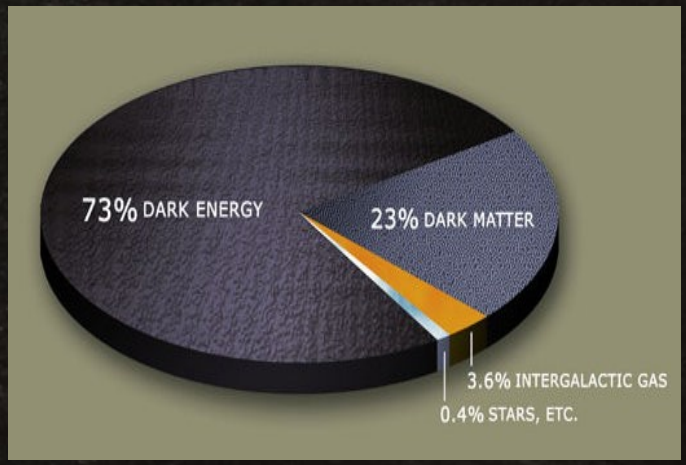

From cosmology to Particle Physics: looking for WIMPs

WIMPs are not part of the standard model. Nonetheless, a very appealing feature of WIMPs is that you don't need to build up a brand new theory to justify them: they naturally arise in extensions of the Standard Model, like SUSY models or models of universe with extra dimensions.

- SUSY models: every particle has a partner with opposite spin.
- R-Parity conservation implies that the lightest supersimmetric particle (neutralino, mix of Zino, Photino and Higgsino) is stable.
- For mass 100 GeV÷1 TeV and σ tipical of weak interactions, the neutralino mass density matches the requested DM density in the Universe.

Gauge Bosons $S=1$ gluon, $W^{\pm}, Z, \gamma$	Gauginos $S=1/2$ gluino, $\widetilde{W}, \widetilde{Z}, \widetilde{\gamma}$
Fermions $S=1/2$ $\begin{pmatrix} u_L \\ d_L \end{pmatrix}\begin{pmatrix} \nu_L^e \\ e_L \end{pmatrix}$ u_R, d_R, e_R	Sfermions $S=0$ $\begin{pmatrix} \widetilde{u}_L \\ \widetilde{d}_L \end{pmatrix}\begin{pmatrix} \widetilde{\nu}_L^e \\ \widetilde{e}_L \end{pmatrix}$ $\widetilde{u}_R, \widetilde{d}_R, \widetilde{e}_R$
Higgs $\begin{pmatrix} H_2^0 \\ H_2^- \end{pmatrix}\begin{pmatrix} H_1^+ \\ H_1^0 \end{pmatrix}$	Higgsinos $\begin{pmatrix} \widetilde{H}_2^0 \\ \widetilde{H}_2^- \end{pmatrix}\begin{pmatrix} \widetilde{H}_1^+ \\ \widetilde{H}_1^0 \end{pmatrix}$

Best WIMPs feature: they may be experimentally accessible!

Ways to look for WIMPs: indirect search (looking for products of neutralino annihilation – high energy gammas coming from the galatic center or high energy neutrinos coming from the centre of Sun or Earth) or direct search.

Dark Matter Direct Search

✔ Look for WIMPs elastically scattering off nuclei within the detector.

✔ Interaction characterized by a low energy release (few–100 keV recoil energy) with an energy spectrum rapidly decreasing and a very low interaction rate ($\leq 10^{-2}$ evts/(kg•day) according to current limits).

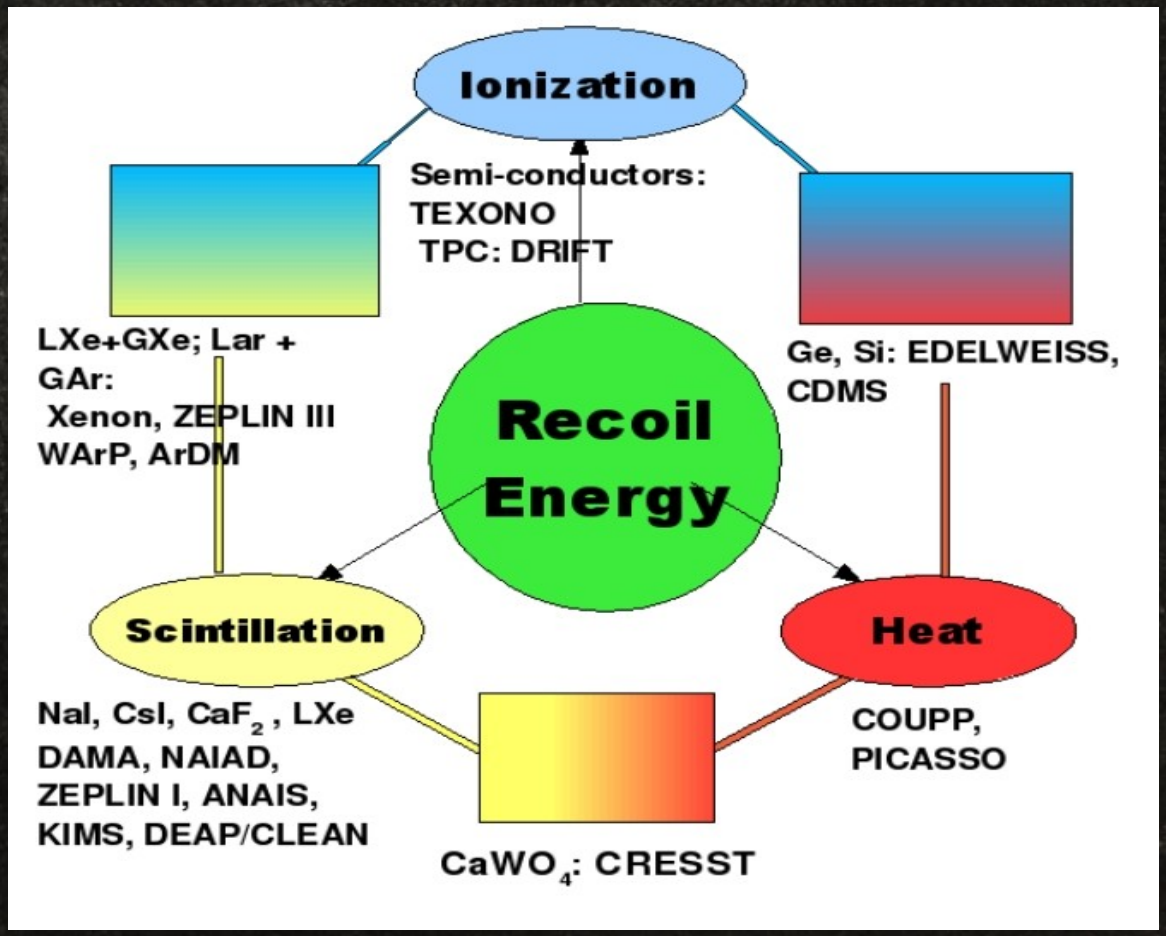

Key features of a successful DM detector are a low energy threshold and a powerful background rejection, especially at the lower energies (where most of the positive signals are expected).

Several kind of detecting materials and detection techniques have been proposed.

Dark Matter Direct Search

WIMP exclusion plot

Situation in DM community is getting hot: several experiments (DAMA, COGENT, CRESST) observe an excess of events inconciliabile with any known background. BUT:

- Positive observations are not fully compatible among them;
- They are not compatible with null experiments (CDMS, XENON);
- Positive data suggests a low mass WIMP, not favorite from theory and accelerator data.

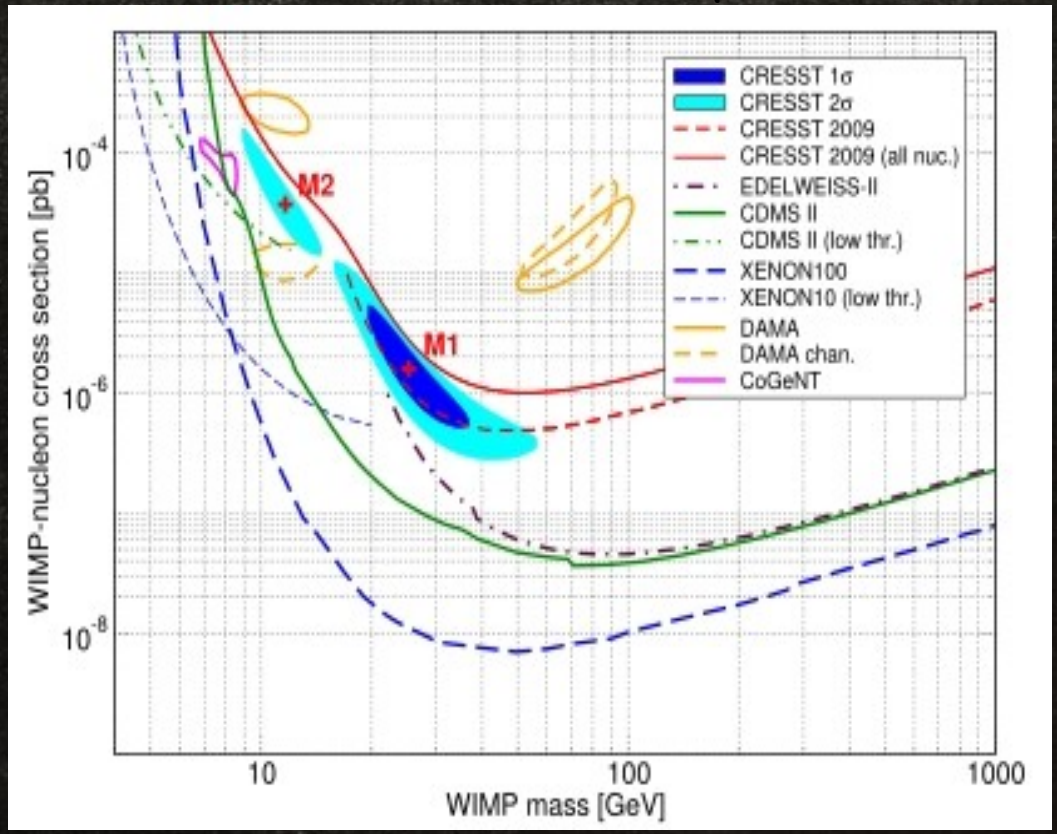

Several publications are coming out, trying to conciliate all the results, suggesting different WIMP–nucleus interactions (inelastic scattering, isospin violating scattering), pointing out possible inefficiencies/parameters not perfectly known the various experiments may experience or uncertainties in the astrophisical modelization.

Liquid Argon for DM detection

- Liquified noble gases (mainly Argon & Xenon) are excellent target/sensitive materials for DM direct search (the best exclusion limit is currently held by a LXe detector). Argon, in particular, offers several advantages:

  - ✔ well mastered technology and ease of purification allow for realization of big mass detectors (tons scale) at relatively low cost;
  - ✔ high scintillation yield ($4 \cdot 10^4$ γ/MeV) allows for a low energy threshold;
  - ✔ characteristics of scintillation light allow for a powerful discrimination method based on the shape of the light pulse - PSD.
  - ✔ simultaneous charge and light readout allow for further particle discrimination.

About my activity...

- Main contribution to the background in a LAr detector comes from ^{39}Ar (269 years half life - cannot be neglected). This is the ultimate background that MUST be reduced to be challenging and push sensitivity to WIMPs down to the most interesting levels of cross section.

- $>10^7$ ^{39}Ar events expected in the energy region of interest in a 100 lt detector in 100 days of data.

- Two ways to reduce this background: depleted Argon (obtained by centrifugation or found in natural underground reservoir) or to develop a discrimination technique able to push the rejection power up to 10^8 and more (looking forward to ton-scale detectors).

- Features of LAr scintillation light are such that a PSD method can be adopted to reject this background. Nevertheless, back to days (2005-2006), little work was done on exploiting PSD techniques for LAr.

About my activity...

- This has been the main core of both my Master and PHD thesis (from 2005 to 2010): *definition, study and optimization of a PSD technique for LAr detectors for DM*. Particular care has been put to the optimization in the low energy range (down to 20 keV), since these are the energies where most of the WIMP signal is expected.

But this it not all...

- In parallel, I actively and extensively worked (2007-2010) on a series of test aimed to the *optimization of the light collection in LAr detectors*.

- The two activities are closely related: a higher efficiency in light collection produce a lower energy threshold (fundamental to access those energy regions where WIMP interactions are more relevant) and increase the number of photoelectrons per unit of energy, thus improving the efficiency of PSD at low energy.

Scintillation light in LAr

- ✓ The interactions of ionizing particles in LAr cause the formation of both electron–hole (ion) pairs $e^- - Ar^+$ and excited atoms Ar^* ($Ar^*/Ar^+ \sim 0.21$).
- ✓ Both states lead to the formation (with times of the order of tens of picoseconds) of the excited dimer Ar_2^* ($^1\Sigma_u$ singlet state and $^3\Sigma_u$ triplet state).
- ✓ The de-excitation of the excited dimer: $Ar_2^* \rightarrow 2Ar + \gamma$ produces a Vacuum Ultra Violet (VUV) photon with $\lambda = 128nm$ ($\sigma \simeq 3nm$).

Time dependence of pure LAr scintillation light emission

$$l(t) = \frac{A_S}{\tau_S}\exp\left(\frac{-t}{\tau_S}\right) + \frac{A_T}{\tau_T}\exp\left(\frac{-t}{\tau_T}\right)$$

+ possible intermediate component with $\tau_i \sim 40ns$

$$\tau_S(^1\Sigma_U) = 2 \div 6\, ns$$

$$\tau_T(^3\Sigma_U) = 1100 \div 1600\, ns$$

$$\int l(t)\,dt = A_S + A_T = 1$$

A_S/A_T depends on ionizing radiation (PSD discrimination)

Pulse Shape Discrimination in LAr

The very different decay times of fast and slow components, together with the dependence of A_S/A_T on the ionizing radiation, allows for the rejection of predominant β and γ background on an event by event basis.

A_S/A_T=1/3 for electron recoils (β and γ interactions): "slow" signal

A_S/A_T=3 for nuclear recoils (neutron and WIMP interactions): "fast" signal

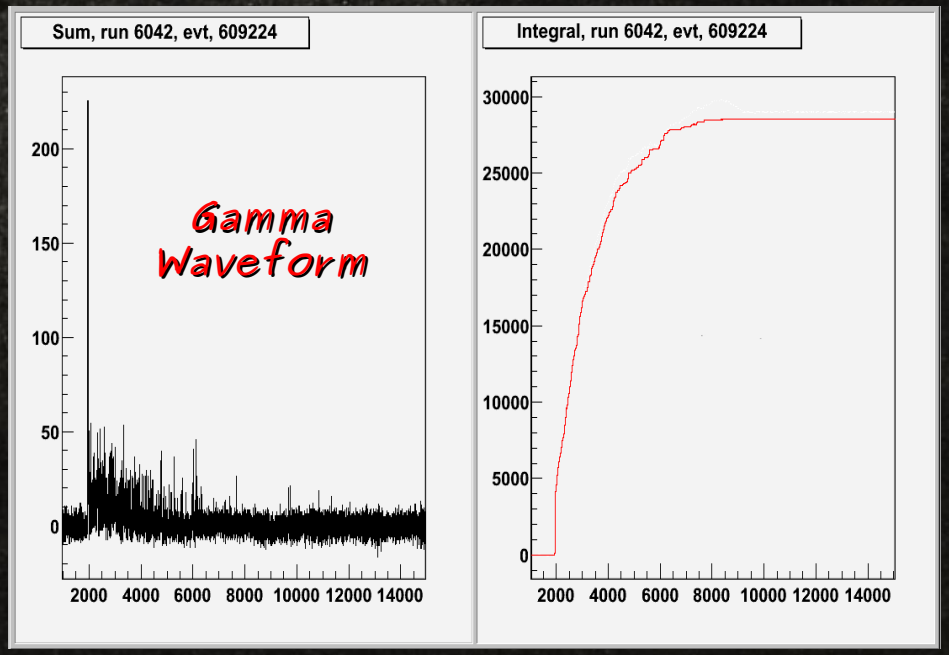

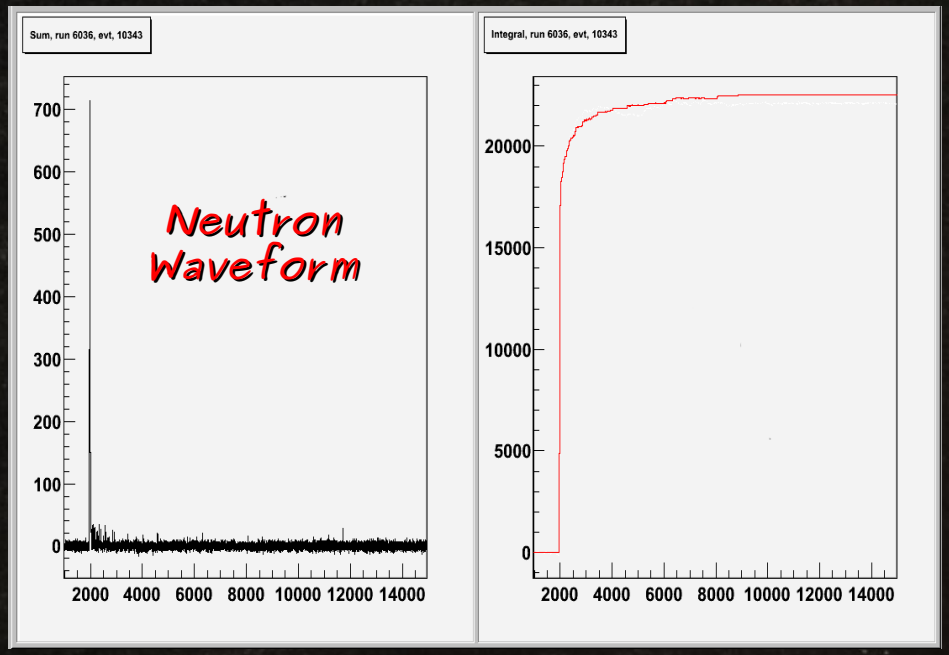

Pulse Shape Discrimination in LAr

The very different decay times of fast and slow components, together with the dependence of A_s/A_T on the ionizing radiation, allows for the rejection of predominant β and γ background on an event by event basis.

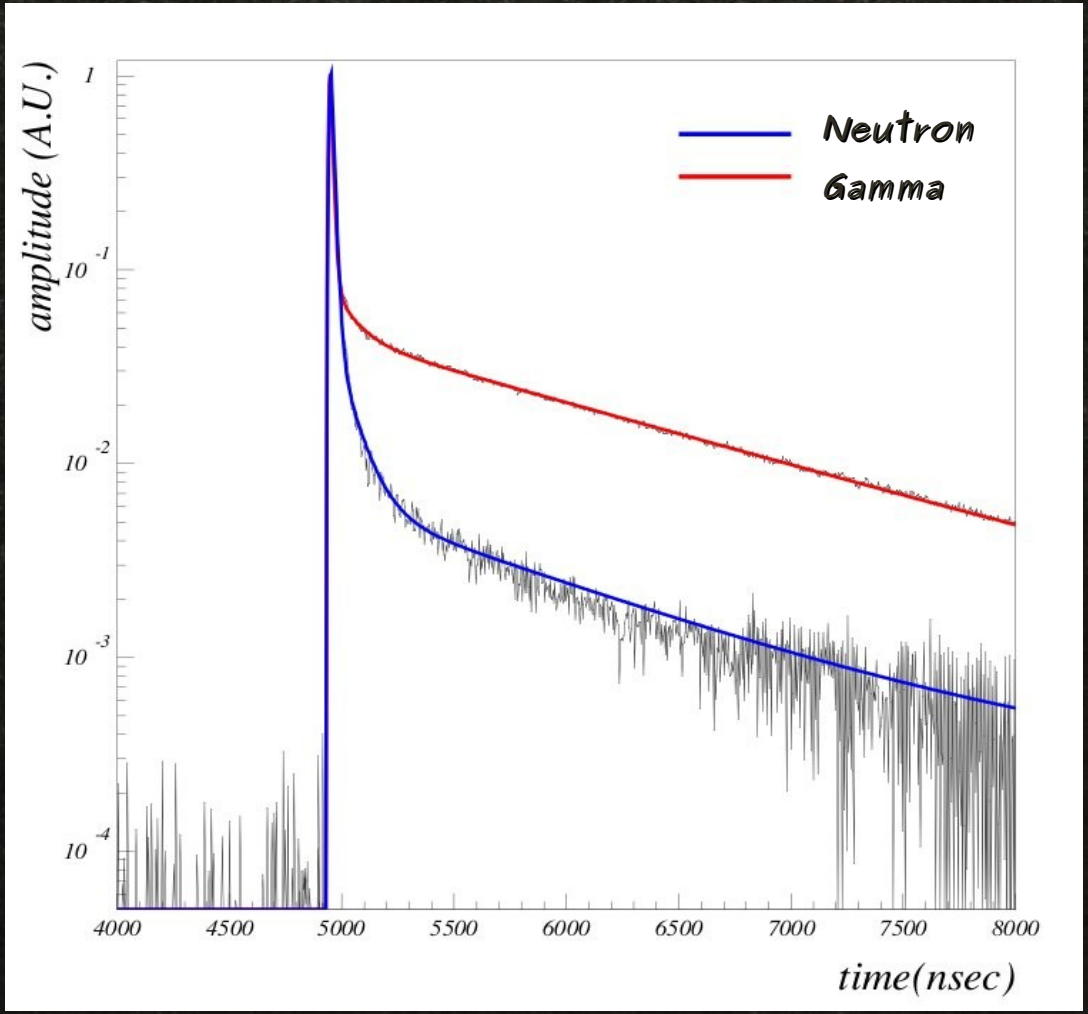

Study and optimization of PSD methods

At the beginning of this work (2005/2006), PSD in LAr was a new idea, totally inexplored from the experimental point of view. Thus, I first looked at PSD in organic liquid scintillator, a subject widely treated in literature. There I selected several PSD techniques (developed for organinc scintillators) and optimized them for LAr scintillation light:

- F-Prompt (Fp): fast and widely used discrimination technique based on the ratio between the integral of the first part of the light pulse and its total integral.

- Average Time (AvT): method based on the determination of the average arrival time of photoelectrons.

- Multibin Method: generalization of Fp method to the case in which the waveform is divided into k time intervals (rather than 2). Prior knowledge of neutron and gamma average waveforms (used as template waveforms) is required.

- Gatti Method: theoretically, the best discrimination method available. It is based on the knowledge of the average waveform of both nuclear recoil and electron recoil events.

A comparison among these techniques has been carried out to choose the most indicated one for LAr. Fp method resulted to be the best compromise in terms of discrimination efficiency, ease of implementation and rapidity of execution.

Detector and Data Sample

- A dedicated experimental set-up has been mounted: a PEEK chamber (4.3 lt inner volume) viewed by 7 2" PMTs (to collect LAr scintillation light).

- A wavelength shifter (TPB) evaporated onto reflective layers covers the inner surfaces of the chamber to down shift the VUV photons produced by LAr scintillation to longer wavelengths accessible by PMTs.

Detector and Data Sample

- Data acquisition and subsequent analysis took place in the Hall Di Montaggio facility of the Gran Sasso National Laboratory.
- Runs with a ^{133}Ba γ source have been acquired for Light Yield (LY, number of photoelectrons collected per unit of energy deposited) evaluation: 1.52 ± 0.05 phe/keV, stable during the data acquisition.
- An Am/Be n and γ source (neutron spectrum up to 11 MeV) has been used to collect data for the analysis. This source, producing both electron and nuclear recoils, represents an ideal source for PSD studies.

F-Prompt technique

The F-prompt (Fp) method is the most common technique to quickly discriminate electron recoils from the nuclear ones.

$$Fp = \frac{\int_{T_i}^{T_{Fp}} V(t)\,dt}{\int_{T_i}^{T_f} V(t)\,dt} = \frac{S_F}{S1}$$

V(t) Signal sum

S_F fast integral

S1 total integral

T_{trig} trigger time

$T_i = t_{trig} - 100$ ns

$T_f = t_{trig} + 7\ \mu s$

$T_{Fp} = t_{trig} + 120$ ns

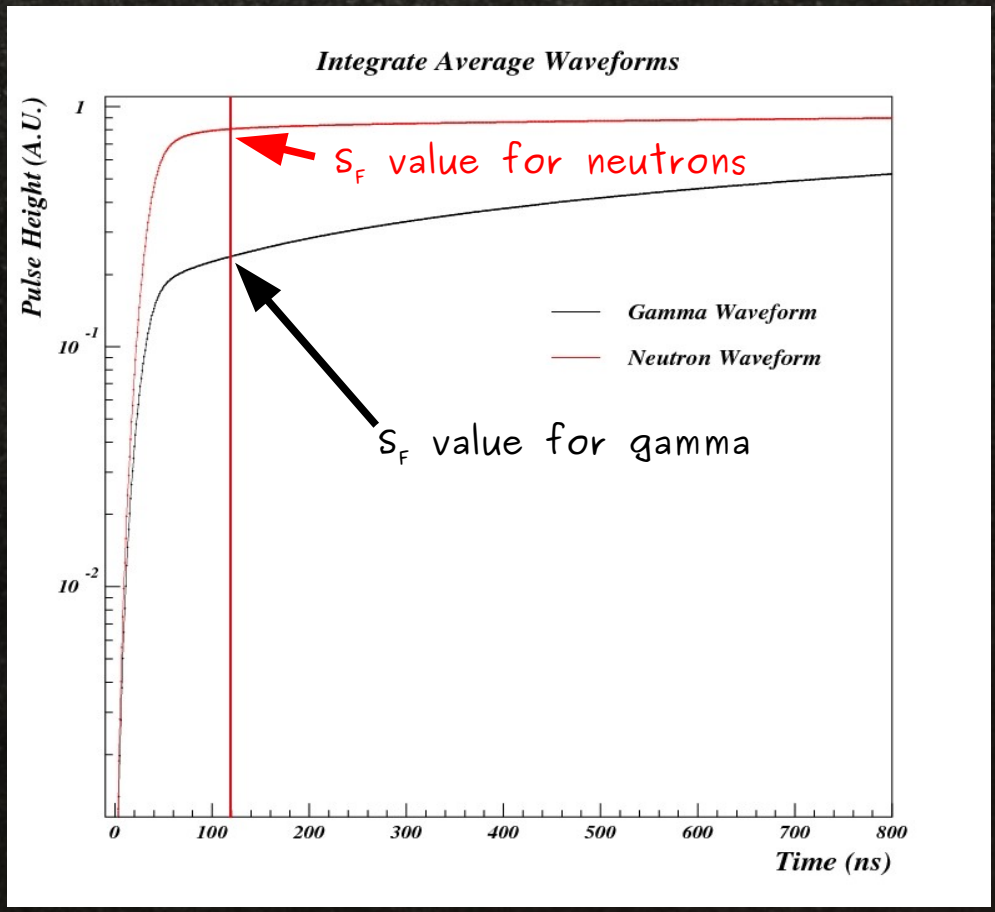

T_{fp} is a free parameter that needs to be optimizaed.

F-Prompt: T_{Fp} Optimization

Two indipendent methods have been applied to determine the optimum "fast" integration time.

I Method

8 different values of T_{Fp} are selected (from 80 ns to 150 ns). A Fp parameter is built from each of these T_{Fp} values and applied to data, to determine the integration time ensuring the best discrimination power.

The parameter adopted to determine the discrimination efficiency is the Normalized Merit Factor (NMF), obtained from the standard Merit Factor (MF) averaged over the energy bins.

$$MF = \frac{X_n - X_g}{\sigma_n + \sigma_g}$$

X_n neutron Fp expectation value

X_g gamma Fp expectation value

σ_i dispersion of Fp distribution

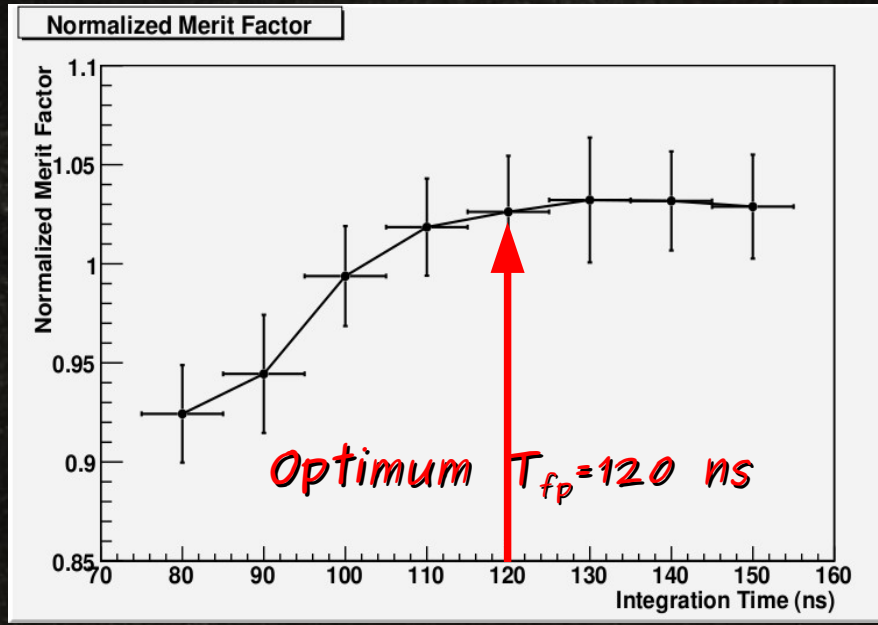

The second method, based on the max difference between integrated average n and γ waveforms, gives compatible results (T_{fp}=116 ns). Indication of the presence of an intermediate scintillation component.

F-Prompt: populations

Once T_{Fp} has been optimized, the Fp parameter can be applied to the data sample and a plot of Fp vs event energy (expressed in phe) obtained.

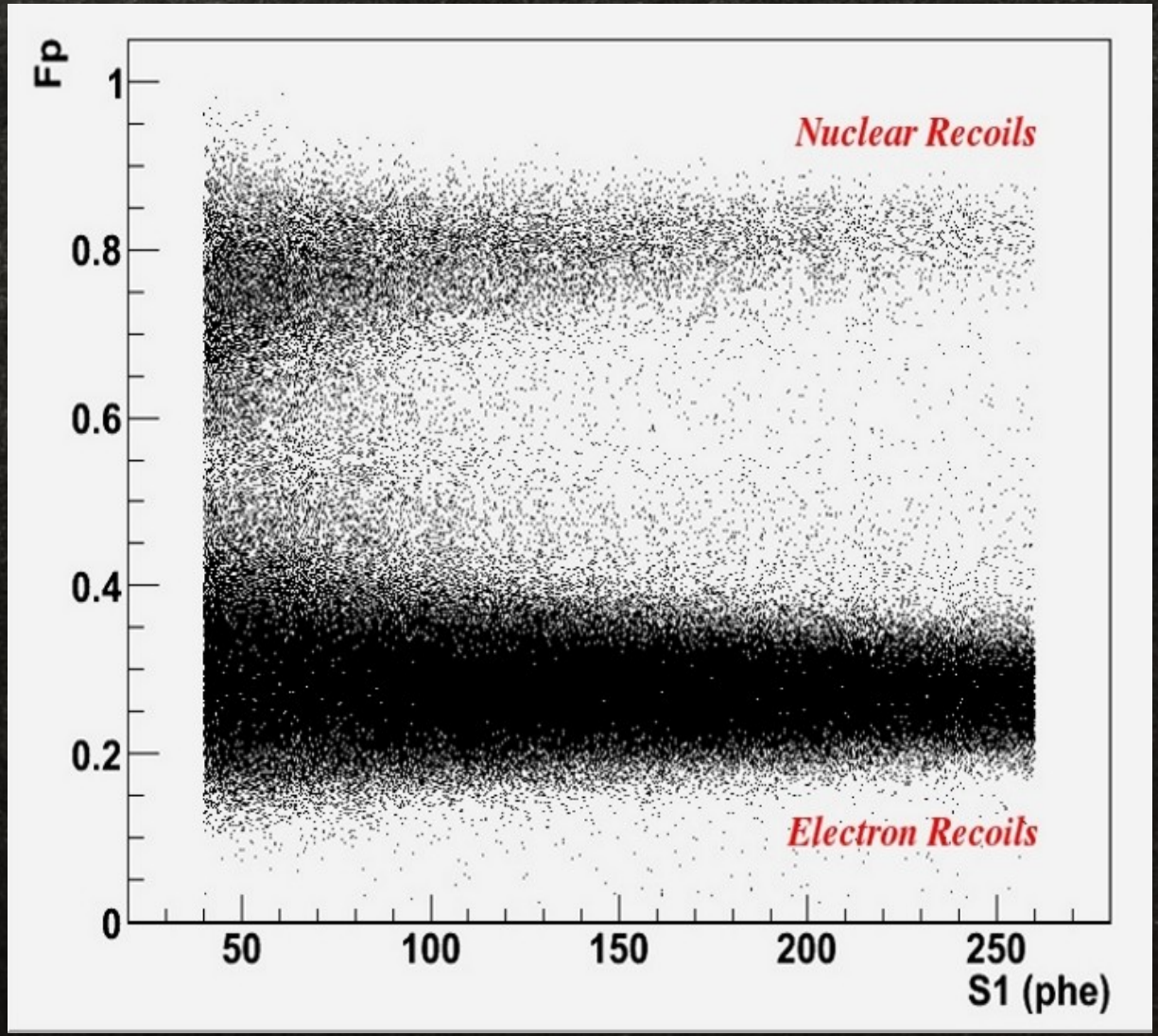

A relevant number of events cluster in between the two expected population of nuclear and electron recoils. Where do they come from?

Intermediate events

The appearance of an intermediate population with $Fp_g < Fp_i < Fp_n$ was something totally unexpected, never observed or reported in literature before. A study of the possible causes and the subsequent definition of a fit function able to correctly reproduce all the features of Fp distributions appeared as necessary.

One of the possible origins of this new population are neutrons inelastically scattering off Ar nuclei.

$$n + Ar \rightarrow Ar^* + n'$$

Neutron like

$$Ar^* \rightarrow \gamma + Ar_{recoil}$$

Gamma like

$$\gamma + e^-(Ar) \rightarrow e^-_{recoil}$$

Recoiling Ar nucleus and emitted γ share the energy of incident neutron, giving origin to an Fp value in between those of the two populations

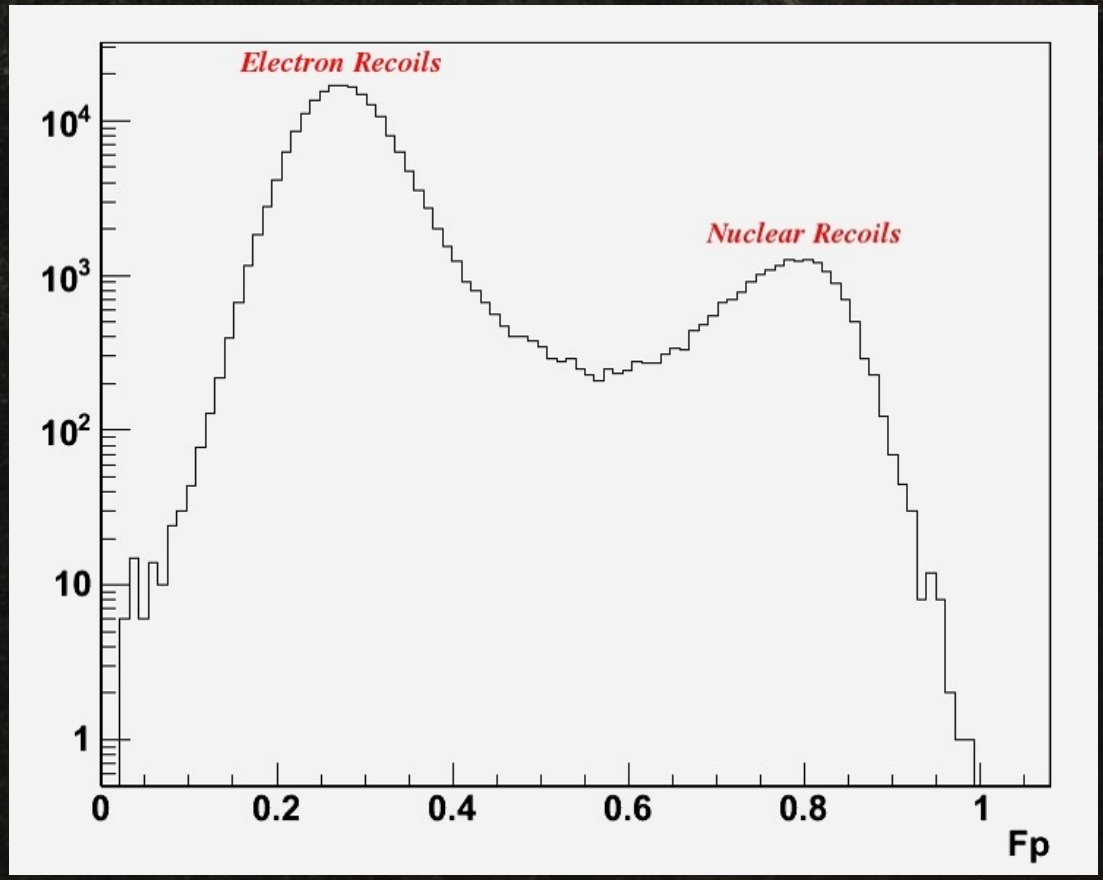

Neutron spectrum and cross section

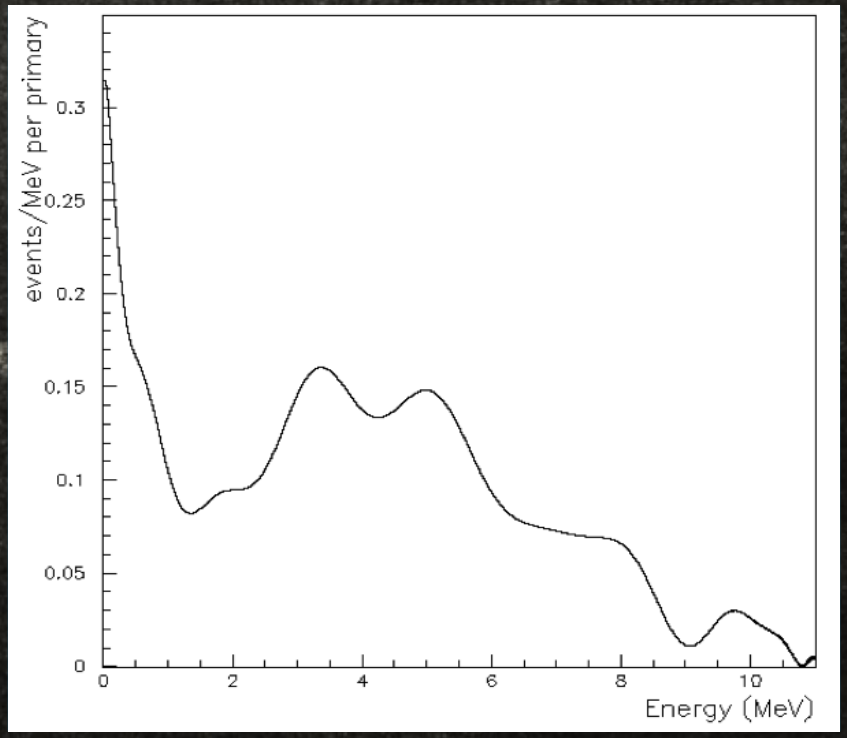

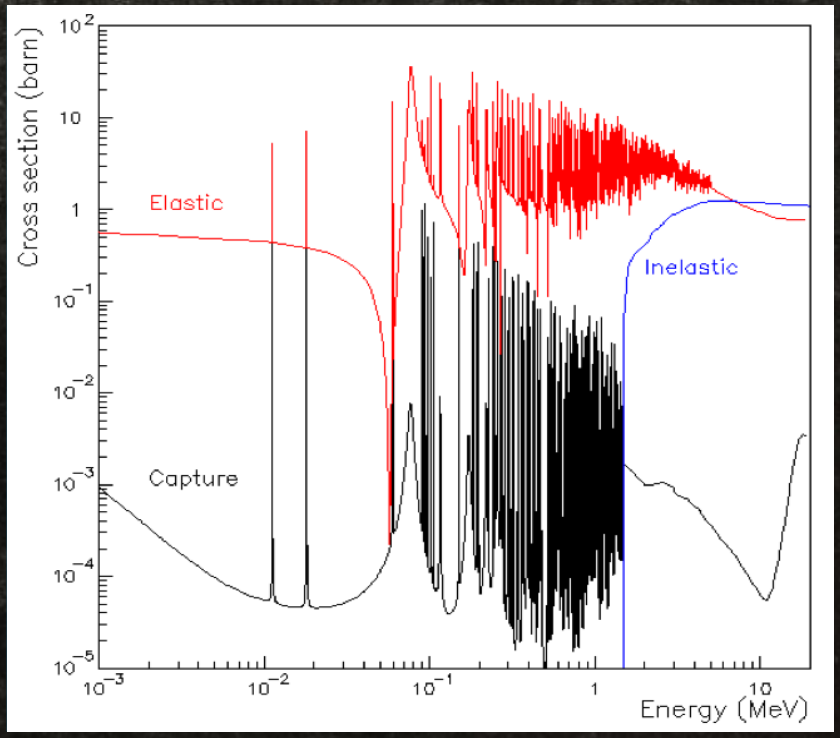

Primary Am/Be n spectrum

Neutron cross section on ^{40}Ar

Am/Be neutron spectrum goes up to 11 MeV. Inelastic cross section becomes relevant for E>2 MeV. A MC simulation of the detector exposed to the Am/Be source has then been realised to:

- ✔ confirm the hypothesis of inelastic scattering as origin of the intermediate population;
- ✔ determine the best fit function for the Fp distribution.

Monte Carlo simulation

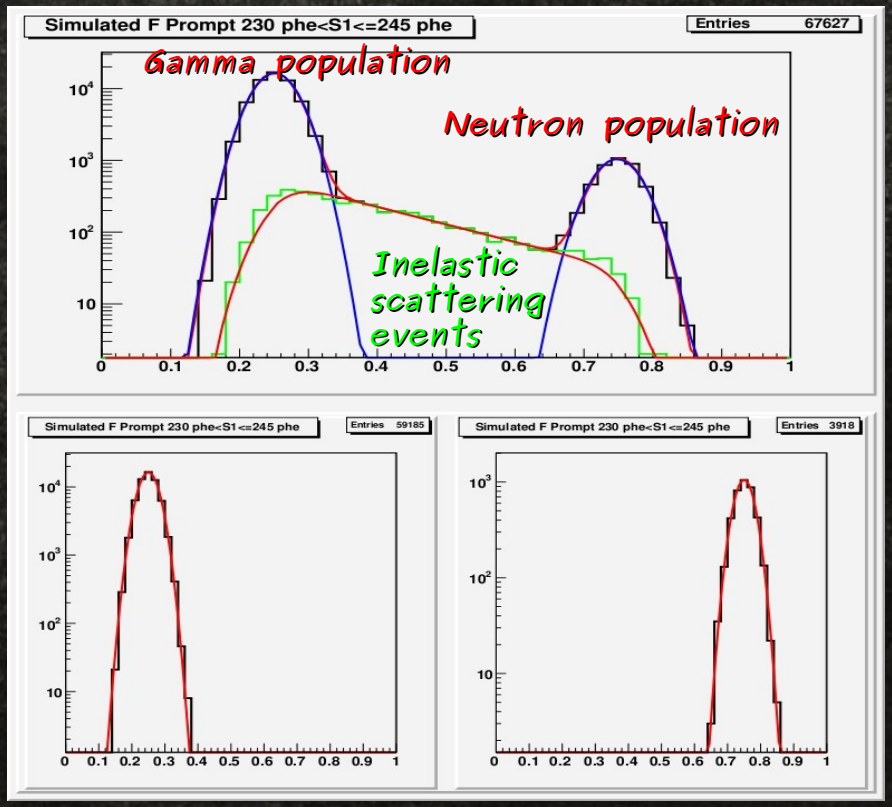

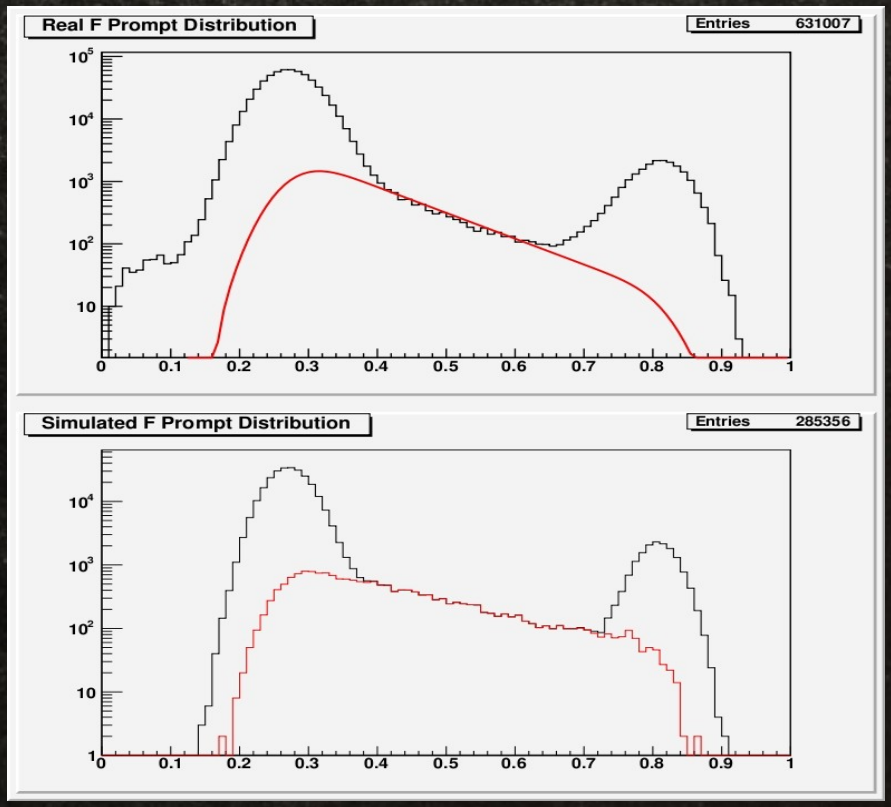

- Intermediate events are originated by neutrons inelastic scattering off Ar nuclei.
- The suitable fitting function able to reproduce the total Fp distribution is given by $F_{tot}(t) = G_\gamma \oplus G_n \oplus (Exp \otimes G)_{int}$.

F-Prompt: results

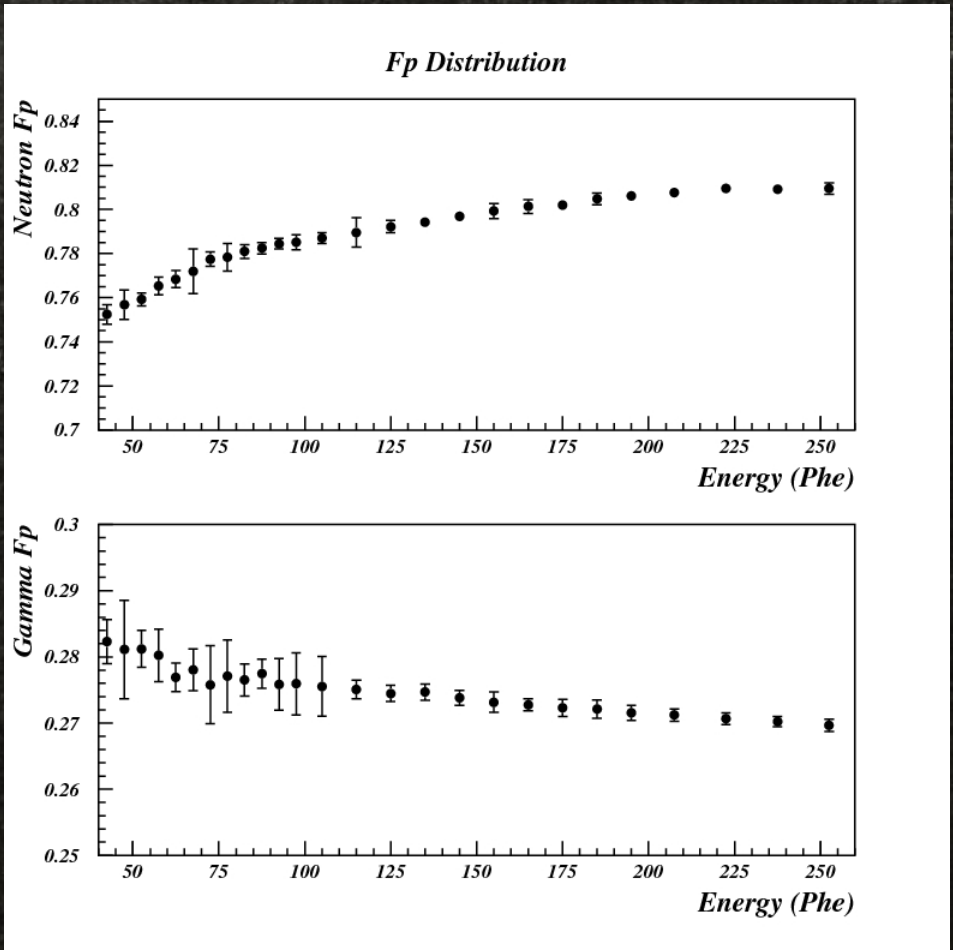

Separation between gamma and neutron populations, hence the discrimination power, worsen at lower energies: statistical or physical effect?

To understand the reason of such a behaviour, a comparison between neutron and gamma <Fp> distributions obtained with this data sample and two other ones, all characterised by different LY values (different phe-to-keV conversion factor) has been done.

F-Prompt: results

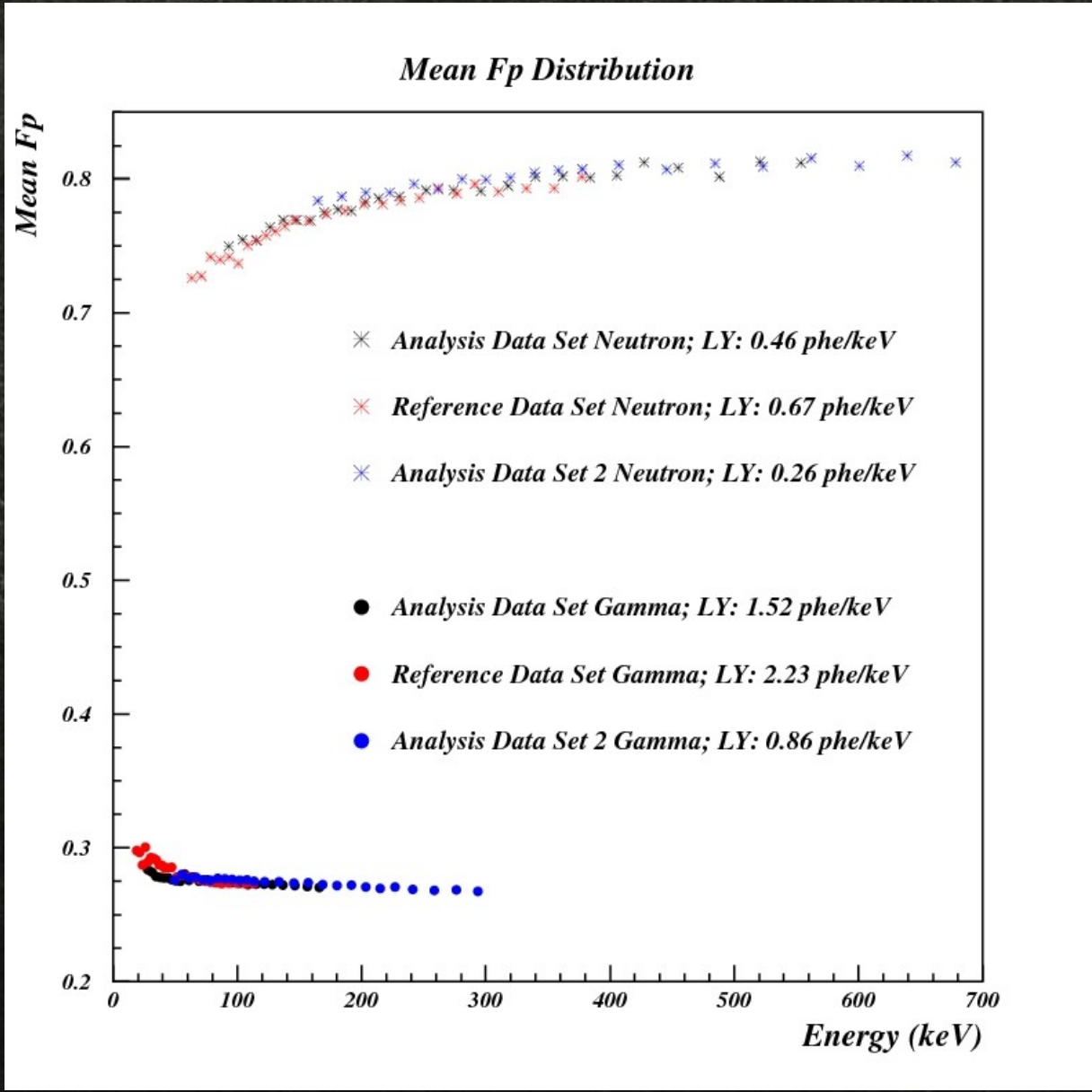

Energetic behaviour of <Fp> distributions is a physical effect.

There is a physical limit to the minimum energy at which an efficient discrimination of β and γ background can be obtained.

Consequences of Fp optimization

- To determine the actual impact the Fp optimization process has on the sensitivity of a LAr detector tailored for DM search, a comparison between results reported here and results found in literature (H. Lippincont *et al.*, Phys. Rev. C 78 (2008), 035801) for a method totally equivalent to Fp has been carried out.

- Lippincont *et al.* data have been collected with a LAr chamber exposed to Am/Be neutron and ^{22}Na gamma sources. They applied to their data set a *prompt fraction* fp discrimination method, defined as:

$$fp = \frac{\int_{T_i}^{\zeta} V(t)\,dt}{\int_{T_i}^{T_f} V(t)\,dt}$$

V(t) Signal sum

$T_i = t_{trig} - 50$ ns

$T_f = t_{trig} + 9$ μs

$\xi = t_{trig} + 90$ ns

t_{trig} trigger time

Consequences of Fp optimization

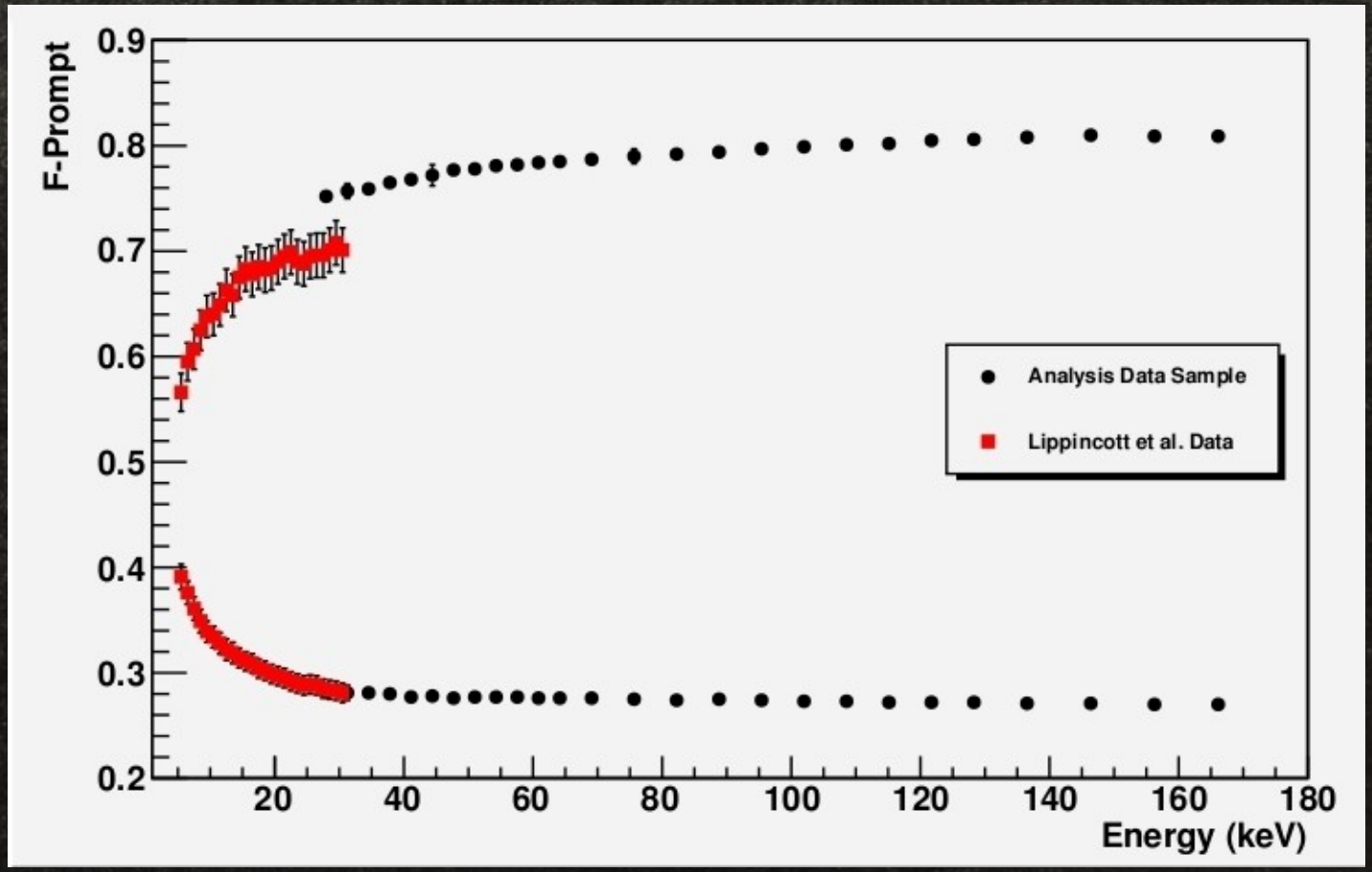

The better separation shown by <Fp> distributions may be attributable to:

✔ A careful choice of the integration time T_{Fp};

✔ A careful choice of the fit function for the Fp distributions.

Consequences of Fp optimization

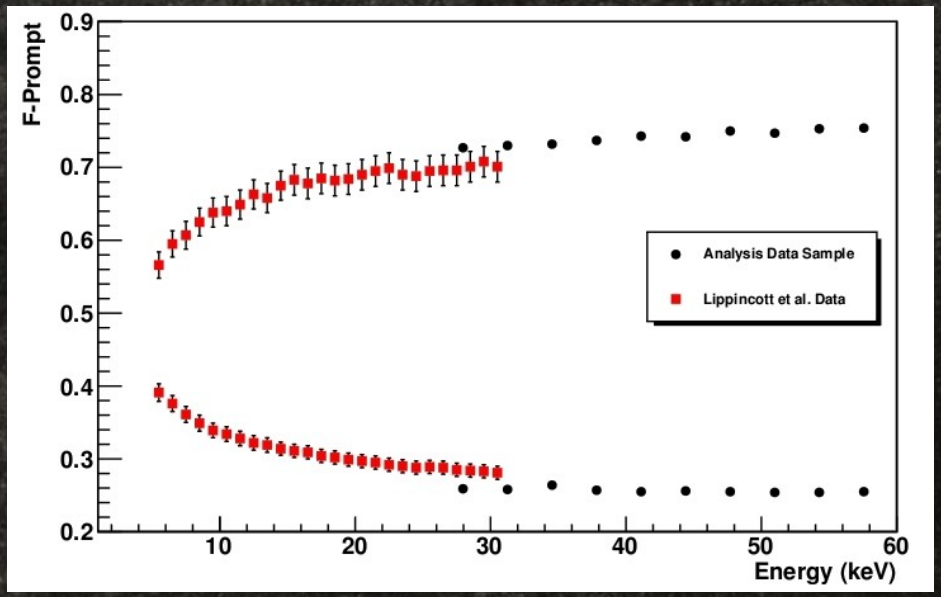

T_{fp}=90 ns: <Fp> values of both gamma and neutron events decrease.

T_{fp}=90 ns and fit function given by the sum of two gaussians: both gamma and neutron <Fp> distributions perfectly match the respective <fp> distributions.

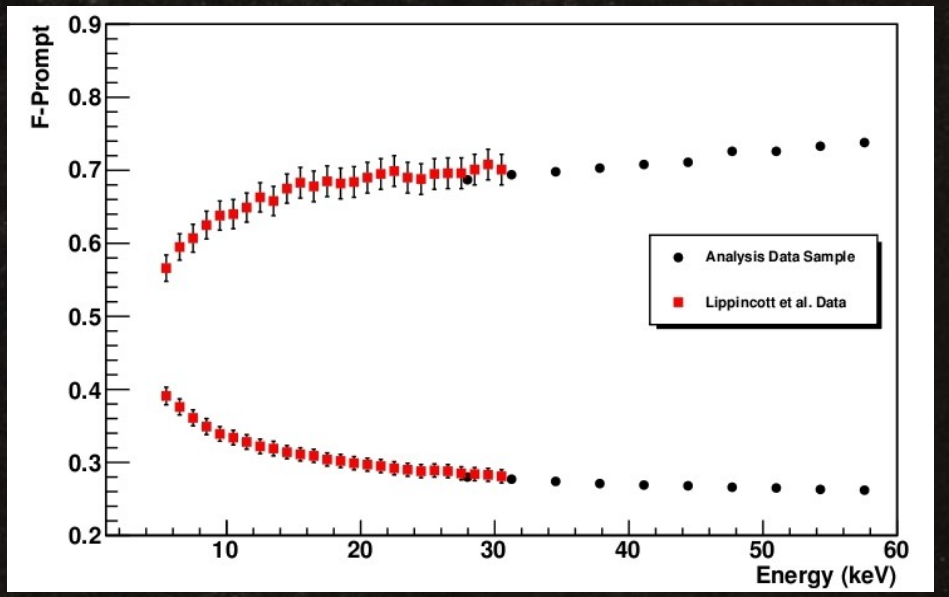

Consequences of Fp optimization

Starting from <Fp> and <fp> values shown, it is possible to realize a projected sensitivity plot for a LAr detector tailored for Dark Matter

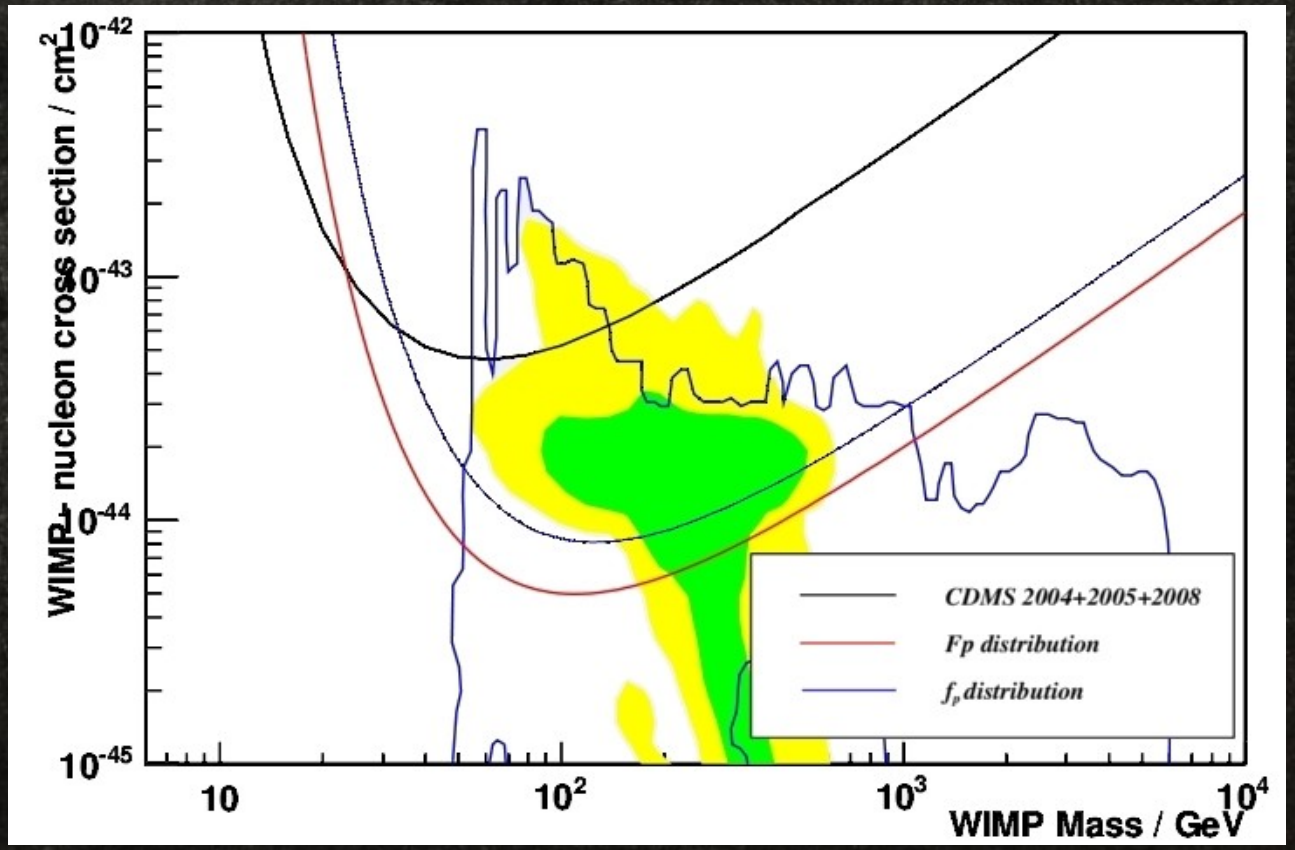

- ✔ LY: 1.6 phe/keV
- ✔ Exposure: 110 kg·day
- ✔ Nulcear Recoil Acceptance: 50%
- ✔ Background dominated by β from ^{39}Ar only. (no neutron bkg).
- ✔ Nuclear recoil efficiency:30% respect to electron recoils.
- ✔ Standard assumption for the galactic halo model.

Fp optimization process and above all a careful choice of the fit function for Fp distributions produces a remarkable increasing of the discrimination power and, consequently, an increasing of the sensitivity to WIMPs.

Consequences of Fp optimization

Recent, preliminary results of the comparison with Lippincont et al. data. They have been obtained after an improvement of the light collection of the detector (LY=6.35 phe/keV, compared to LY=1.52 phe/keV of this work): energy threshold for electron recoil pushed under 10 keV!

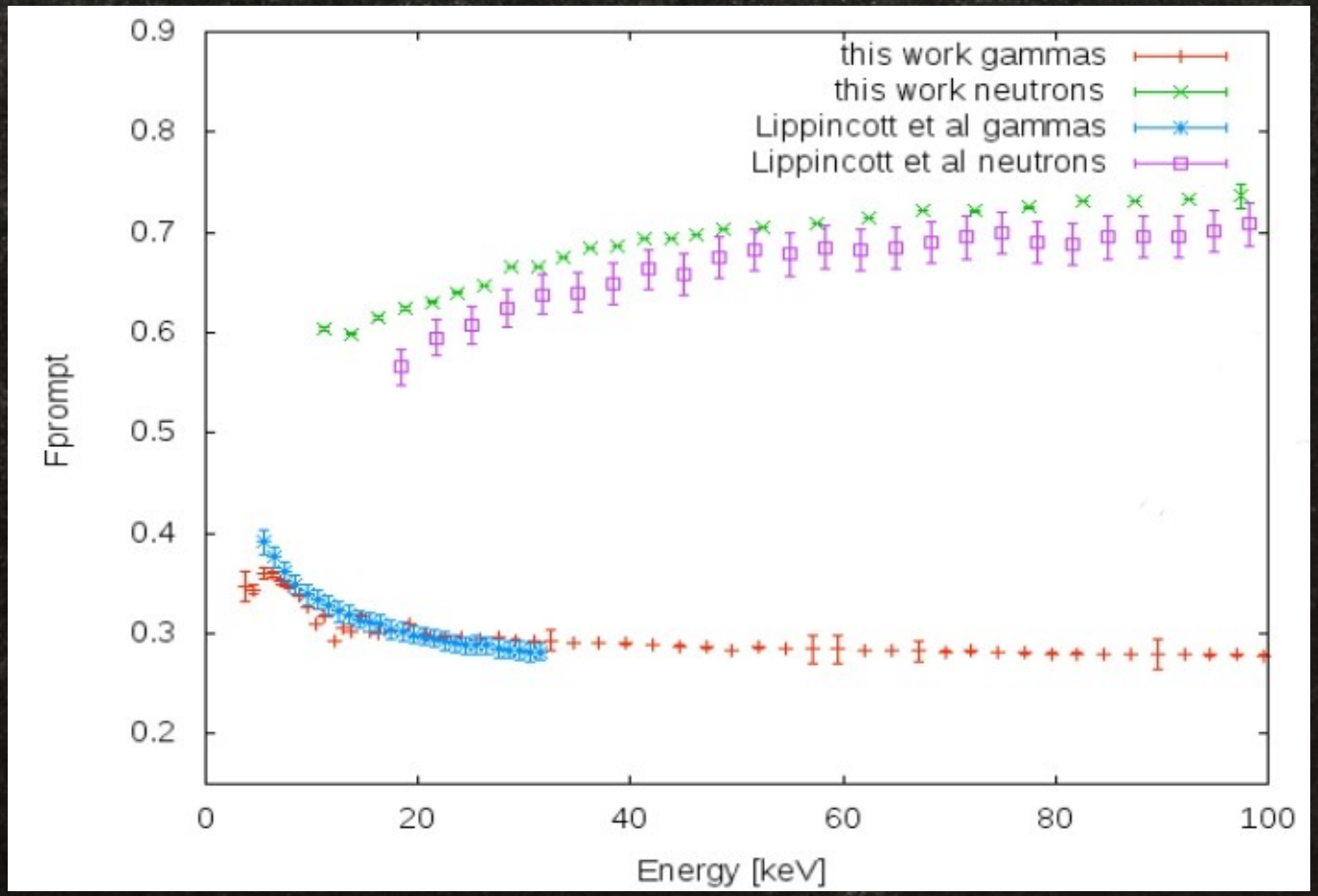

Light collection optimization will be the subject of next slides

Consequences of Fp optimization

Results of the two studies (with low and high LY chambers) presented at TIPP2011 conference

ELSEVIER

Available online at www.sciencedirect.com

ScienceDirect

Physics Procedia 00 (2011) 1–9

Physics Procedia

Neutron to Gamma Pulse Shape Discrimination in Liquid Argon Detectors with High Quantum Efficiency Photomultiplier Tubes

R. Acciarri[a], N. Canci[b,*], F. Cavanna[a,d], P. Kryczynski[c], L. Pandola[b], E. Segreto[b], A.M. Szelc[1a,c]

[a] *Università degli Studi dell'Aquila e INFN, L'Aquila, Italy*
[b] *INFN - Laboratori Nazionali del Gran Sasso, Assergi, Italy*
[c] *IFJ PAN, Krakow, Poland*
[d] *Yale University - New Haven, Connecticut, USA.*

Abstract

A high Light Yield Liquid Argon chamber has been radiated with an Am/Be source for signal-to-background separation level characterization in a Dark Matter Liquid Argon based detector. Apart from the standard nuclear recoil and electron events, from neutron elastic interactions and gamma conversions respectively, an intermediate population has been observed which is attributed to inelastic neutron scatters on Argon nuclei producing Argon recoil and simultaneous gammas from nuclear de-excitation. Taking account of these events results in a better determination of the recoil-like to electron-like separation based on the shape of the scintillation pulse. The results of this recent study as well as from a previous study with a chamber with a lower Light Yield are presented.

Keywords: Liquid Argon, Noble Liquid detectors, Cryogenic Detectors, Dark Matter search, Pulse Shape Discrimination, Particle identification
PACS: 29.40.Mc, 61.25.Bi, 33.50.Hv, 95.35.+d

Improving the light collection

- Maximization of light collection in a DM LAr detector represents a crucial step on the way to achieve a low energy threshold and an efficient background discrimination. Because of this, I actively worked on this topic as well (2007–2011).

- Optimization of light collection has been performed through:

  - ✔ study of the effects of N_2 and O_2 contamination in LAr;

  - ✔ characterization of a new generation of high QE cryogenic PMTs;

  - ✔ characterization of the conversion properties of wavelength shifter films and their response to exposition to light and air (not shown here).

Quenching process by X_2 molecules

The quenching process can be sketched as:

$$Ar_2^* + X_2 \rightarrow 2\,Ar + X_2$$

Where X can represent either Nitrogen or Oxygen molecule.

This non-radiative collisional reaction, in competition with de-excitation process leading to VUV emission, brings to a reduction of Ar_2^*.

$$l'(t) = \frac{A'_S}{\tau'_S}\exp\left(\frac{-t}{\tau'_S}\right) + \frac{A'_T}{\tau'_T}\exp\left(\frac{-t}{\tau'_T}\right)$$

$$\frac{1}{\tau'_j}([X_2]) = \frac{1}{\tau_j} + k[X_2]$$

$$A'_j([X_2]) = \frac{A_j}{1+\tau_j k[X_2]}$$

k: quenching process rate constant

$[X_2]$: contaminant concentration

$$\int l'(t)\,dt = A'_S + A'_T \leq 1$$

$$Q_F = A'_S + A'_T$$

$$0 \leq Q_F \leq 1$$

N_2 and O_2 contamination in LAr

While ionization charge quenching by electro-negative impurities in LAr has been widely studied, scintillation light quenching from X_2 contaminants is less precisely explored. This effect is important because it reduces light collection and deteriorates the PSD discrimination capabilities of the detector. A systematic study of the effects of Oxygen and Nitrogen contamination in LAr has then been pursued to:

- determine the effective lifetimes τ_j' as a function of the O_2 and N_2 contamination, as well as the quenched amplitudes A_j';

- extract the main characteristics of the scintillation light emission in pure LAr and the value of the rate constant k of the quenching process associated to the presence of either O_2 or N_2 contaminant.

A small (0.7 lt) dedicated detector has been realised for this purpose, coupled with a system for the injection of controlled amounts of gaseous contaminants.

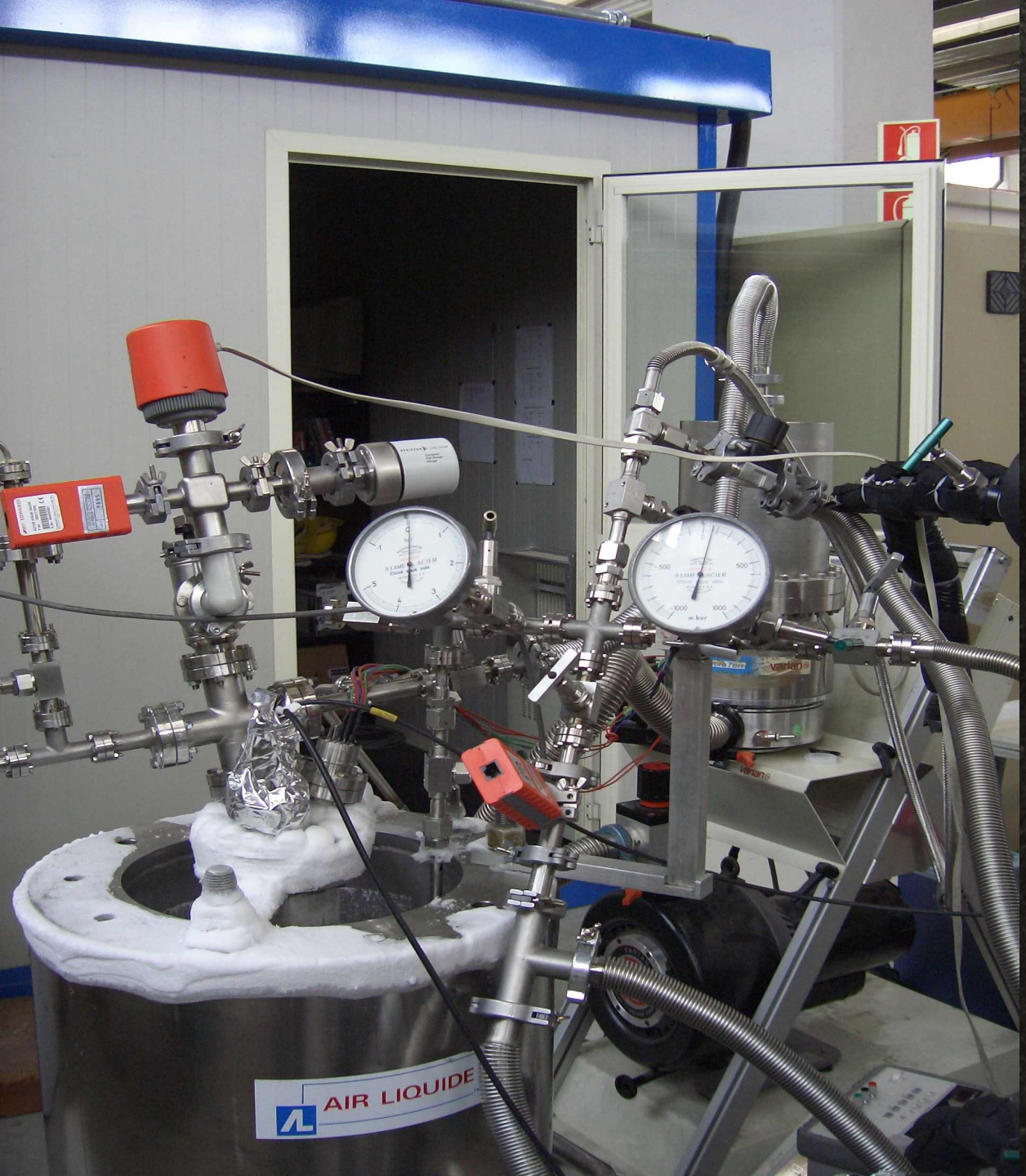

0.7 lt

single

phase

detector

0.7 lt single phase detector: schematic view

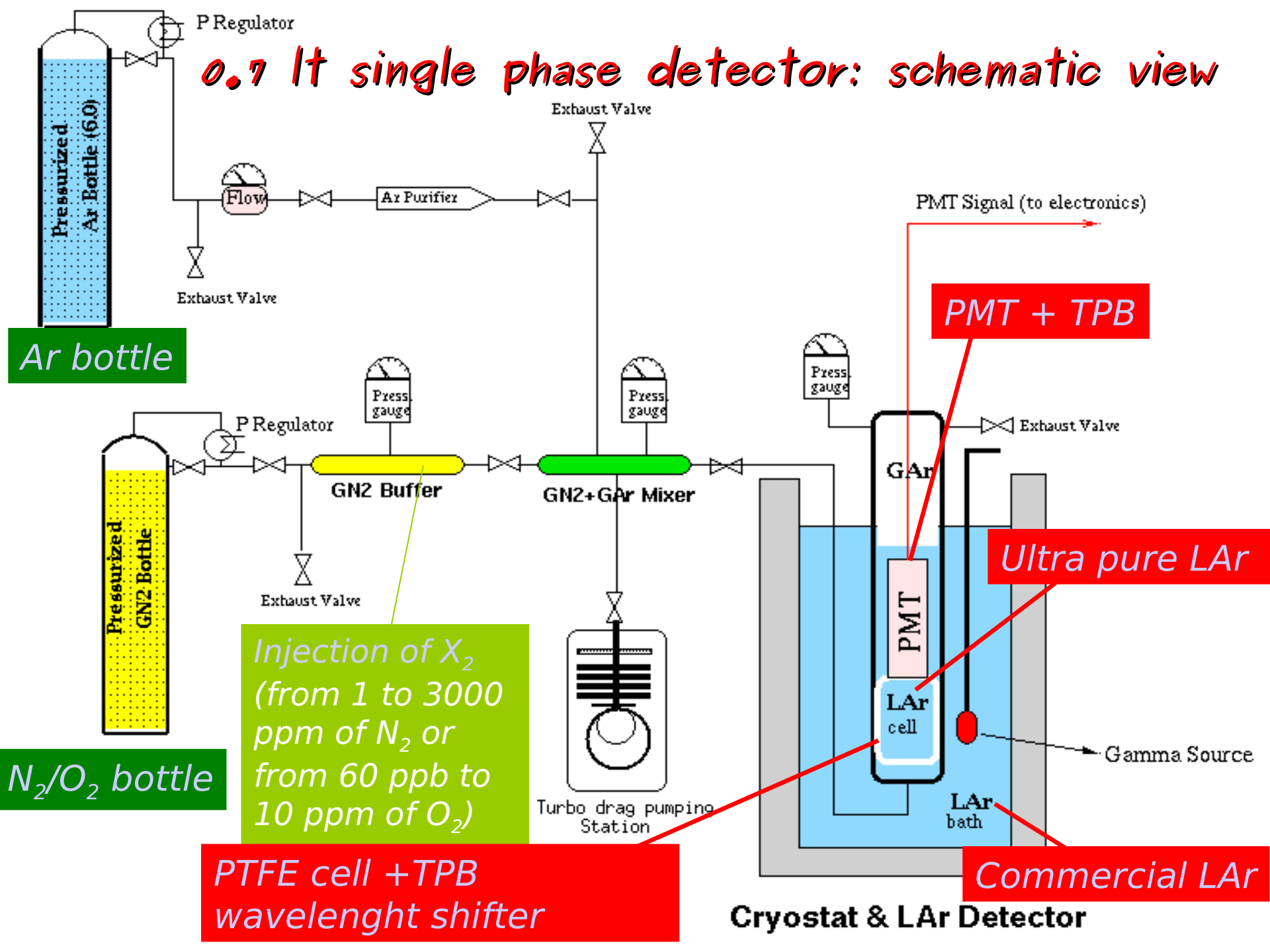

O_2 contamination test

Wfm recording of PMT signal (1 ns sampling time) allows for a detailed study of the LAr scintillation: individual components, relative amplitude and decay time.

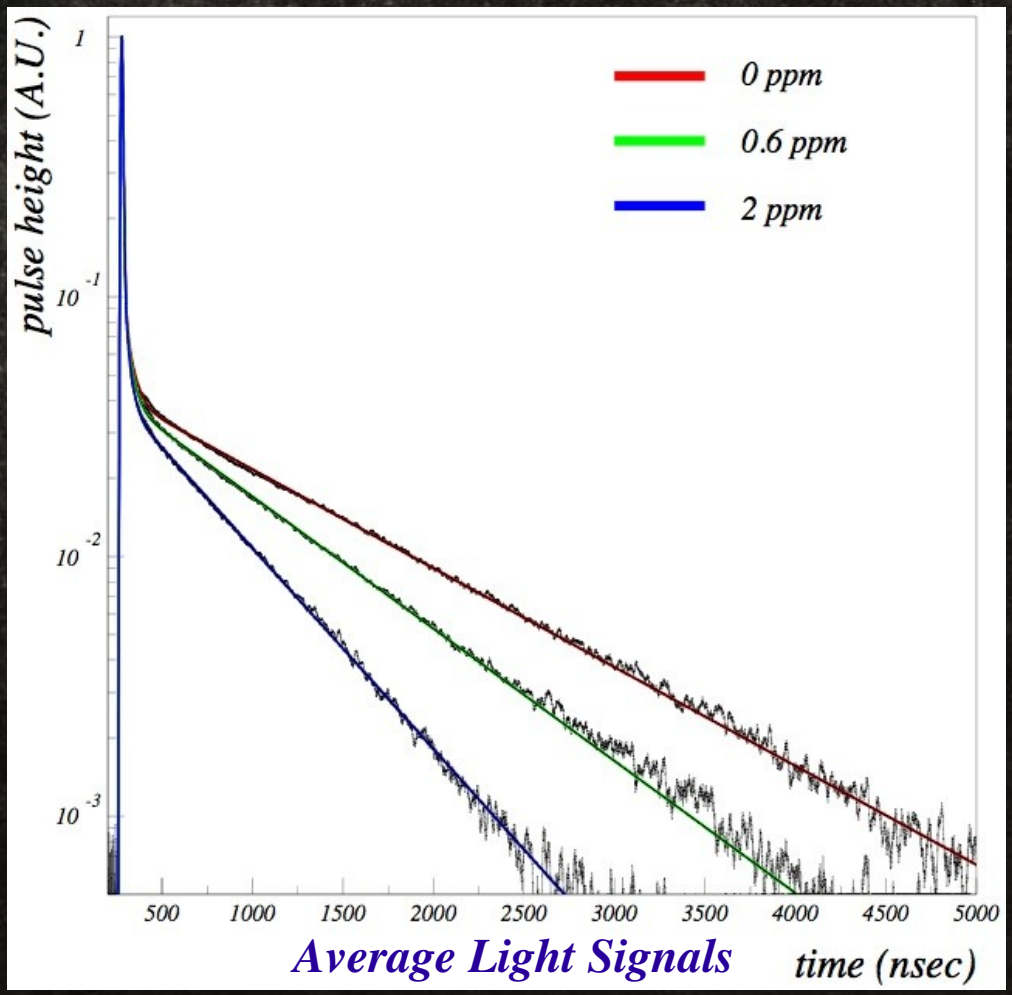

- Argon was progressively contaminated with increasing quantities of O_2 (0 ppm, 0.06 ppm, 0.3 ppm, 0.6 ppm, 2ppm, 5 ppm, 10 ppm).
- Single waveforms produced by a ^{60}Co γ source have been acquired at each level of contamination.
- Average signal V(t) is calculated (100k wfms) for each $[O_2]$.

Slow component decay time vs O_2 concentration

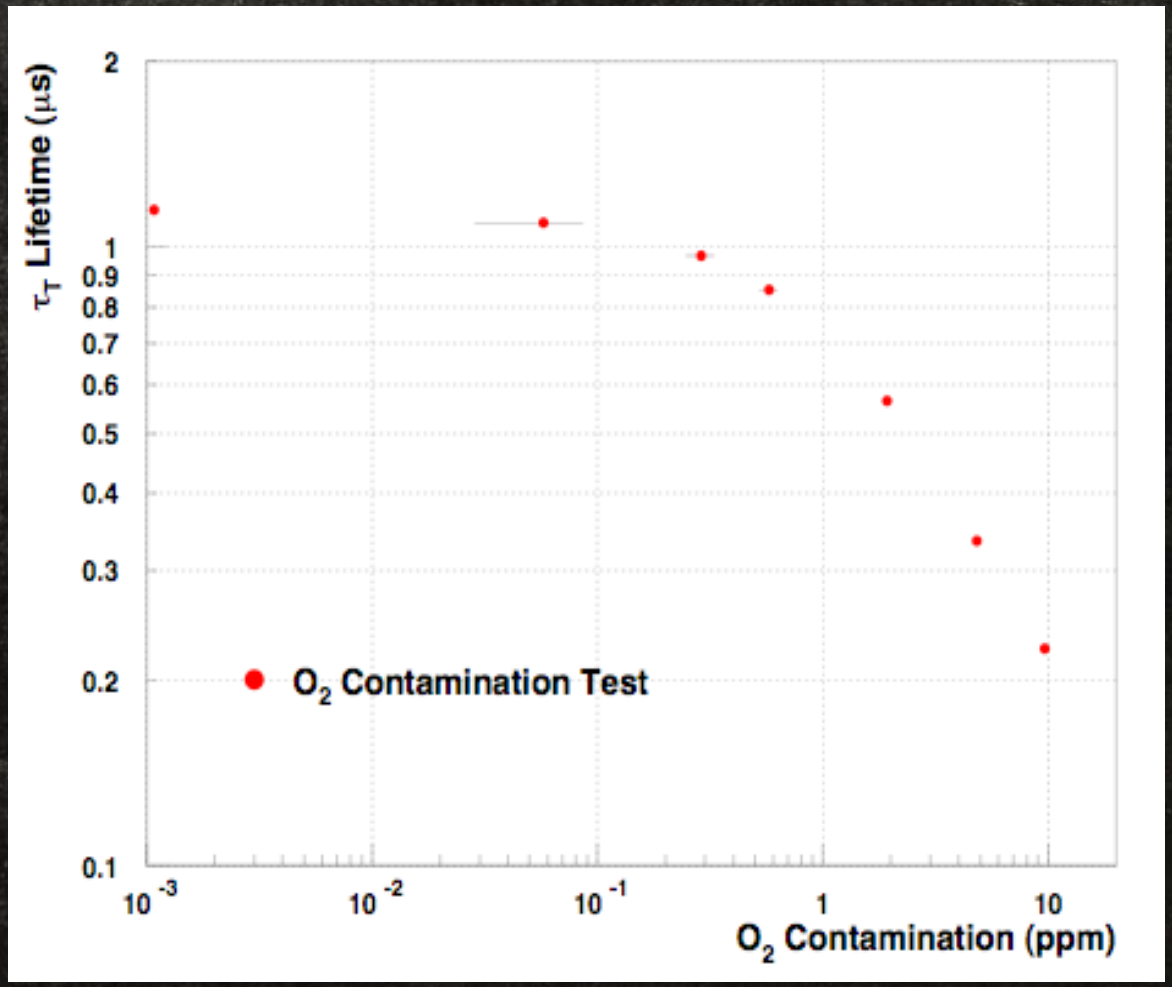

- Because of the quenching process, τ_T clearly decreases as the $[O_2]$ exceeds the ~100 ppb level.

- τ_S is instead almost unaffected even at largest contaminations.

N_2 contamination test

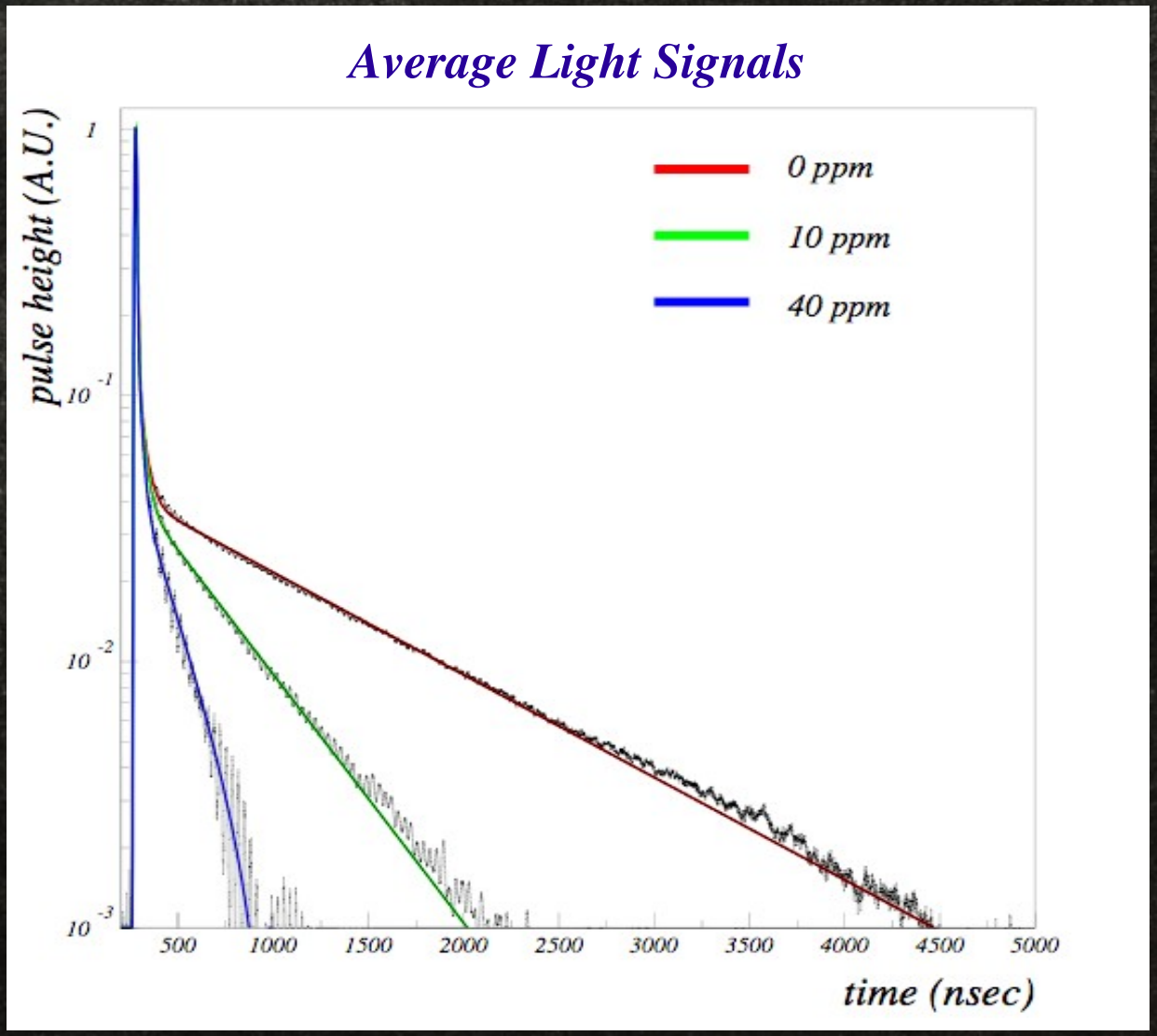

- Argon was progressively contaminated with increasing quantities of N_2 (0 ppm, 1 ppm, 2 ppm, 5 ppm, 10 ppm, 20 ppm, 40 ppm, 60 ppm, 100 ppm, 500 ppm, 1000 ppm, 3000 ppm).
- Single waveforms produced by a ^{60}Co γ source have been acquired at each level of contamination.
- Average signal V(t) is calculated (100k wfms) for each $[N_2]$.

Overall fit of Amplitudes and Lifetimes

Relative Intensities

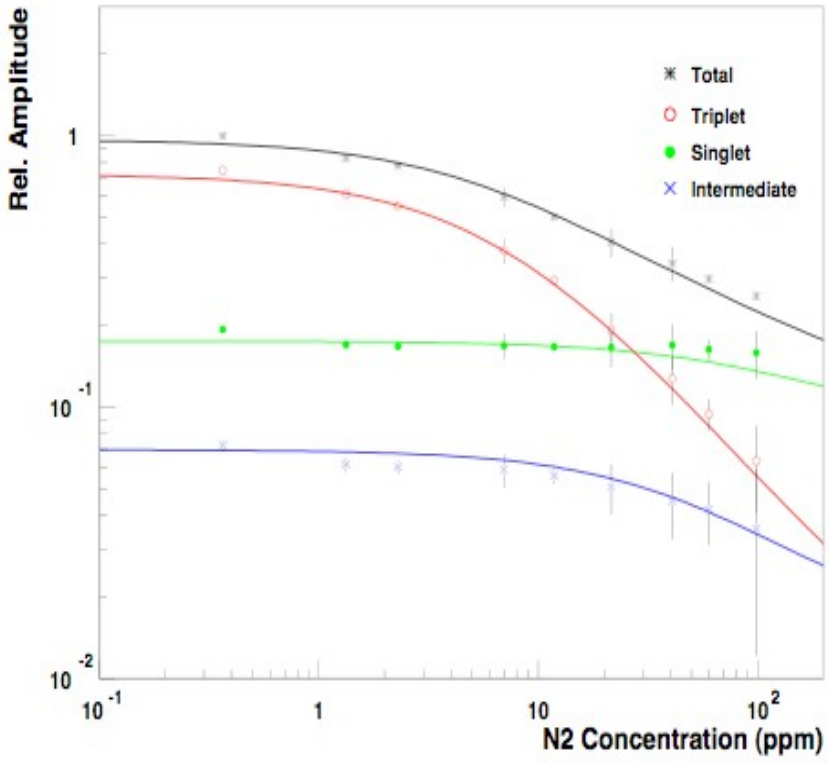

Lifetimes

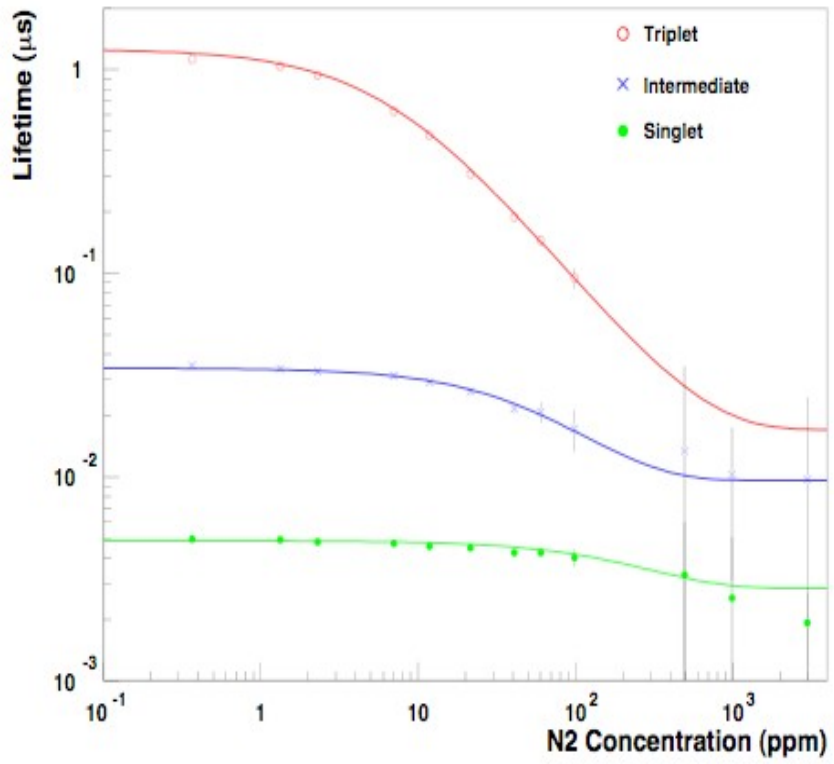

$$A'_j([N_2]) = \frac{A_j}{1+\tau_j k[N_2]}$$

$$\frac{1}{\tau'_j}([N_2]) = \frac{1}{\tau_j} + k[N_2]$$

Analysis results

	Lifetimes τ_i	Amplitudes A_i
Short-Lived Component	4.9±0.2 ns	18.8%
Intermediate Component	34±3 ns	7.4%
Long-Lived Component	1260±30 ns	73.8%

	Rate Constant k	Initial Concentration $[X_2]_{in}$
O_2	0.54±0.03 $\mu s^{-1} ppm^{-1}$	65±15 ppb
N_2	0.11±0.05 $\mu s^{-1} ppm^{-1}$	0.40±0.20 ppm

- ✓ The overall minimization procedure I developed (minimize at the same time all the average wvfs for a given contamination test) allowed to determine uncontaminated τ_i and A_i values, as well as rate constants and initial concentration of contaminants.
- ✓ A_s/A_t = 0.35 in agreement with available reference data for light ionizing particles.
- ✓ The rate constant k of the N_2 quenching process is in agreement with earlier measurements (but with an higher precision than before).
- ✓ The rate constant k' of the O_2 quenching process is five times higher than that of N_2 process.
- ✓ Initial O_2 and N_2 concentrations are within the specification for ultra-pure Ar.

Jinst

PUBLISHED BY IOP PUBLISHING FOR SISSA

RECEIVED: *February 26, 2010*
REVISED: *May 3, 2010*
ACCEPTED: *May 16, 2010*
PUBLISHED: *June 15, 2010*

Effects of Nitrogen contamination in liquid Argon

R. Acciarri,[a] M. Antonello,[a,b] B. Baibussinov,[c] M. Baldo-Ceolin,[d] P. Benetti,[e] F. Calaprice,[f] E. Calligarich,[g] M. Cambiaghi,[e] N. Canci,[a] F. Carbonara,[h] F. Cavanna,[a,1] S. Centro,[d] A.G. Cocco,[i] F. Di Pompeo,[a,b] G. Fiorillo,[h] C. Galbiati,[f] V. Gallo,[i] L. Grandi,[a,b] G. Meng,[c] I. Modena,[a] C. Montanari,[g] O. Palamara,[b] L. Pandola,[b] G.B. Piano Mortari,[a] F. Pietropaolo,[c] G.L. Raselli,[g] M. Roncadelli,[g] M. Rossella,[g] C. Rubbia,[b] E. Segreto,[b,1] A.M. Szelc,[j,a] S. Ventura[c] and C. Vignoli[g]

[a]*Università dell'Aquila e INFN, L'Aquila, Italy*
[b]*INFN - Laboratori Nazionali del Gran Sasso, Assergi, Italy*
[c]*INFN - Sezione di Padova, Padova, Italy*
[d]*Università di Padova e INFN, Padova, Italy*
[e]*Università di Pavia e INFN, Pavia, Italy*
[f]*Princeton University - Princeton, New Jersey, U.S.A.*
[g]*INFN - Sezione di Pavia, Pavia, Italy*
[h]*Università di Napoli e INFN, Napoli, Italy*
[i]*INFN - Sezione di Napoli, Napoli, Italy*
[j]*IFJ PAN, Krakow, Poland*
E-mail: ettore.segreto@lngs.infn.it, flavio.cavanna@aquila.infn.it

ABSTRACT: A dedicated test to study the effects of Nitrogen contamination in liquid Argon has been performed at the INFN-Gran Sasso Laboratory (LNGS, Italy) within the WArP R&D program.

A detector has been designed and assembled for this specific task and connected to a system for injection of controlled amounts of gaseous Nitrogen into the liquid Argon volume. The purpose of the test is to detect the reduction of the Ar scintillation light emission as a function of the amount of the Nitrogen contaminant injected in the Argon volume. A wide concentration range, spanning from $\sim 10^{-1}$ ppm up to $\sim 10^{3}$ ppm, has been explored.

Measurements have been done with electrons in the energy range of minimum ionizing particles (γ-conversion from radioactive sources). Source spectra at different Nitrogen contaminations are analyzed, showing sensitive reduction of the scintillation yield at increasing concentrations.

Direct PMT signal acquisition exploiting high time resolution by fast waveform recording allowed high precision extraction of the main characteristics of the scintillation light emission in contaminated LAr. In particular, the decreasing behavior in lifetime and relative amplitude of the

[1]Corresponding author

doi:10.1088/1748-0221/5/06/P06003

2010 JINST 5 P06003

Jinst

PUBLISHED BY IOP PUBLISHING FOR SISSA

RECEIVED: *February 26, 2010*
ACCEPTED: *March 13, 2010*
PUBLISHED: *May 4, 2010*

Oxygen contamination in liquid Argon: combined effects on ionization electron charge and scintillation light

R. Acciarri,[a] M. Antonello,[a,b] B. Baibussinov,[c] M. Baldo-Ceolin,[d] P. Benetti,[e] F. Calaprice,[f] E. Calligarich,[g] M. Cambiaghi,[e] N. Canci,[a,1] F. Carbonara,[h] F. Cavanna,[a,1] S. Centro,[d] A.G. Cocco,[i] F.Di Pompeo,[a,b] G. Fiorillo,[h] C. Galbiati,[f] V. Gallo,[i] L. Grandi,[a,b] G. Meng,[c] I. Modena,[a] C. Montanari,[g] O. Palamara,[b] L. Pandola,[b] G.B. Piano Mortari,[a] F. Pietropaolo,[c] G.L. Raselli,[g] M. Roncadelli,[g] M. Rossella,[g] C. Rubbia,[b] E. Segreto,[b] A.M. Szelc,[j,a] F. Tortorici,[b] S. Ventura[c] and C. Vignoli[g]

[a]*Università dell'Aquila e INFN, L'Aquila, Italy*
[b]*INFN - Laboratori Nazionali del Gran Sasso, Assergi, Italy*
[c]*INFN - Sezione di Padova, Padova, Italy*
[d]*Università di Padova e INFN, Padova, Italy*
[e]*Università di Pavia e INFN, Pavia, Italy*
[f]*Princeton University - Princeton, New Jersey, U.S.A.*
[g]*INFN - Sezione di Pavia, Pavia, Italy*
[h]*Università di Napoli e INFN, Napoli, Italy*
[i]*INFN - Sezione di Napoli, Napoli, Italy*
[j]*IFJ PAN, Krakow, Poland*
E-mail: nicola.canci@lngs.infn.it, flavio.cavanna@aquila.infn.it

ABSTRACT: A dedicated test to study the effects of Oxygen contamination in liquid Argon has been performed at the INFN-Gran Sasso Laboratory (LNGS, Italy) within the WArP R&D program. Two detectors have been used: the WArP 2.3 lt prototype and a small (0.7 lt) dedicated detector, coupled with a system for the injection of controlled amounts of gaseous Oxygen.

O_2 contamination in LAr leads to depletion of both the free electron charge (via *attachment* process) and the scintillation light (via *quenching* and *absorption* mechanisms) available for ionization signal detection. Purpose of the test with the 0.7 lt detector was to detect the reduction of the long-lived component lifetime of the Argon scintillation light emission and of the overall light yield at increasing O_2 concentration. Data from the WArP prototype were used for determining the

[1]Corresponding author.

doi:10.1088/1748-0221/5/05/P05003

2010 JINST 5 P05003

Results of this work have been published on JINST. Since then, they received many citations and have been taken has a reference point by the LAr community. I also presented this work at the IPRD08 conference

Test of new cryogenic PMTs

- On the way to maximize the light collection in LAr detectors for Dark Matter search, our last step has been the choice of a set of PMTs featuring the highest possible level of performance and stability.

- The cryogenic temperature of LAr (87 K) induces problems on common PMTs (mechanical fragility, change on photocatode resistivity). Some years ago the WArP experiment started a collaboration with Hamamatsu Photonics for the production of new cryogenic PMTs with a high quantum efficiency.

- The result of this collaboration has been a first set of a new generation of PMTs (Mod. R11065), with Quantum Efficiency (QE) of the photocatode over 30% (up to 35%) at LAr temperatures (to be compared to <20% QE of the ETL PMTs commonly adopted by the WArP experiment).

- We assembled three different prototypes (housing respectively 1,2 and 4 PMTs) to subject this first set of PMTs to a series of tests aiming at their characterization in reference working conditions.

Single PMT test

- A first test on a single PMT (Fall '09, repeated beginning 2010) has been performed to determine its main characteristics (gain, response to single photoelectron, stability).
- The detector is constitued by a PTFE cell containing 0.7 kg of LAr (cylinder shaped h=9cm Ø=8.4cm) closed on top by a 3" R11065 PMT viewing the active volume.
- Internal surfaces of the cell were covered with a TPB film.

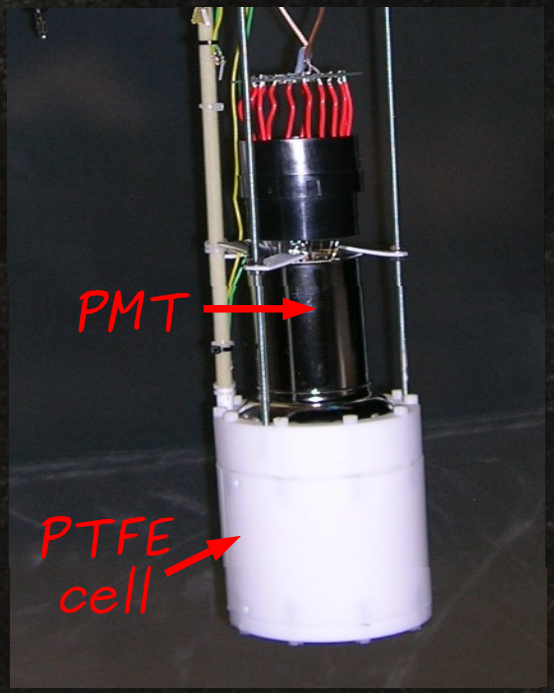

- ✔ PMT signal acquired with a fast Waveform Recorder with 1 ns sampling time over a full record length of 15 μs;
- ✔ The detector is exposed to a ^{241}Am source – monochromatic γ-emission E_γ=59.54 keV;

Single PMT test: Light Yield measurement

^{241}Am γ energy spectrum (bkg sub.)

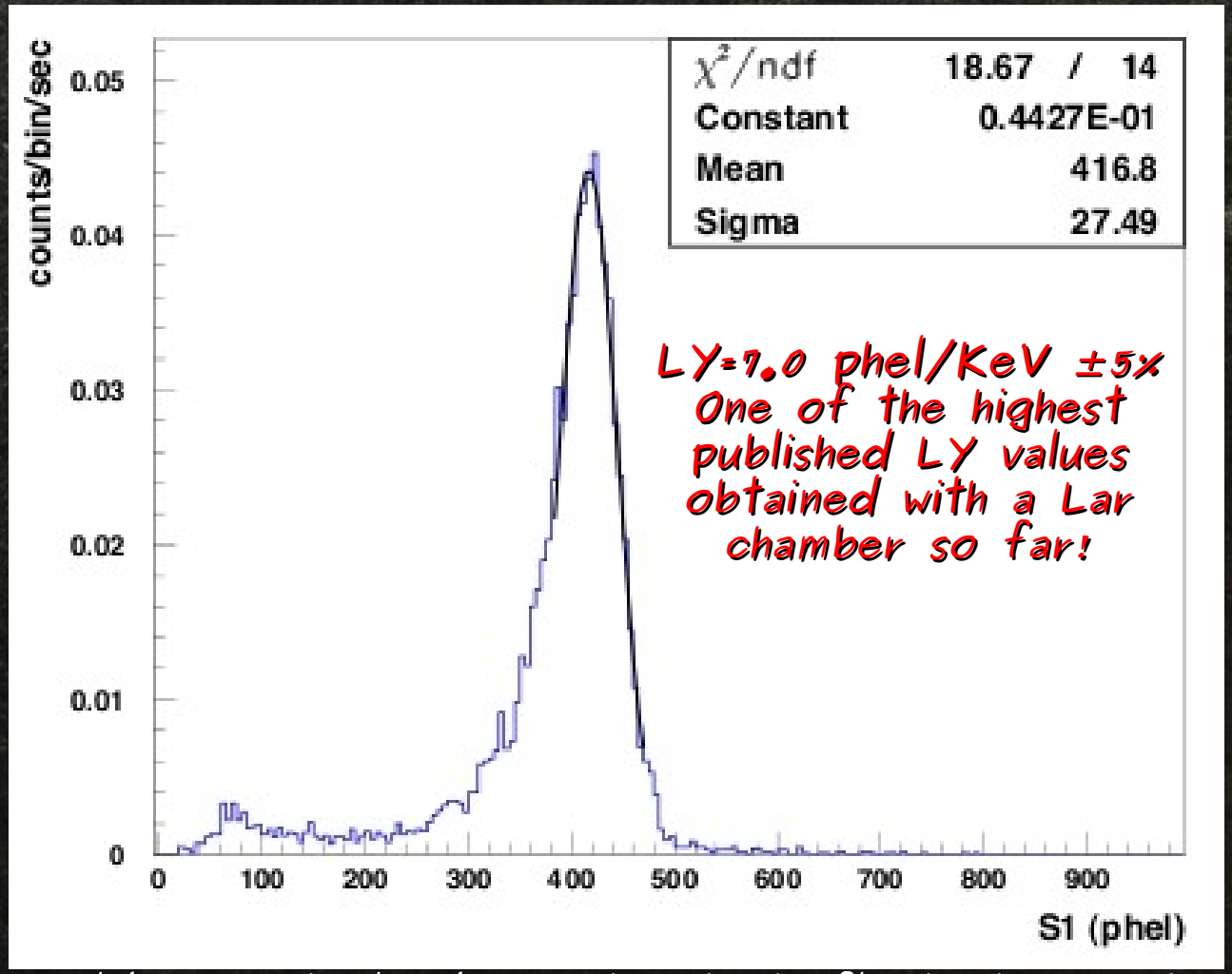

LY=7.0 phel/KeV ±5%
One of the highest published LY values obtained with a Lar chamber so far!

- ✔ Light Yield very stable during the test: fluctuations within ±1.5%.
- ✔ Test repeated after few weeks. LY result fully confirmed.

Two PMTs test: ETL vs Hamamatsu

- The second test (mid 2010) aims to the direct comparison of two tipes of PMTs: 3" HQE Hamamatsu R11065 (same used before) and 3" ETL-D750 (pre-production series of the PMTs for WArP 100 lt experiment).

- LAr volume viewed simultaneously by the two PMT. This allows for comparison of the light outputs independently from actual detector conditions.

- Detector is a PTFE cell of about 0.4 lt internal volume (h=8 cm and Ø=7.6 cm) lined with TPB coated reflector layer on lateral walls.

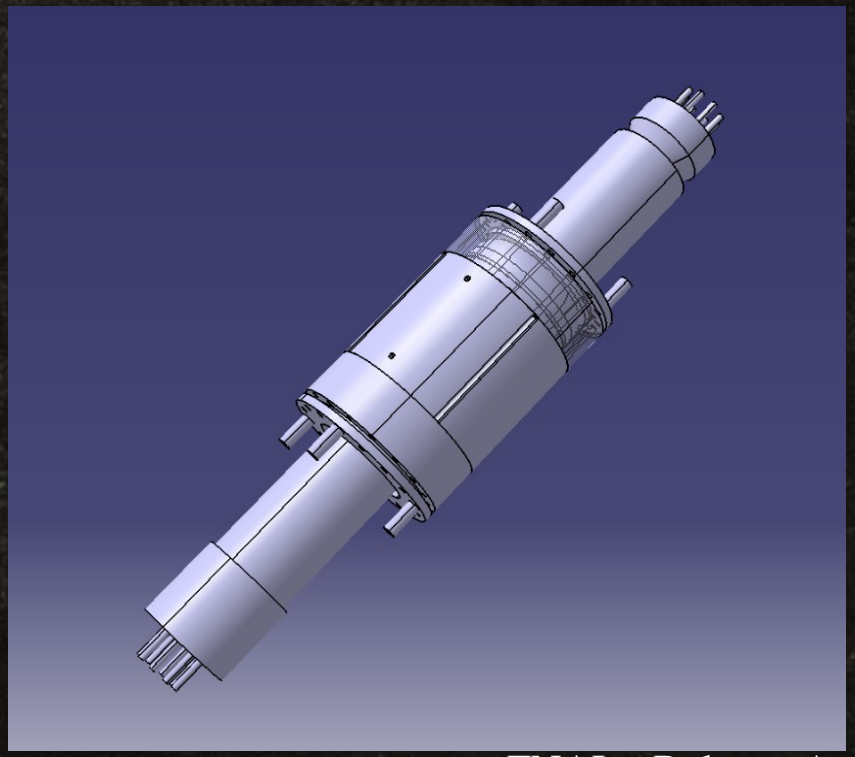

- Signals from each PMT are directly recorded by the 8-bit Fast Waveform Digitizer Acqiris board (DP235) @ 1 GHz over 15μs window time.

- Data analysis is the same as for the single PMT test.

ETL vs Hamamatsu: Light Yield

LY values are determined by exposure to the ^{241}Am γ source (E_γ=59.54 keV)

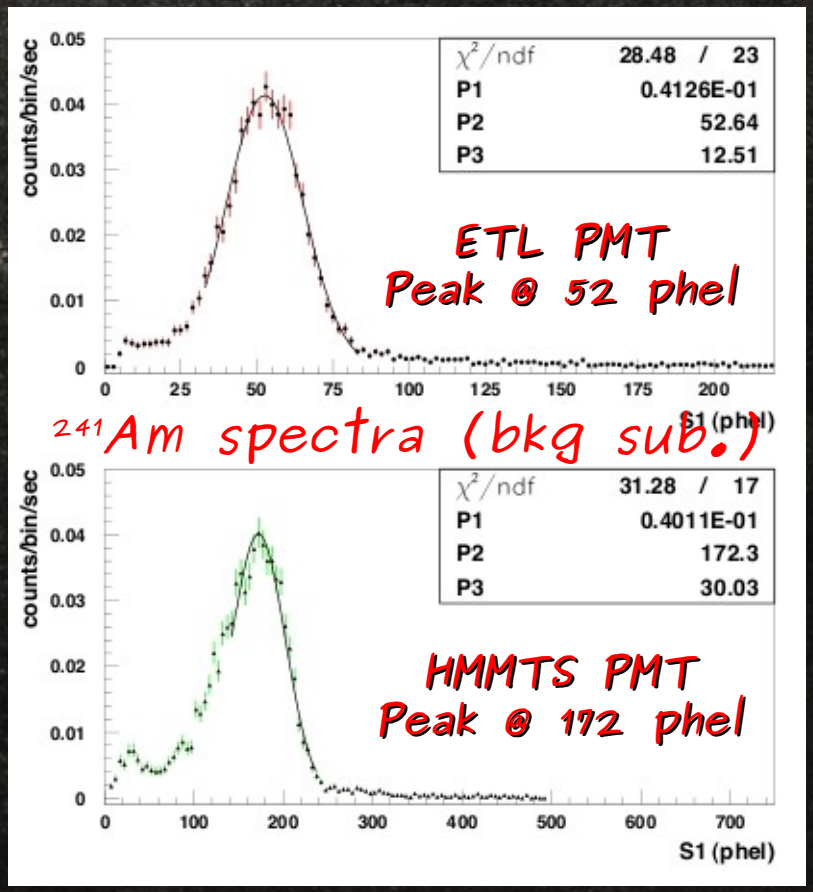

^{241}Am spectra (bkg sub.)

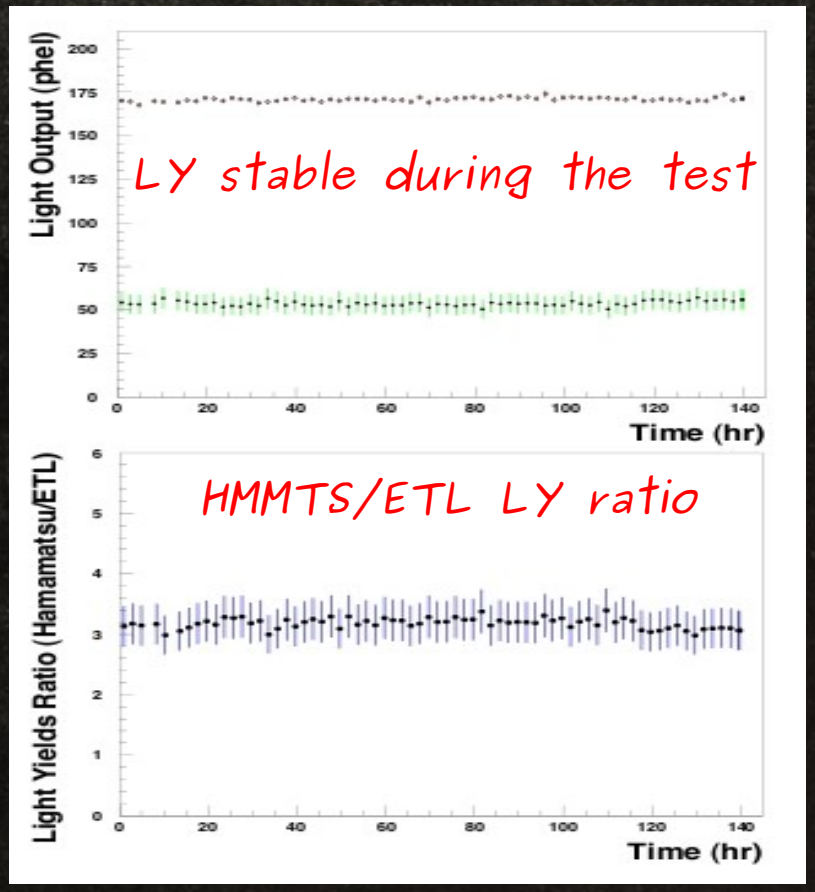

The Hamamatsu-to-ETL LY ratio found in the 3:1 range, consistent with the ratio of the Global Efficiency GE (GE=QE*CE, being CE the collection efficiency at the first dynode).

Four PMT test

- It is not generally obvious or easy to reproduce a LY result obtained with a small prototype in a bigger detector.
- Scaling up capability of the implemented technology has been tested with a detector about ten times bigger than the one with one PMT, a ~4.3 lt chamber equipped with 4 HMMS PMTs (~12% photocatodic coverage, as for the single PMT test).

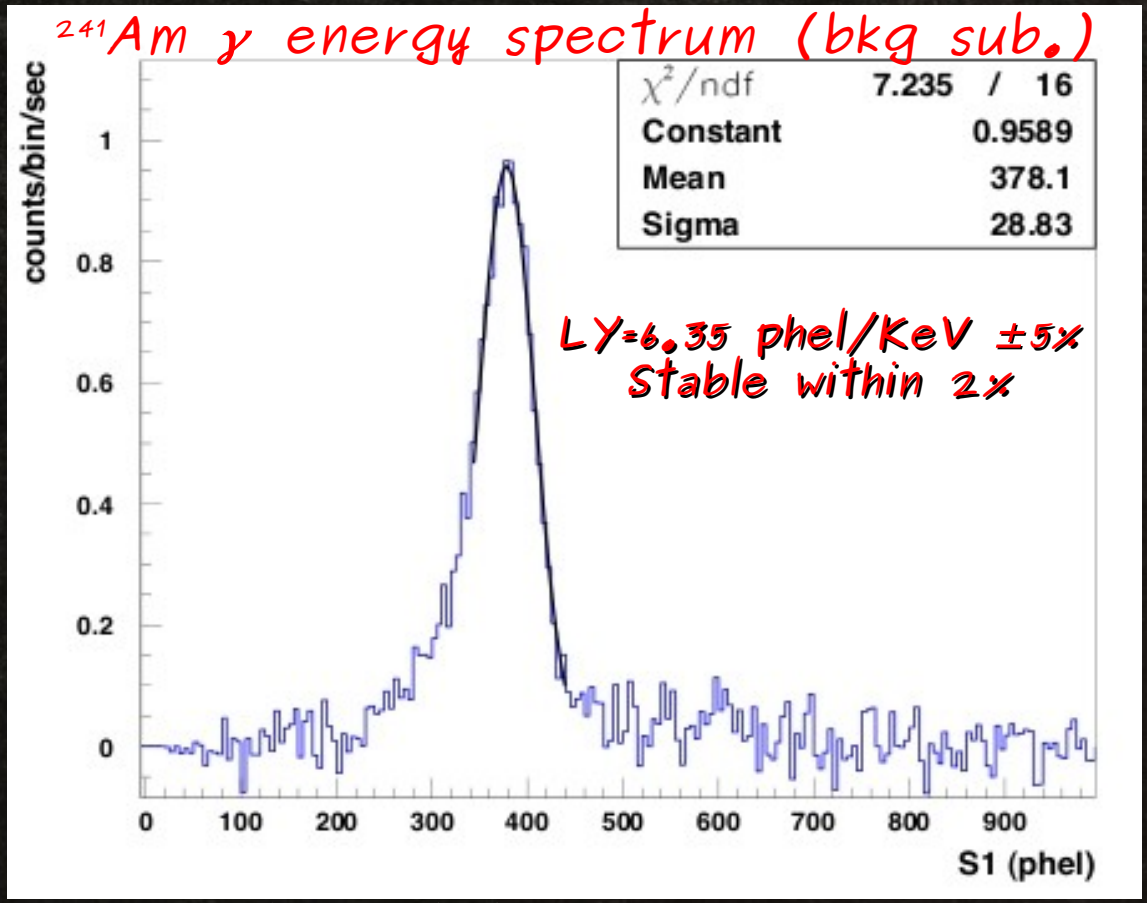

Four PMT test

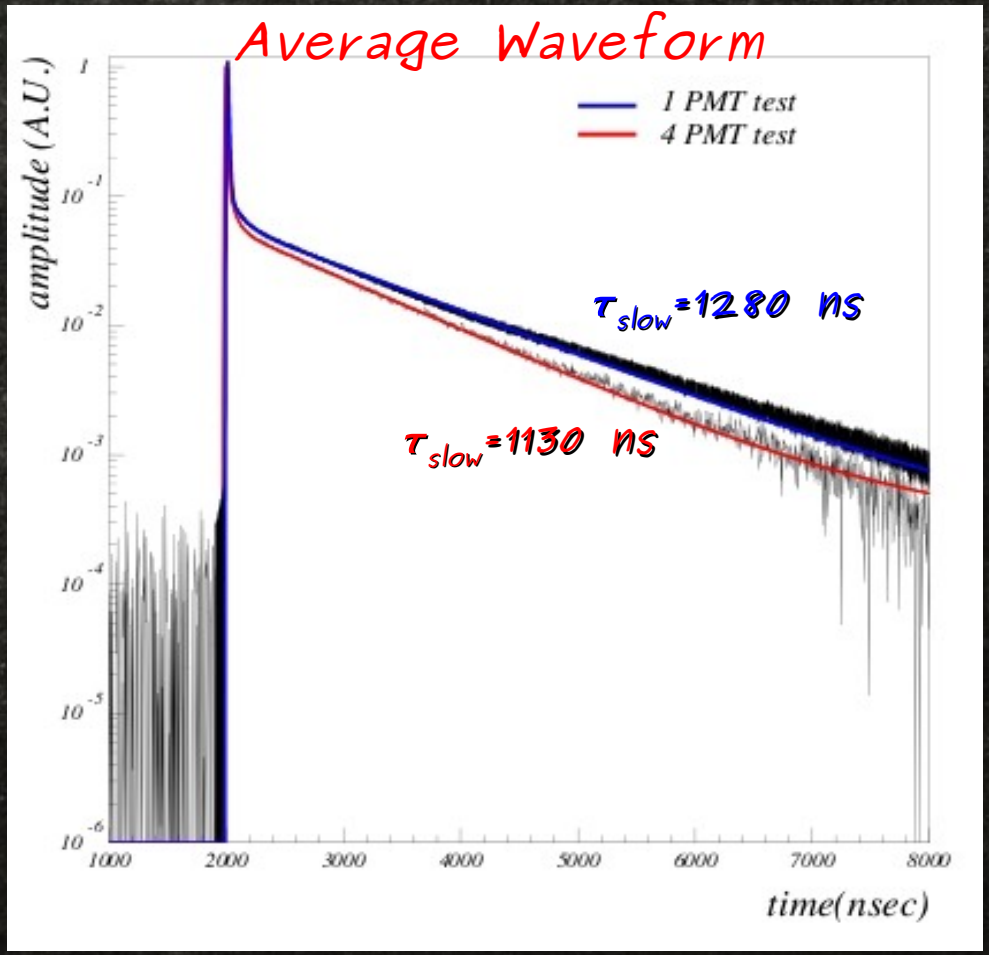

- ✔ τ_{slow}=1130 ns (1300 ns for clean argon). This implies a 10% reduction of the LY.
- ✔ Direct measurement with mass spectrometer showed the presence of ~1 ppm N_2 (not captured by our filters).

In the case of clean Argon LY would have been in the range of 7 phe/keV.

Detector geometry is a scaled-down version of WArP 100 lt detector (100 lt active volume, 37 PMTs, ~12% photocatodic coverage).

LY from this detector test can be assumed as predective of the LY from the WARP 100 lt inner detector, when operated under equivalent conditions.

Jinst

PUBLISHED BY IOP PUBLISHING FOR SISSA

RECEIVED: *October 18, 2011*
REVISED: *December 22, 2011*
ACCEPTED: *January 1, 2012*
PUBLISHED: *January 20, 2012*

Demonstration and comparison of photomultiplier tubes at liquid Argon temperature

R. Acciarri,[a] **M. Antonello,**[b] **F. Boffelli,**[c] **M. Cambiaghi,**[c] **N. Canci,**[b] **F. Cavanna,**[a,1] **A.G. Cocco,**[d] **N. Deniskina,**[d] **F. Di Pompeo,**[a,b,2] **G. Fiorillo,**[e] **C. Galbiati,**[f] **L. Grandi,**[f] **P. Kryczynski,**[g] **G. Meng,**[h] **C. Montanari,**[i] **O. Palamara,**[b,1] **L. Pandola,**[b] **F. Perfetto,**[e] **G.B. Piano Mortari,**[a] **F. Pietropaolo,**[h] **G.L. Raselli,**[i] **C. Rubbia,**[b] **E. Segreto,**[b,3] **A.M. Szelc,**[g,a,1] **A. Triossi,**[j] **S. Ventura,**[h] **C. Vignoli**[b] **and A. Zani**[c]

[a] *Università dell'Aquila e INFN, L'Aquila, Italy*
[b] *INFN - Laboratori Nazionali del Gran Sasso, Assergi, Italy*
[c] *Università di Pavia e INFN, Pavia, Italy*
[d] *INFN - Sezione di Napoli, Napoli, Italy*
[e] *Università di Napoli e INFN, Napoli, Italy*
[f] *Princeton University, Princeton, New Jersey, U.S.A.*
[g] *APC, PAN, Kraków, Poland*
[h] *INFN - Sezione di Padova, Padova, Italy*
[i] *INFN - Sezione di Pavia, Pavia, Italy*
[j] *INFN - Laboratori Nazionali di Legnaro, Legnaro, Italy*

E-mail: ettore.segreto@lngs.infn.it

ABSTRACT: Liquified noble gases are widely used as target in present Dark Matter searches. Signals from scintillation in the liquid, following energy deposition from the recoil nuclei scattered by Dark Matter particles (e.g. WIMPs), should be recorded down to very low energies by photosensors suitably designed to operate at cryogenic temperatures. Liquid Argon based detectors for Dark Matter searches currently implement photomultiplier tubes for signal readout. In the last few years PMTs with photocathodes operating down to liquid Argon temperatures (87 K) have been specially developed with increasing Quantum Efficiency characteristics. The most recent of these, Hamamatsu Photonics K.K. Mod. R11065 with peak QE up to about 35%, has been extensively tested within the R&D program of the WArP Collaboration. During these tests the Hamamatsu PMTs showed excellent performance and allowed obtaining a light yield around 7 *phel*/keV$_{ee}$ in a Liquid Argon detector with a photocathodic coverage in the 12% range, sufficient for detection of

[1] Currently at Yale University, New Haven, Connecticut, U.S.A.
[2] Currently at ITAB, Chieti, Italy.
[3] Corresponding author.

doi:10.1088/1748-0221/7/01/P01016

2012 JINST 7 P01016

One of the highest Published LY values obtained with LAr chambers so far!

and that's not all...

✔ Along with my work on PSD and light collection optimization, as member of the WArP collaboration I took part to several runs of the WArP 2.3 lt detector (detector mounting, data taking).

✔ I took part to underground runs of the WarP 100 lt detector (production and test of TPB films for inner and veto detector, data taking) as well.

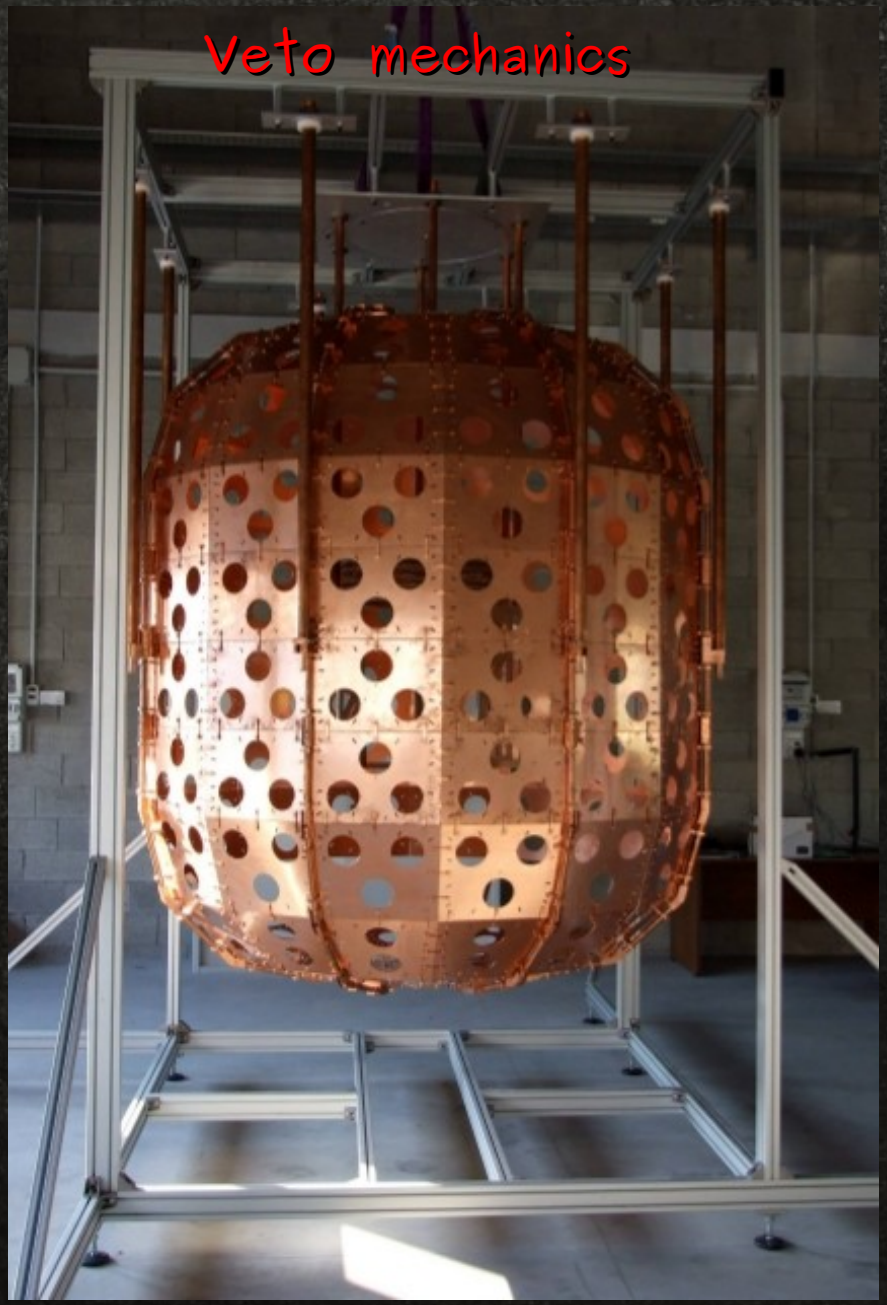
Veto mechanics


Detector mechanics


Veto structure after TPB evaporation

and that's not all...

I also took part to the physics underground run @ LNGS (data taking, event visual scan) that produced the publication of the first world results from a Dark Matter search with a LAr detector.

Available online at www.sciencedirect.com
ScienceDirect
Astroparticle Physics 28 (2008) 495–507
ELSEVIER
Astroparticle Physics
www.elsevier.com/locate/astropart

First results from a dark matter search with liquid argon at 87 K in the Gran Sasso underground laboratory

WARP Collaboration
P. Benetti [a], R. Acciarri [f], F. Adamo [b], B. Baibussinov [g], M. Baldo-Ceolin [g], M. Belluco [a], F. Calaprice [d], E. Calligarich [a], M. Cambiaghi [a], F. Carbonara [b], F. Cavanna [f], S. Centro [g], A.G. Cocco [b], F. Di Pompeo [f], N. Ferrari [c,✠], G. Fiorillo [b], C. Galbiati [d], V. Gallo [b], L. Grandi [a], A. Ianni [c], G. Mangano [b], G. Meng [g], C. Montanari [a], O. Palamara [c], L. Pandola [c], F. Pietropaolo [g], G.L. Raselli [a], M. Rossella [a], C. Rubbia [a,*], A.M. Szelc [e], S. Ventura [g], C. Vignoli [a]

[a] *Dipartimento di Fisica Nucleare e Teorica, INFN and University of Pavia, Italy*
[b] *Dipartimento di Scienze Fisiche, INFN and University Federico II, Napoli, Italy*
[c] *Laboratori Nazionali del Gran Sasso dell'INFN, Assergi (AQ), Italy*
[d] *Department of Physics, Princeton University, Princeton, NJ, USA*
[e] *Instytut Fizyki Jadrowej PAN, Krakow, Poland*
[f] *Dipartimento di Fisica, INFN and University of L'Aquila, Italy*
[g] *Dipartimento di Fisica, INFN and University of Padova, Italy*

Received 18 January 2007; received in revised form 17 May 2007; accepted 3 August 2007
Available online 17 August 2007

Abstract

A new method of searching for dark matter in the form of weakly interacting massive particles (WIMP) has been developed with the direct detection of the low energy nuclear recoils observed in a massive target (ultimately many tons) of ultra pure liquid argon at 87 K. A high selectivity for argon recoils is achieved by the simultaneous observation of both the VUV scintillation luminescence and of the electron signal surviving columnar recombination, extracted through the liquid–gas boundary by an electric field.

First physics results from this method are reported, based on a small 2.3 l test chamber filled with natural argon and an accumulated fiducial exposure of about 100 kg day, supporting the future validity of this method with isotopically purified ^{40}Ar and for a much larger unit presently under construction with correspondingly increased sensitivities.

PACS: 95.35.+d; 29.40.Mc; 13.85.Dz; 14.80.−j

Keywords: Dark matter; WIMP; Liquid argon

Thank you

for your attention!!!

Backup Slides

T_{FP} Optimization

II Method

- Neutron and γ average waveforms are realised for different energy bins (12 bins from 50 phe to 350 phe).
- For every bin, the time T^{i}_{max} at which the difference between the integrated average neutron and γ waveform reaches its maximum is determined.

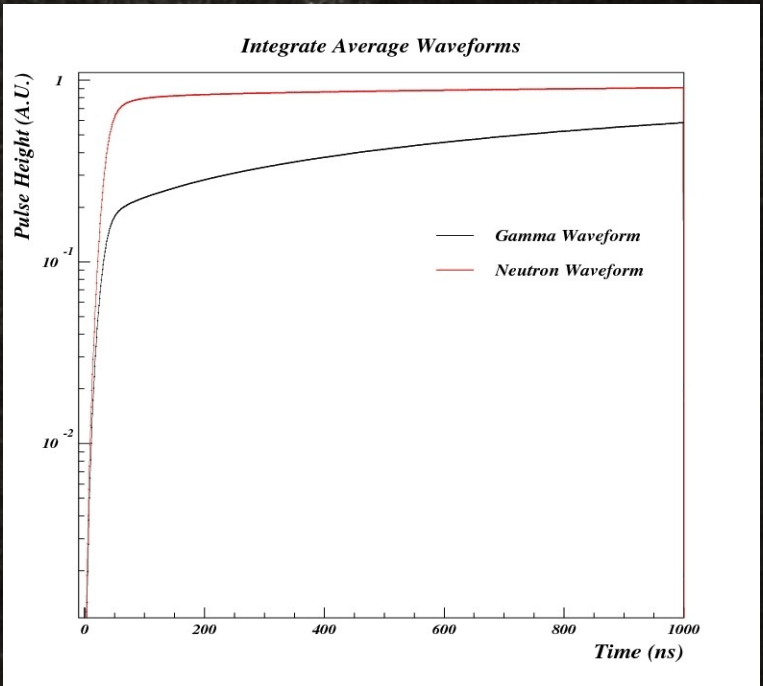

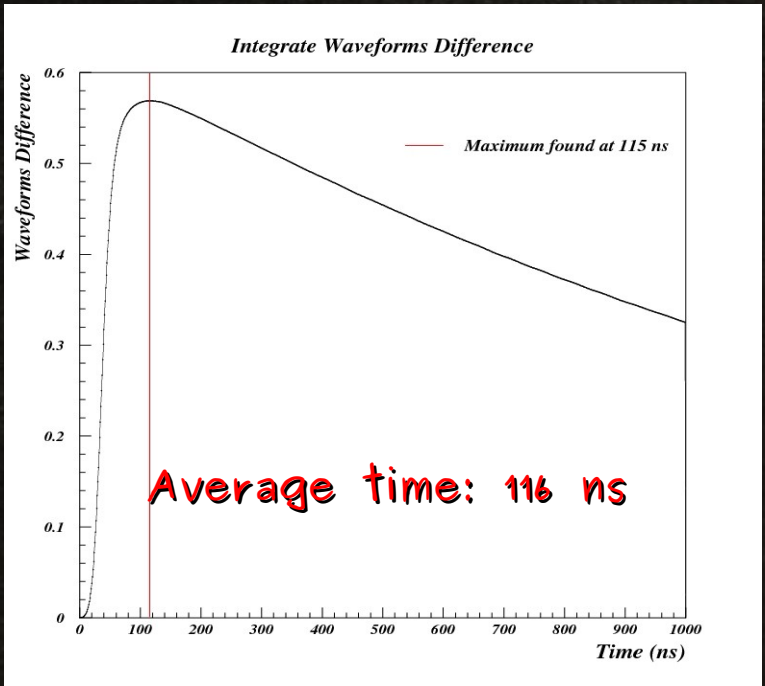

Optimum T_{fp}=120 ns

F-Prompt: results

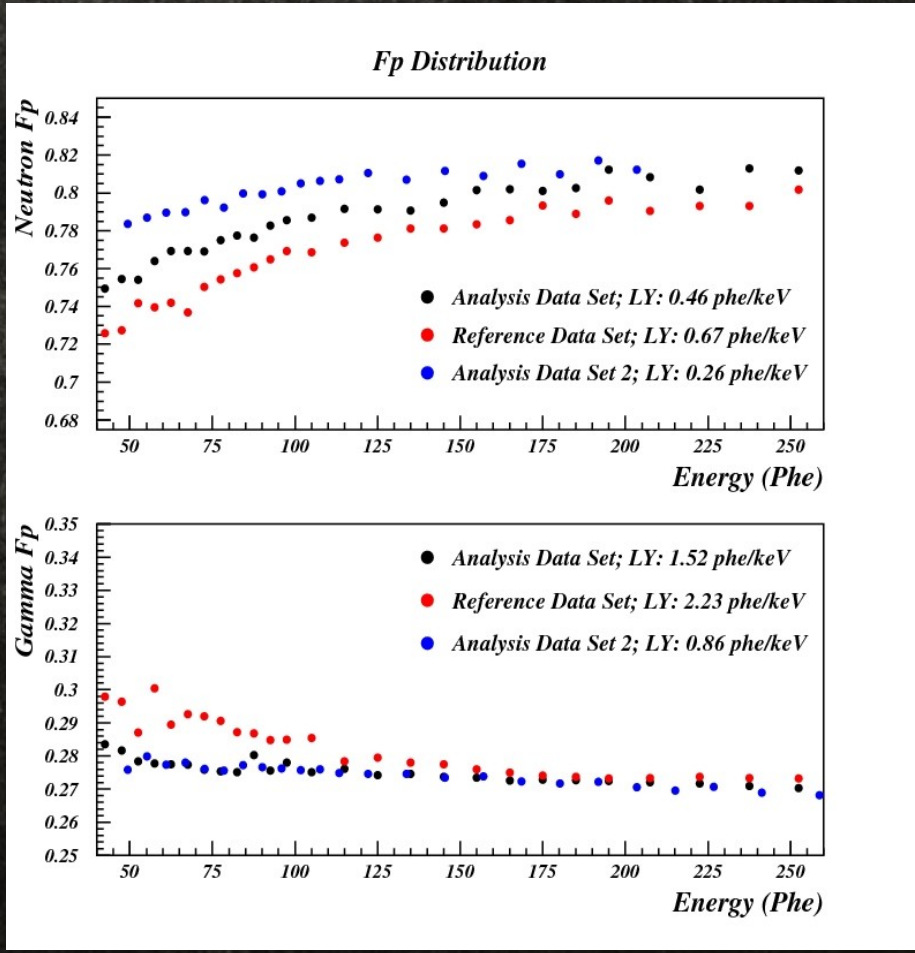

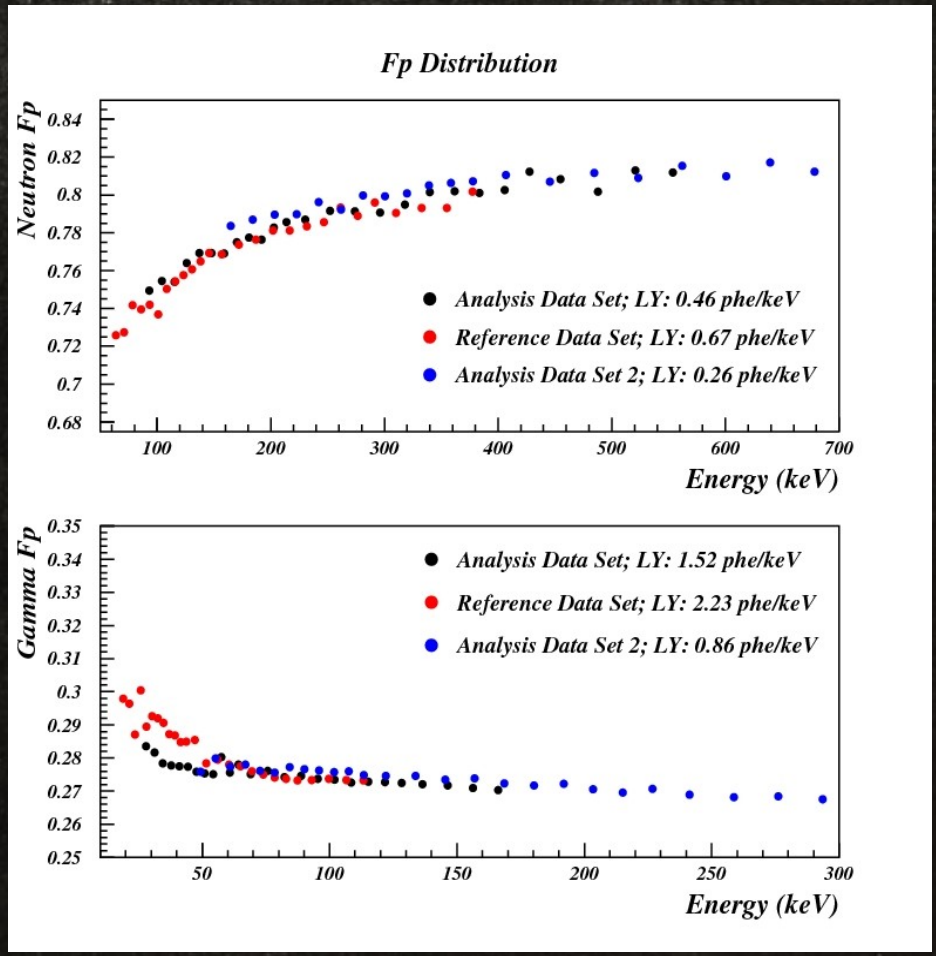

Average Time

$$\tilde{T} = \frac{1}{N_{phe}} \sum_{i=1}^{N_{phe}} t_i \quad \Rightarrow \quad AvT = 1 - \frac{\tilde{T}}{T_{ref}}$$

T_{ref} scale factor

$0 < AvT < 1$

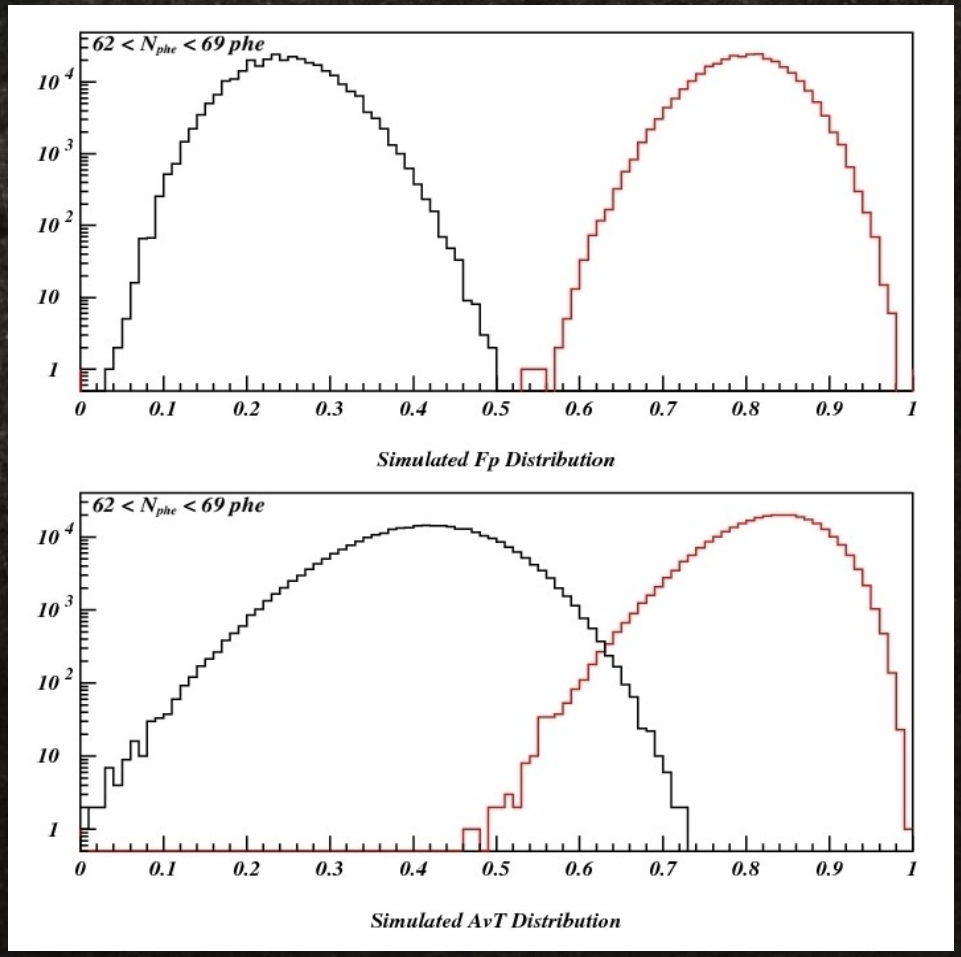

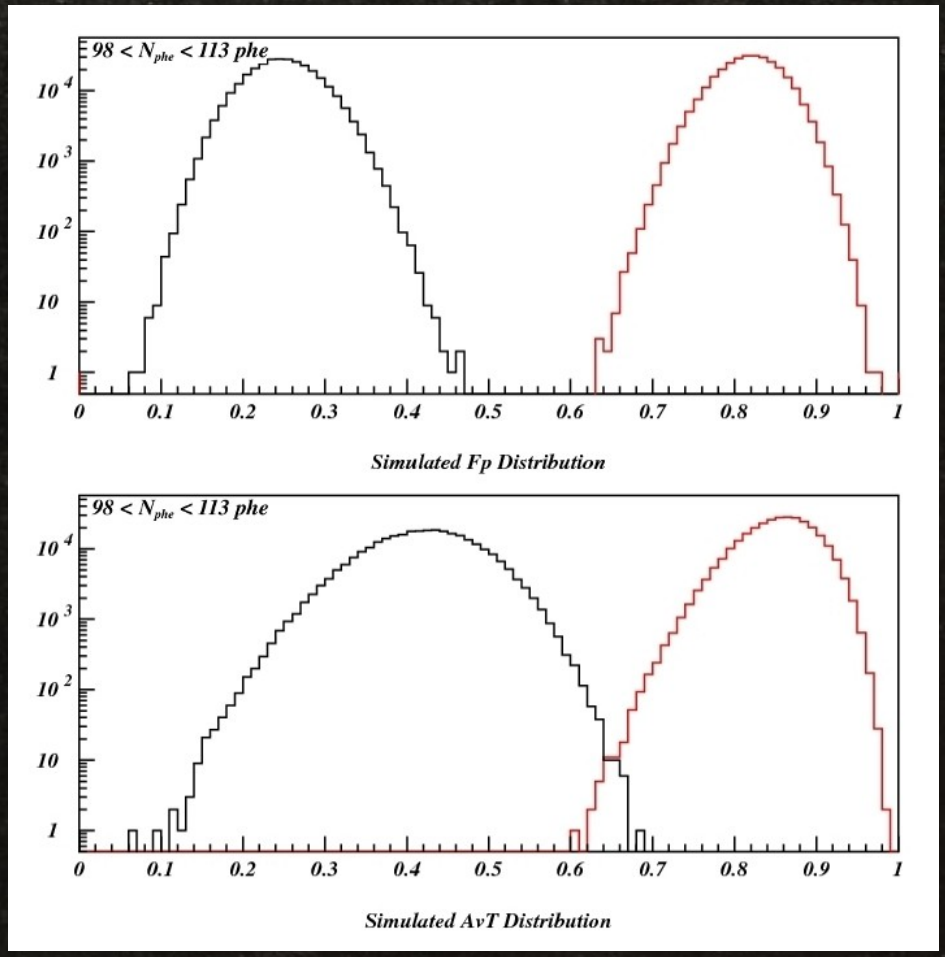

Average Time

$$\tilde{T} = \frac{1}{N_{phe}} \sum_{i=1}^{N_{phe}} t_i \quad \Rightarrow \quad AvT = 1 - \frac{\tilde{T}}{T_{ref}}$$

T_{ref} scale factor

$0 < AvT < 1$

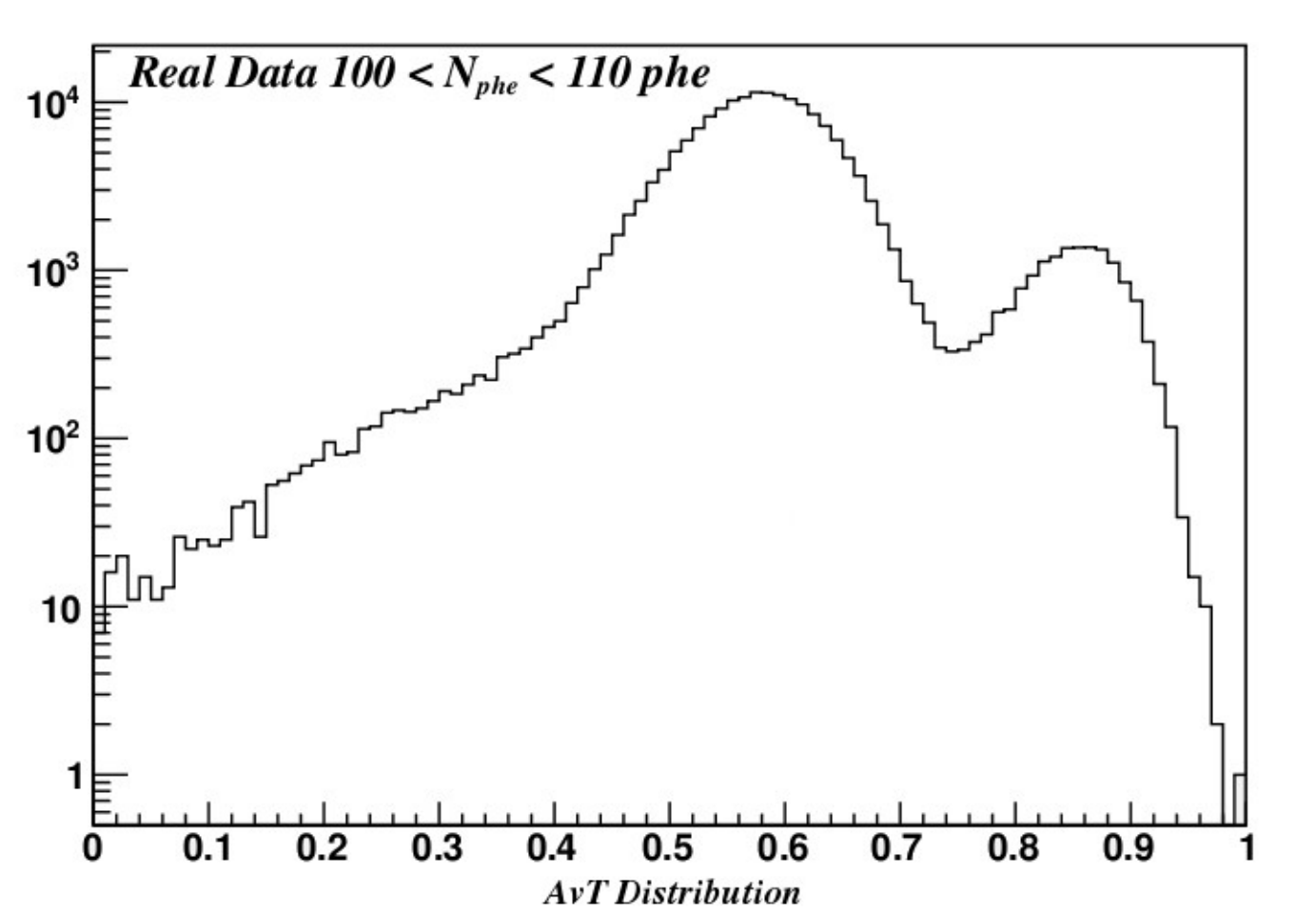

Multibin Method

- Both average waveforms and data set are organised in a K x L matrix, where L is data division in energy bins, while k is the time division of bot data waveforms and average wavaforms.
- In the ideal case, given a total number of phe, the number of phe falling in a given time bin is a mutinomial variable. It is thus possible to assign an event either to the electron recoil or the nuclear recoil family on the basis of a multinomial statistics.
- Being $p_m(k,l)$ the number of phe detected in the k-th time bin for an event falling in the l-th energy bin, multinomial statistics for the electron recoil (lnY_e) and nuclear recoil (lnY_n) class will be given by:

$$lnY_e = N_{tot} \sum_{k=1}^{K} \sum_{l=1}^{L} \delta_{ll'} p_m(k,l) \, lnp_e(k,l') + const$$

$$lnY_n = N_{tot} \sum_{k=1}^{K} \sum_{l=1}^{L} \delta_{ll'} p_m(k,l) \, lnp_n(k,l') + const$$

N_{tot} total phe number

Multibin Method

Given lnY_e and lnY_n the multibin parameter is defined as:

$$M = \frac{1}{N_{tot}}(lnY_e - lnY_n)$$

- According to this definition, electron recoil events will have M>0, while nuclear recoil events will have M<0
- Applying the M parameter, a single neutron and gamma waveform can be considered for the whole dataset, as well as different waveforms at different energies, covering the whole energetic range. Both approaches have been adopted, resulting in the Total Multibin Method and Local Multibin Method, respectively.

Multibin Method

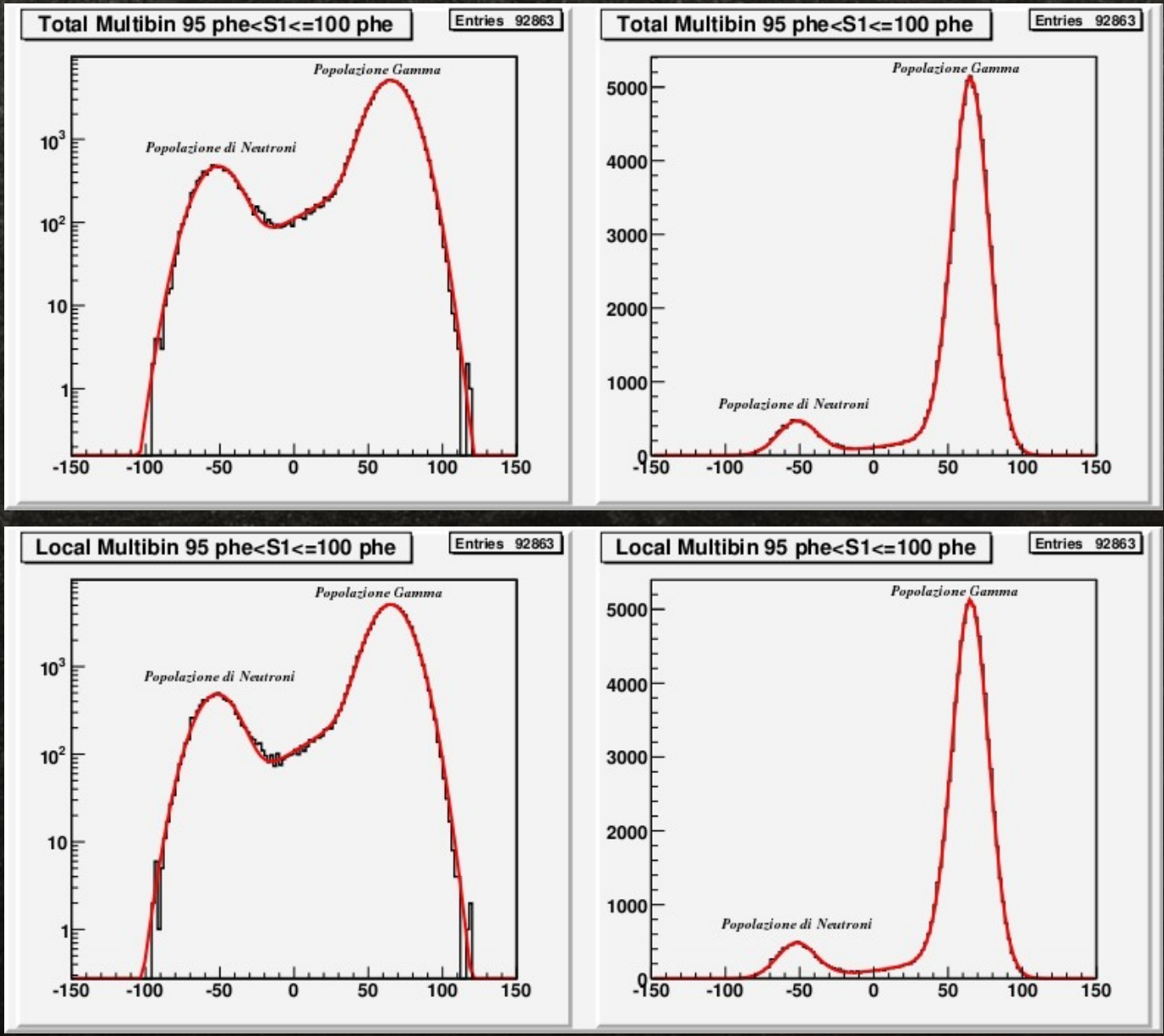

Multibin Method

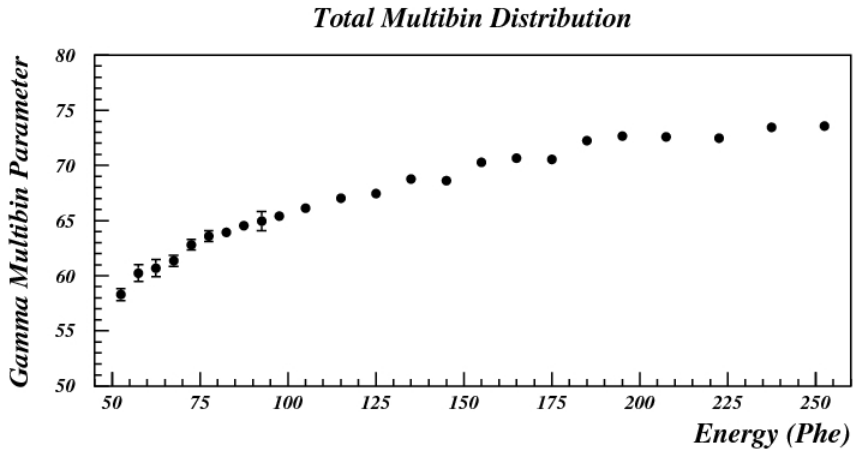

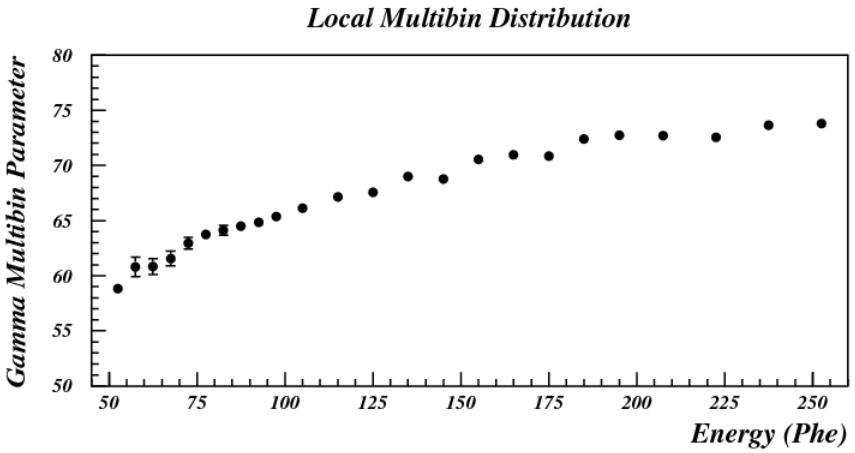

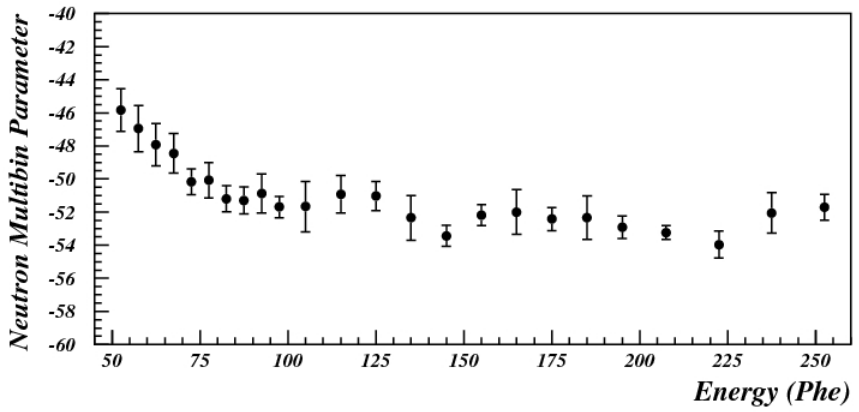

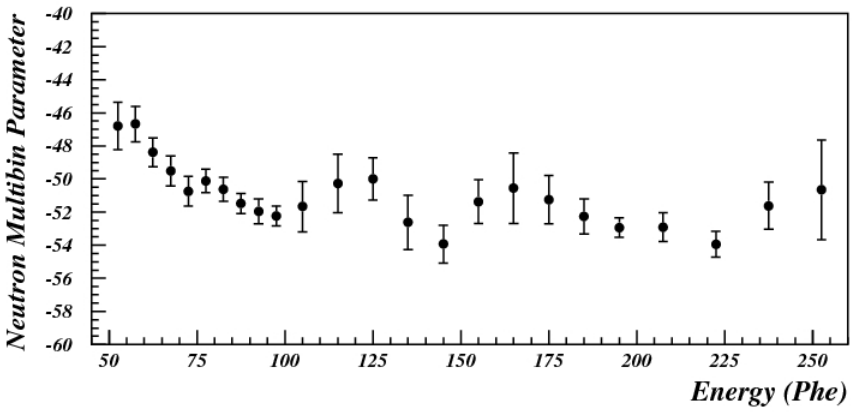

The Gatti Method

- For any given pulse S, it can be divided in short time intervals δt_i, being S_i the value of S at the time δt_i.

- Denoting with $\alpha(t)$ and $\beta(t)$ the average time function of the two particle types, the Gatti parameter G is defined as:

$$G = \sum_i P_i S_i$$

$$P_i = \frac{(\alpha_i - \beta_i)}{(\alpha_i + \beta_i)}$$

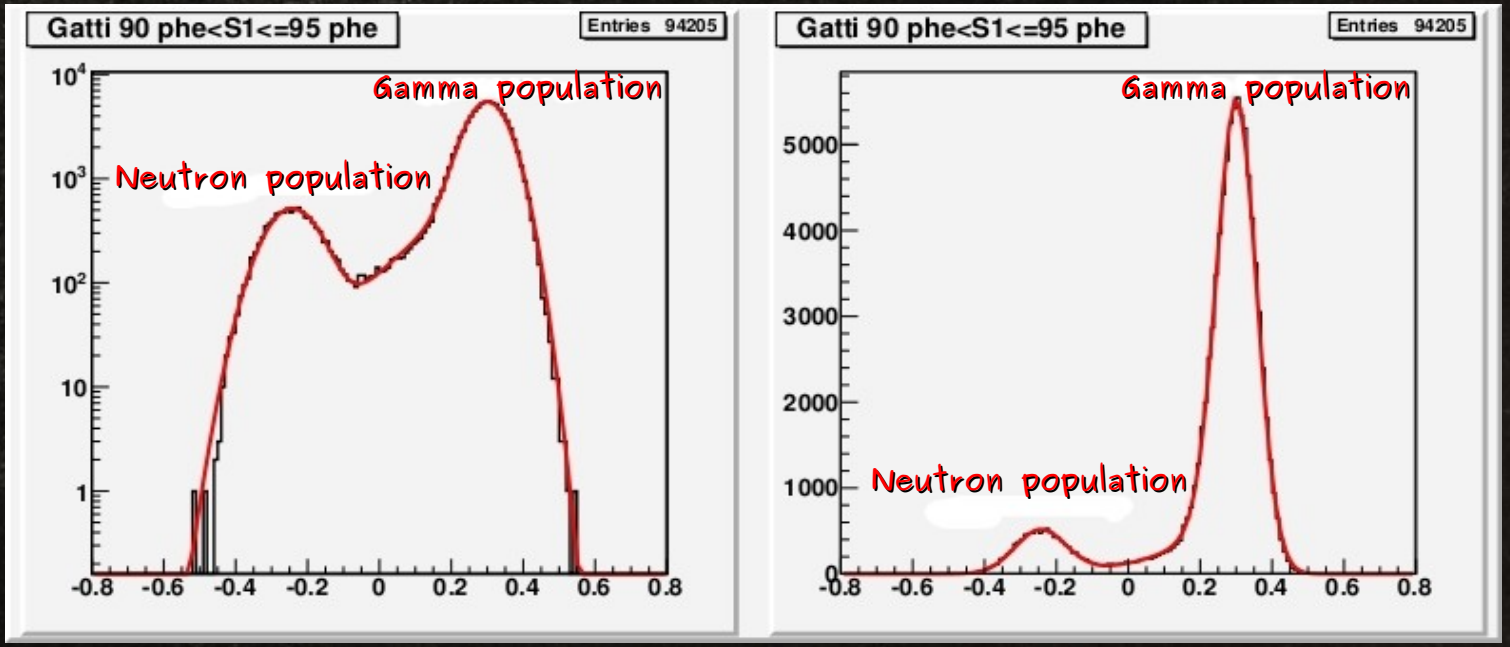

The Gatti Method

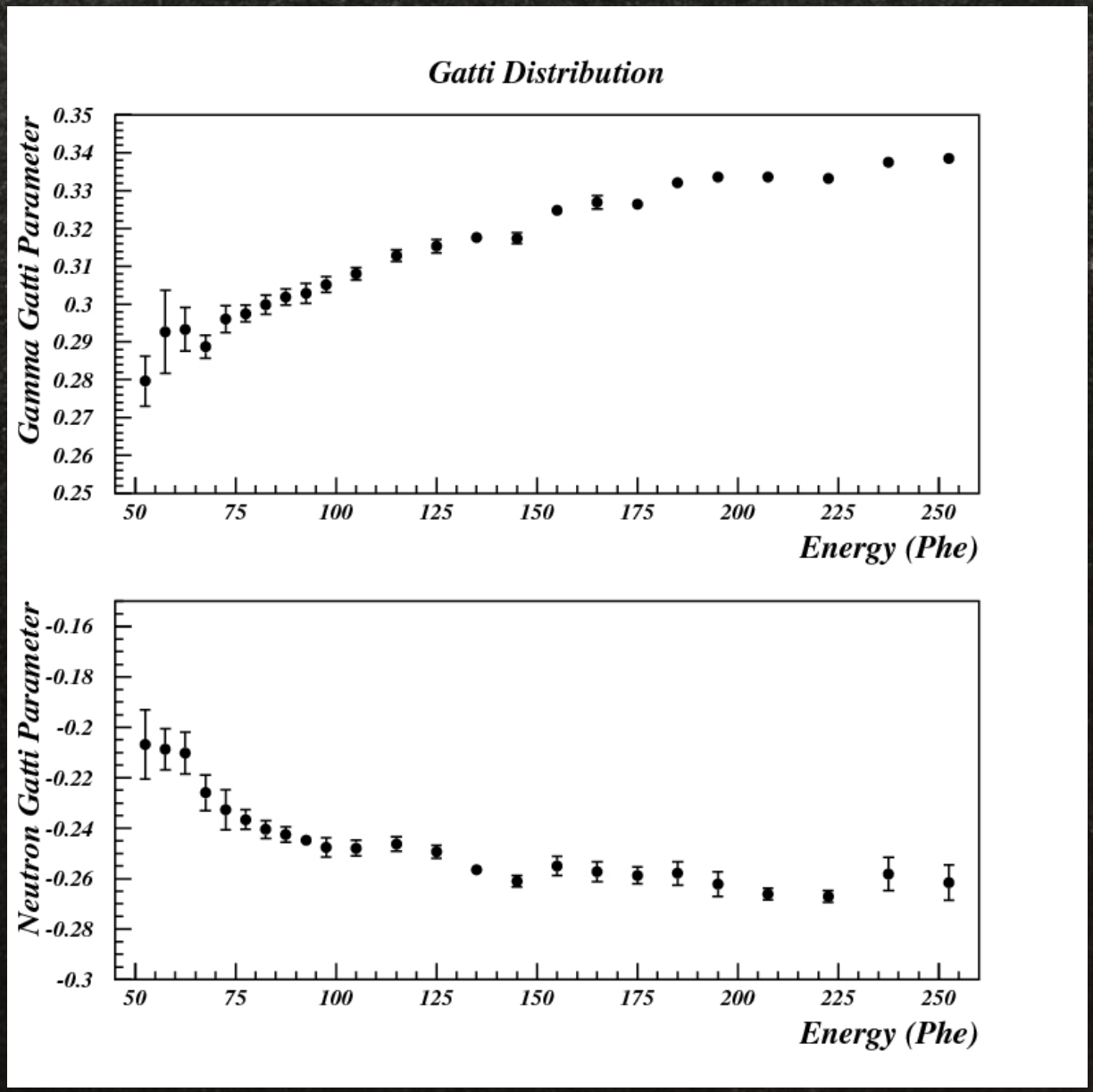

Comparison between PSD techniques

Two parameters have been adopted to compare discrimination powers of the proposed PSD techniques: *Electron Recoil Discrimination* (ERD) and *Nuclear Recoil Acceptance* (NRA).

ERD is defined as the fraction of non-neutron events (gamma + inelastic scattering events) discrimined once a nuclear recoil acceptance of 50% is set.

NRA is defined as that fraction of the neutron population exhibiting a contamination from gamma and intermediate events <1 in 10^3 events.

According to their definition ERD=99.9% when NRA=50%

Comparison between PSD techniques

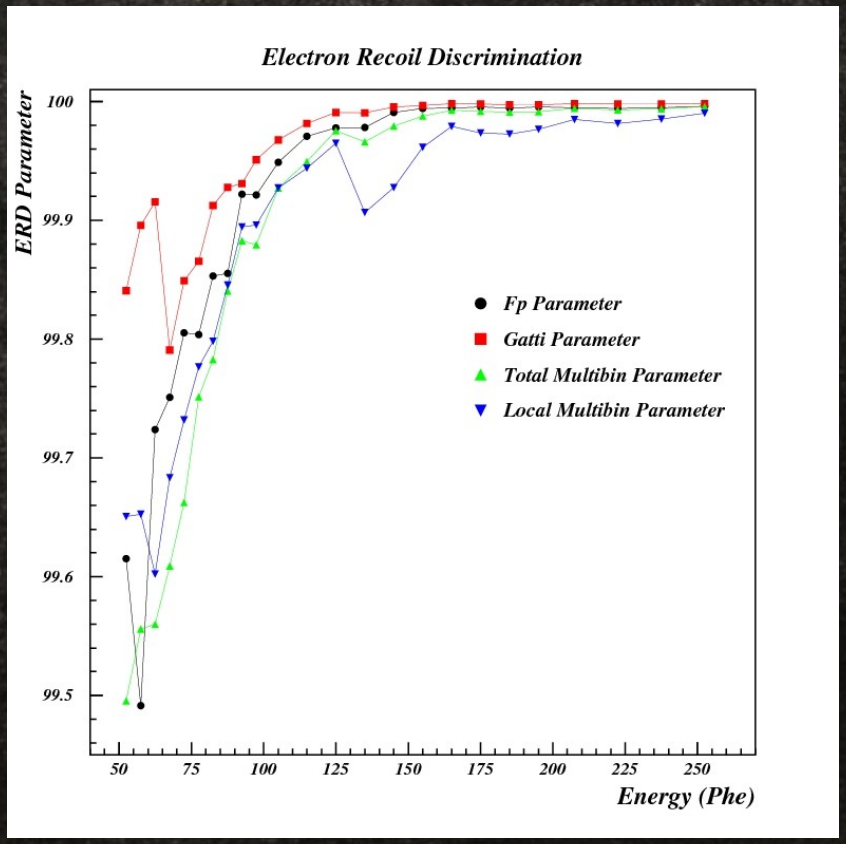

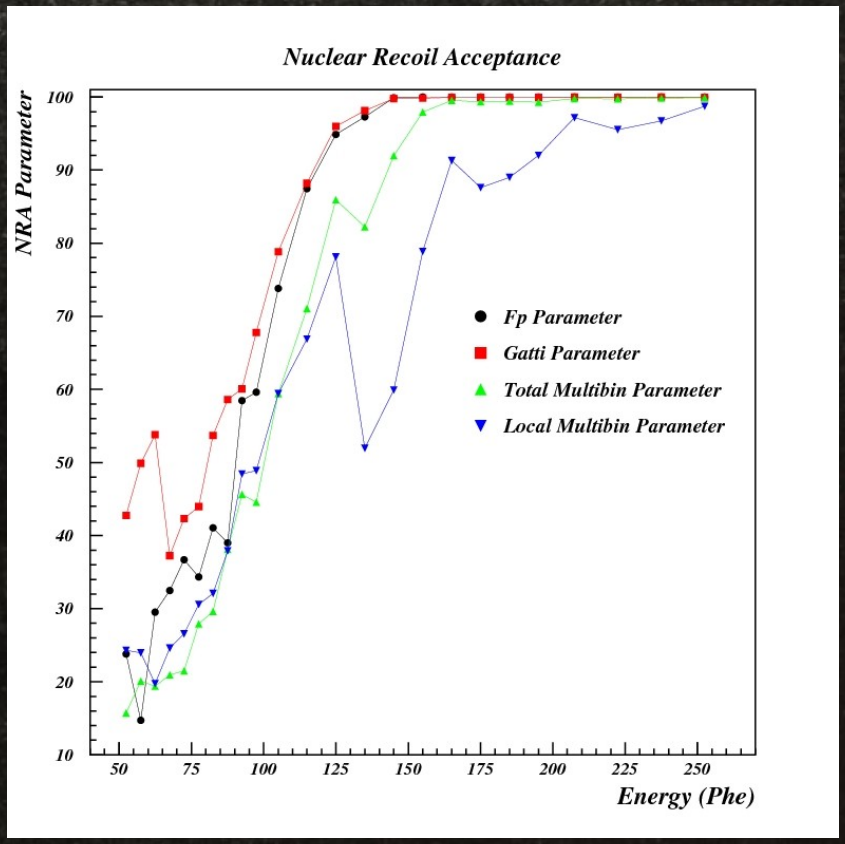

✔ Gatti method is the most powerful one, but troublesome to implement in a running analysis program (knowledge of average waveforms needed).

✔ Fp is slightly less efficient but fast and easy to implement.

Fp standard method for on-line discrimination and main analysis. Gatti more suitable for a final analysis.

F-Prompt: results

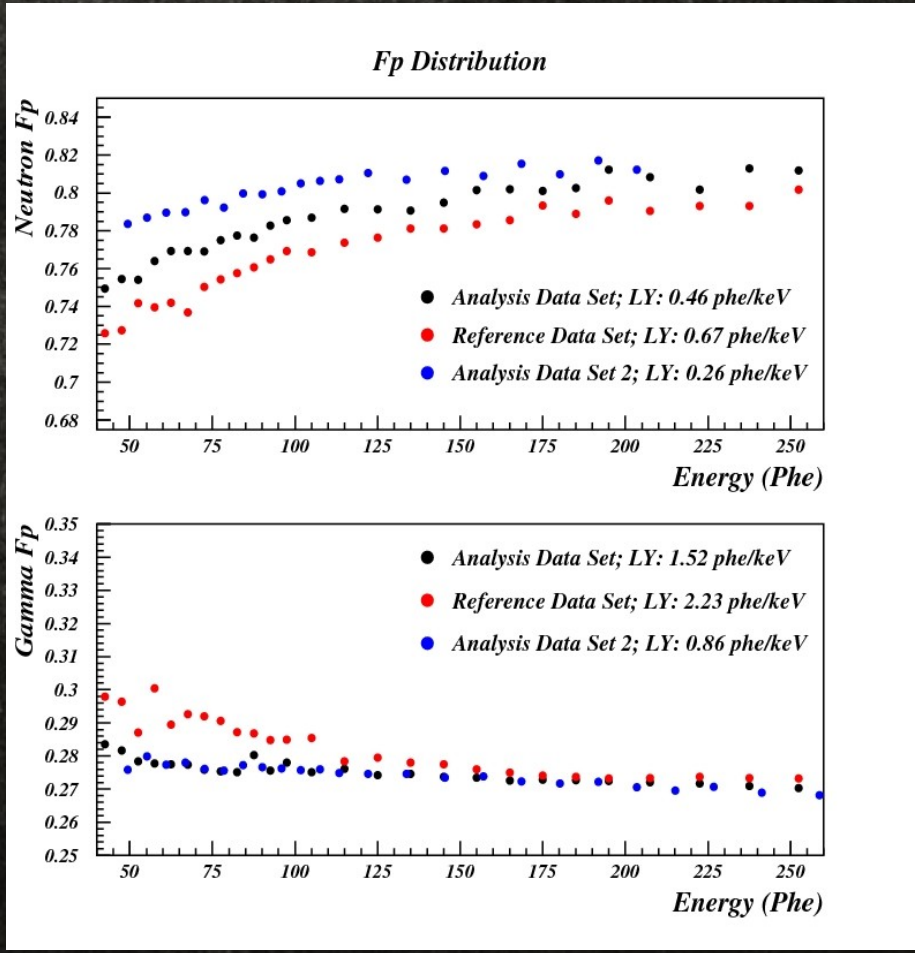

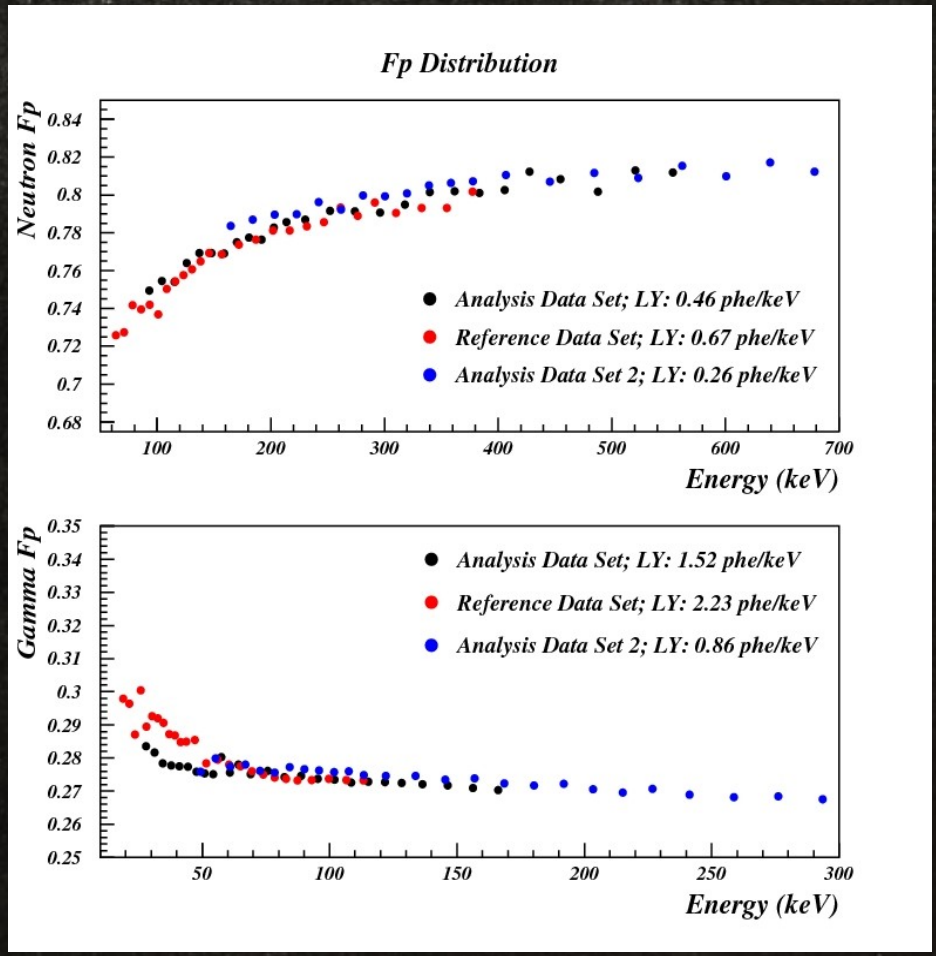

0.7 lt detector Data Acquisition

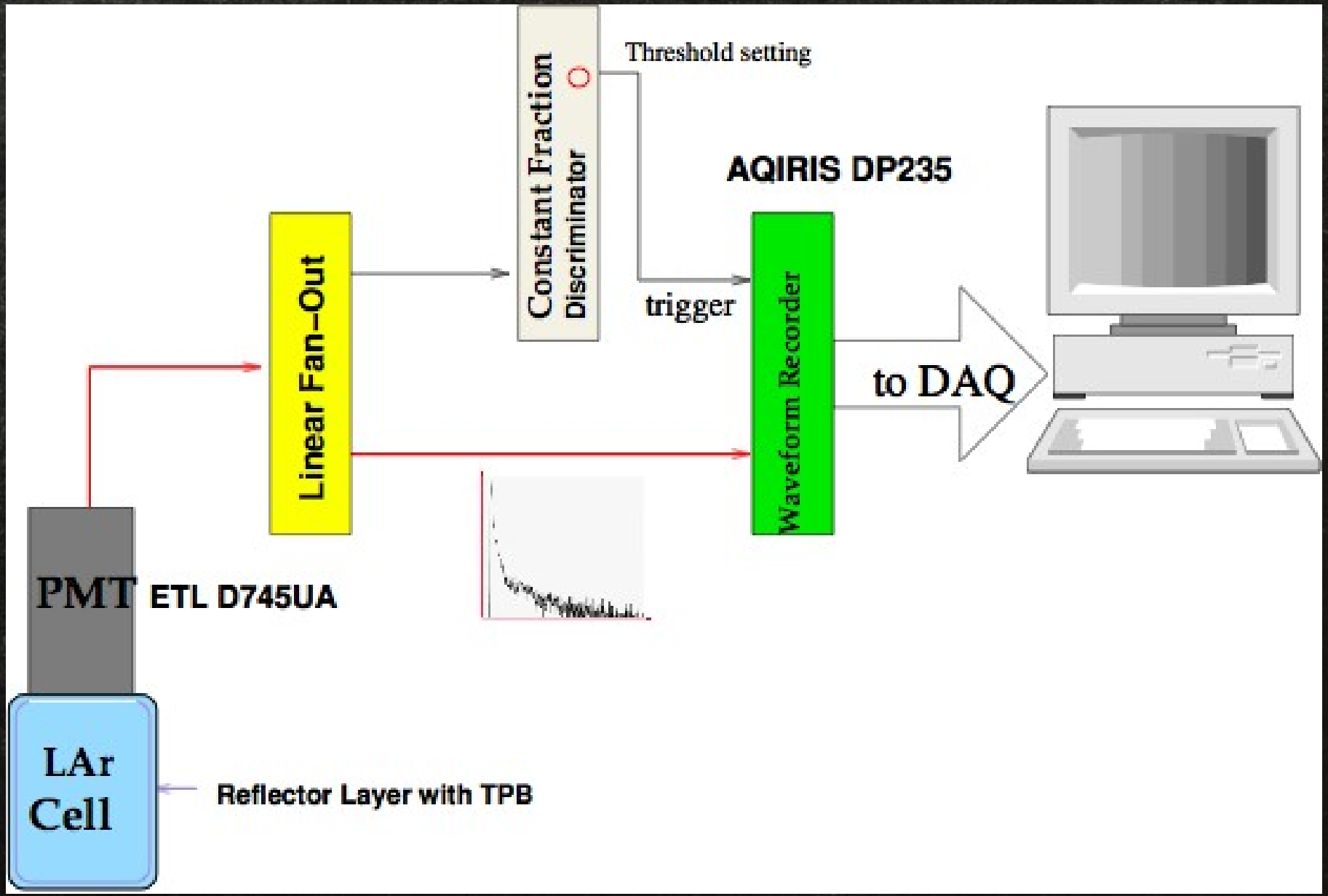

WArP 2.3 lt prototype

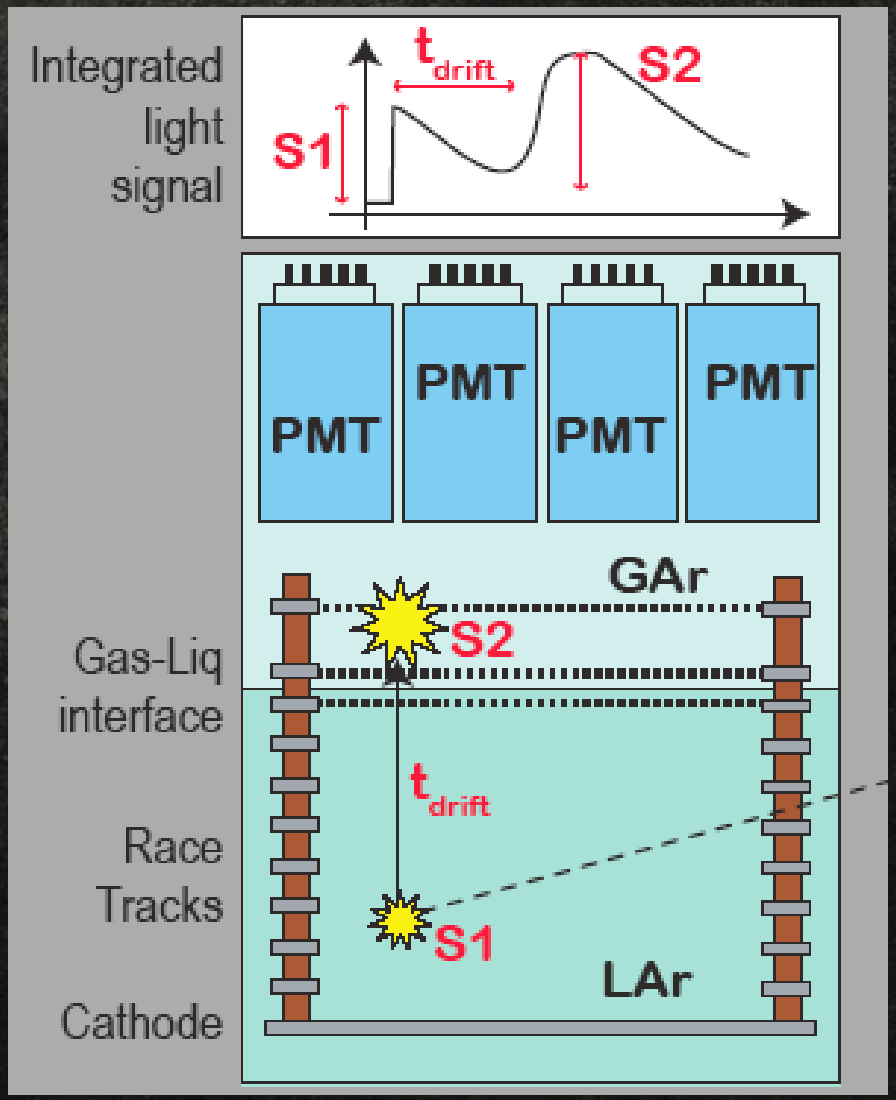

- Particle hits Ar atom, causing ionization and excitation.
- Partial recombination of electron–ion pairs produces scintillation S1 in LAr.
- Remaining electrons from ionization are drifted by the costant field to the gas–liquid interface.
- Electrons are extracted from liquid by E2 and accelerated in Gas to produce scintillation S2.
- Anode signal from each PMT is integrated (shaping time 120 μs) and sent to a 10 bit Flash ADC with 100 MHz sampling frequency.

Measurements with WarP prototype

By the means of WArP prototype it has been possible to describe the behaviour of the long-lived scintillation light lifetime determining the $[O_2]$ by the electron lifetime measurement.

Electronegative molecules, as O_2, reduce the full collection of free electrons:

$$e^- + O_2 \rightarrow O_2^-$$

if $[e^-] \ll [O_2] \Rightarrow [e^-]$ decreases in time as:

$$\frac{d[e^-]}{dt} = -k_e[O_2][e^-] \Rightarrow [e^-(t)] = [e^-(0)]e^{-\frac{1}{\tau_e}}$$

Electron Lifetime $\tau_e = \frac{1}{k_e[O_e]}$

the value of the rate constant k_e depends on drift field applied to the active LAr volume

$$k_e = 5.5 \cdot 10^{10}\, lt \cdot mol \cdot s^{-1} = 1.9\, ppm^{-1} \cdot \mu s^{-1} @ EF = 1\, kV \cdot cm^{-1}$$

O_2 contamination: measurement with WArP prototype

From WArP data is possible to determine both the absolute $[O_2]$ and the slow component decay time (τ_T) (determined by fitting the shape of background electron signals).

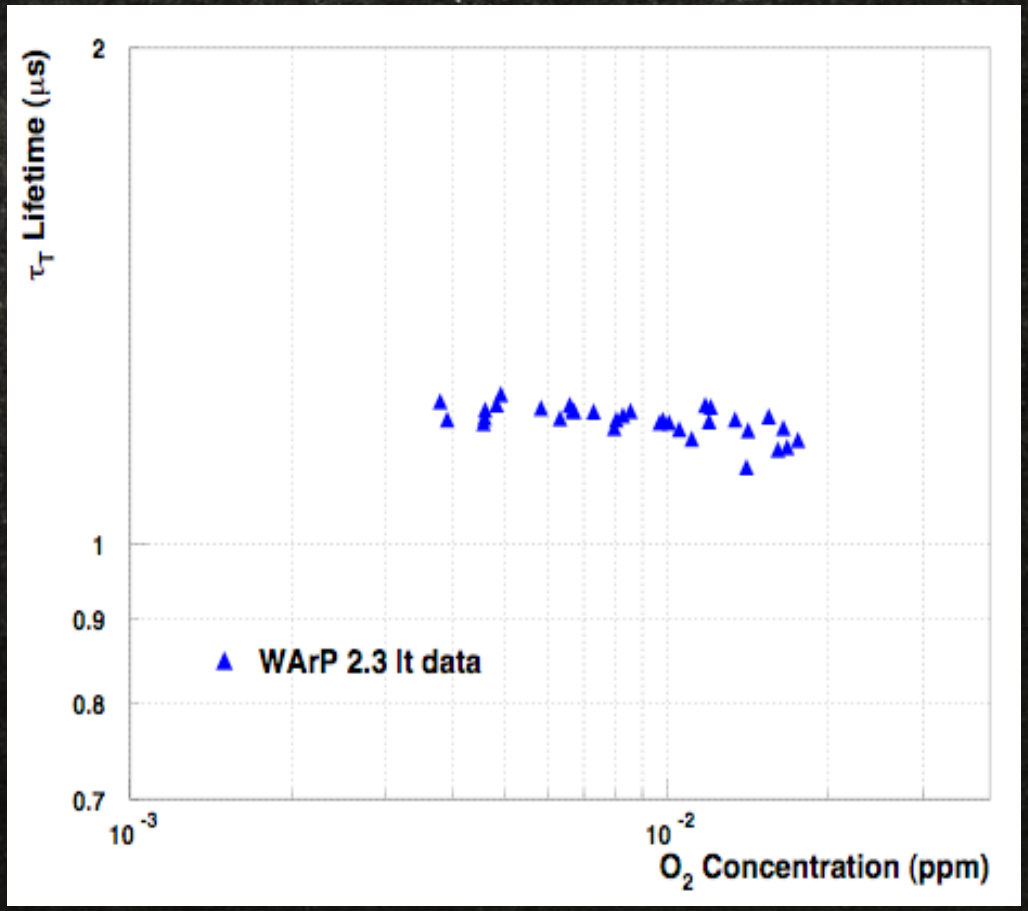

- Variation on $[O_2]$ is due to activation of the recirculation/purification system
- τ_T is almost constant in the range below ≈20 ppb

Scintillation emission is roughly unaffected by the quenching process at this low contamination

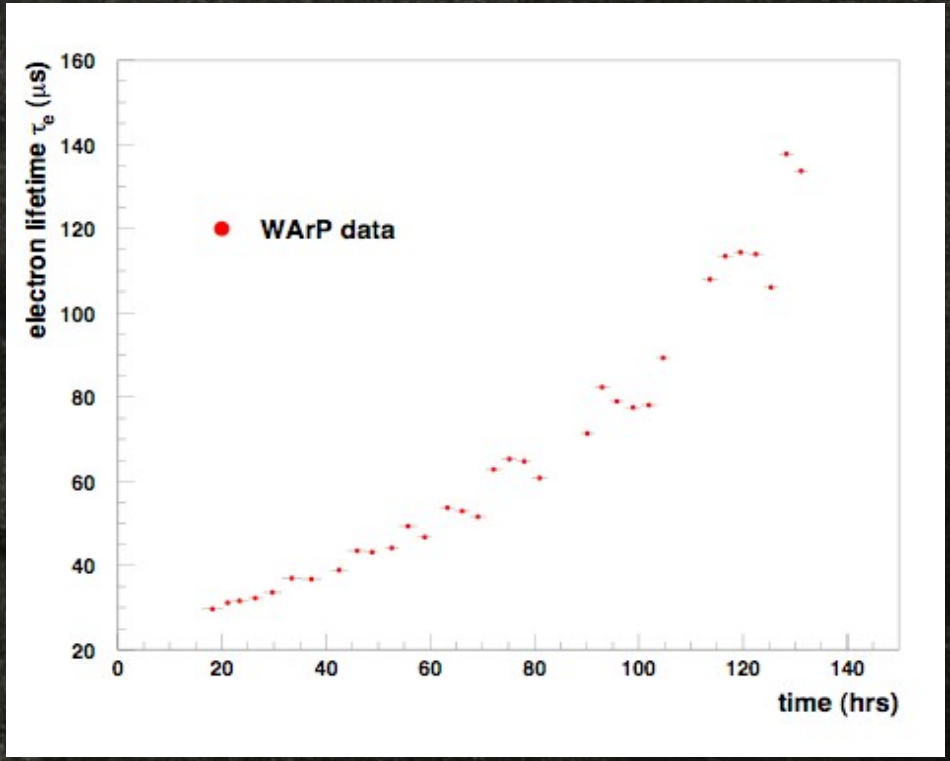

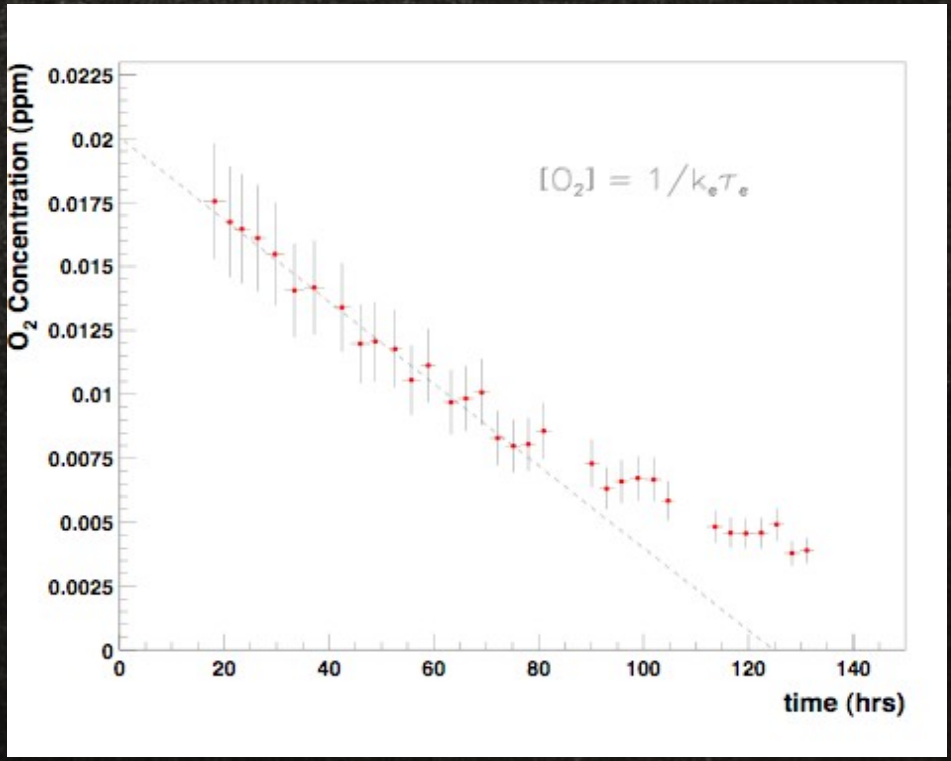

✔ τ_e increases up to the limit of sensitivity (≥ 200 μs) during measurement performed in successive time segments (of about 3 hrs each).

✔ Extrapolation of initial $[O_2]$ of the Ar in the detector up to 20 ppb (coming from O_2 content in Ar 6.0, outgassing materials and residual leaks).

Slow component decay time vs O_2 concentration: combined results

T_T, characterizing the scintillation signal shape in LAr, has been measured over a wide range of O_2 concentrations.

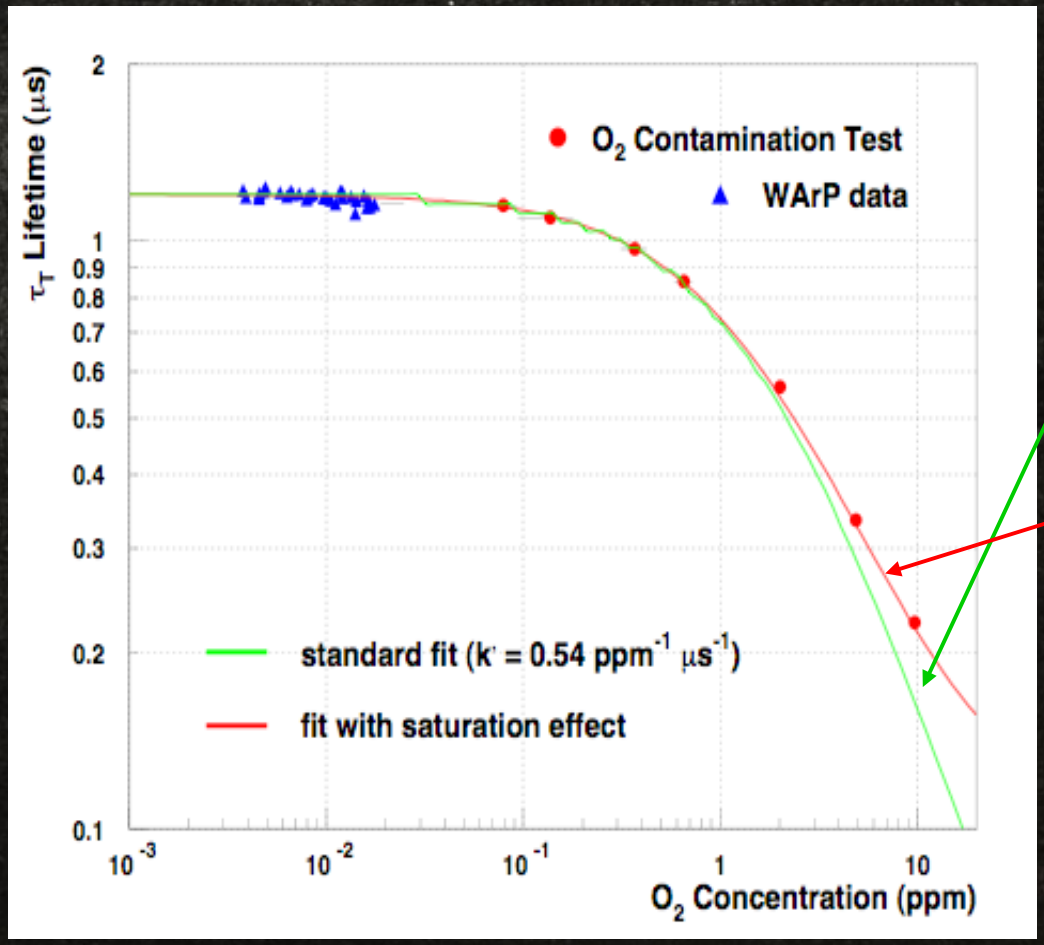

$$\frac{1}{\tau'_T} = \frac{1}{\tau_T} + k'[O_2]$$

Fit with saturation effect:

$$\frac{1}{\tau'_T} = \frac{1}{\tau_T} + k'\beta\left(1 - e^{-[O_2]/\beta}\right)$$

β represents the concentration scale where saturation becomes effective (C.L. ≈ 90%)

Read out system response

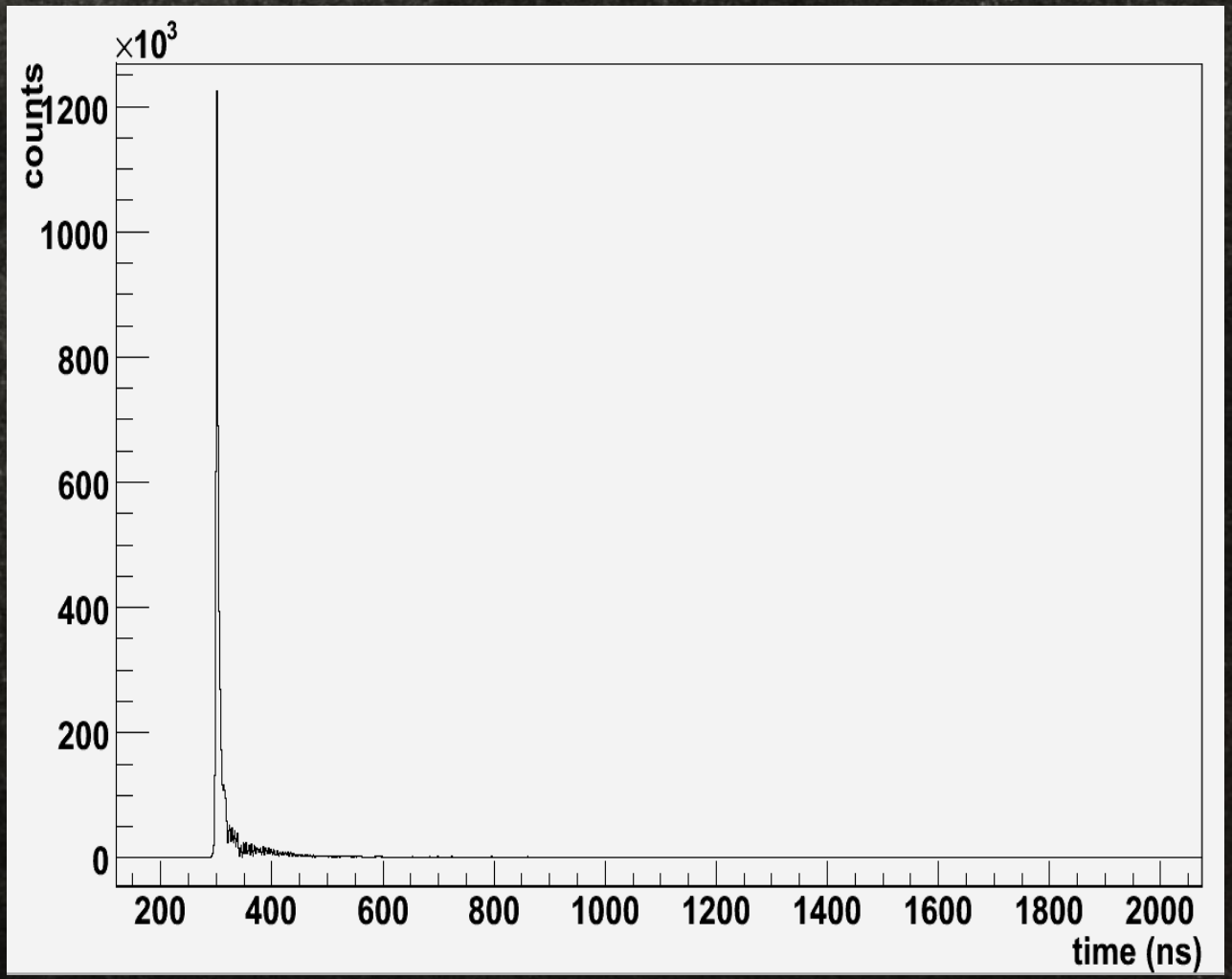

- ✓ The average signal can be expressed as: $V(t)=S(t)\otimes R(t)$ where $S(t)$ is the light signal and $R(t)$ is the response function of the read-out system.

- ✓ The signal $S(t)$ is obtained from $V(t)$ by a deconvolution procedure using the function $R(t)$ experimentally determined.

Evidence for a third component

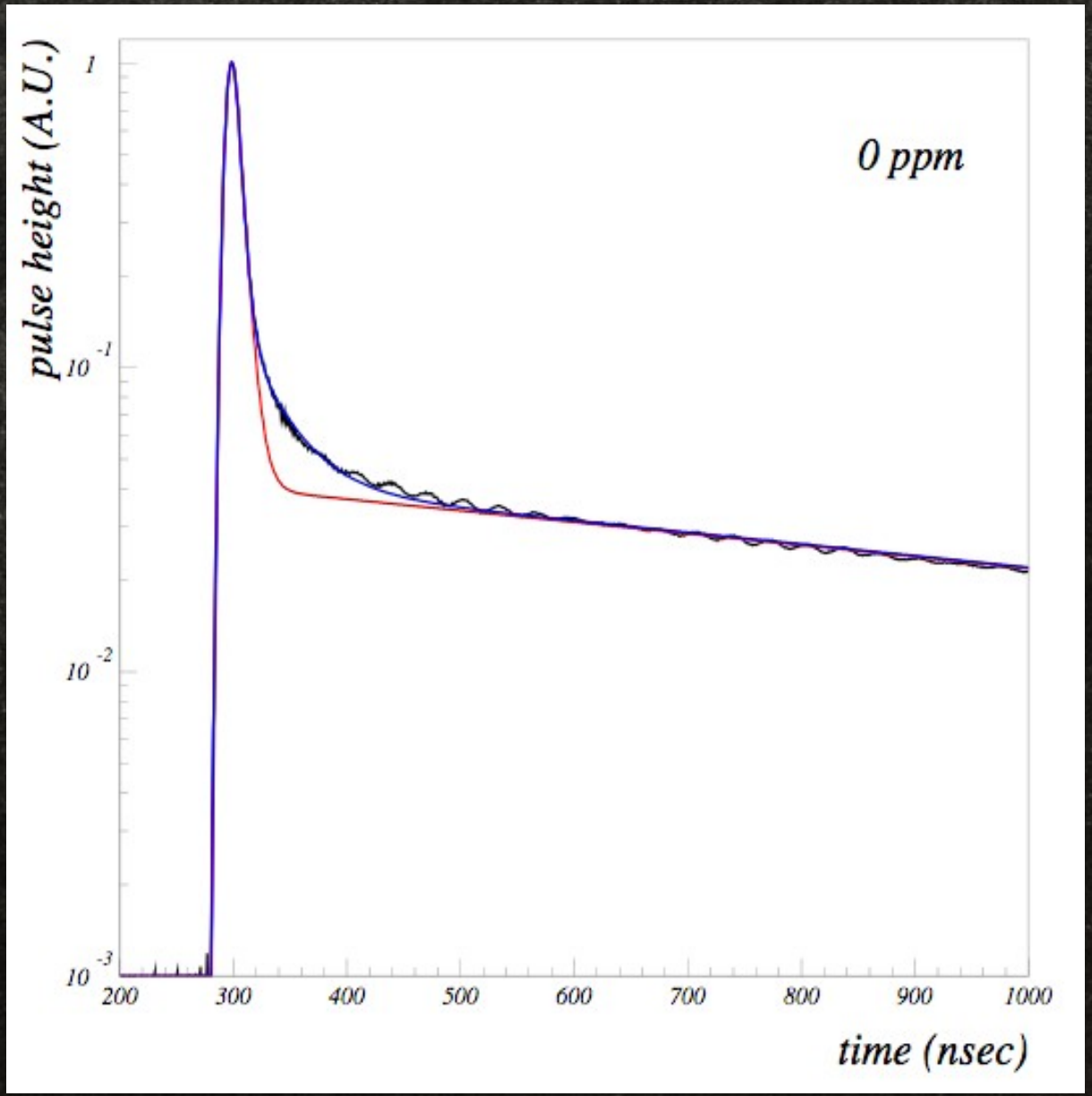

- ✓ Attempts to perform a fit of the average wfm with a two component signal failed.
- ✓ This leads to use a three component model, nicely fitting present data.
- ✓ The origin of this component is not yet determined.

Signal amplitude analysis

The signal amplitude, obtained by single waveform integration, is proportional to the energy deposited by ^{60}Co γ source.
Pulse amplitude spectra (from Compton scattering) are obtained for each run at different $[O_2]$ value.

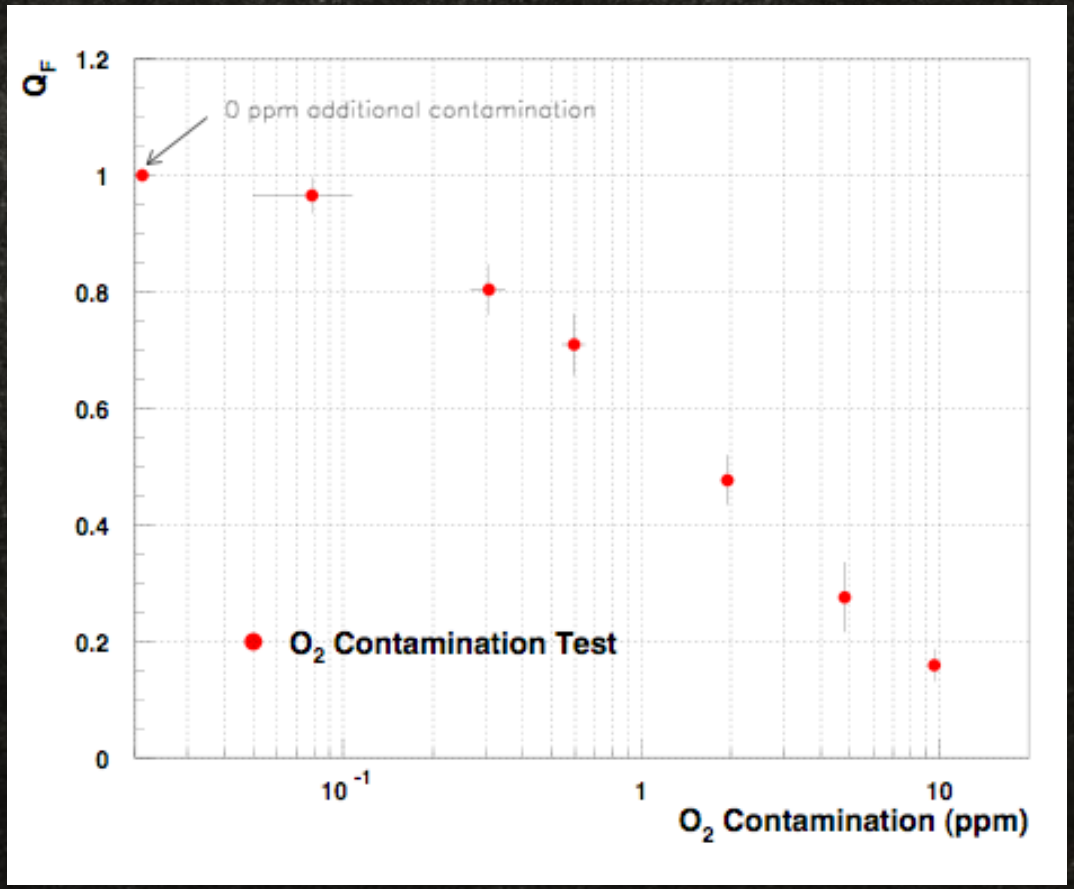

- ✔ Due to the quenching process, the spectra result down-scaled at increasing $[O_2]$
- ✔ Dedicated fitting procedure has been developed to determine the quenching scale factor Q_F relative to each $[O_2]$
- ✔ A sensitive reduction of the scintillation Light Yield is found in the high concentration range ($[O_2] \geq 100$ ppb), e.g. the presence of 1 ppm of O_2 causes a loss of ~40% of the light available

Signal amplitude analysis

By single waveform integration pulse height spectrum is obtained for each $[N_2]$.

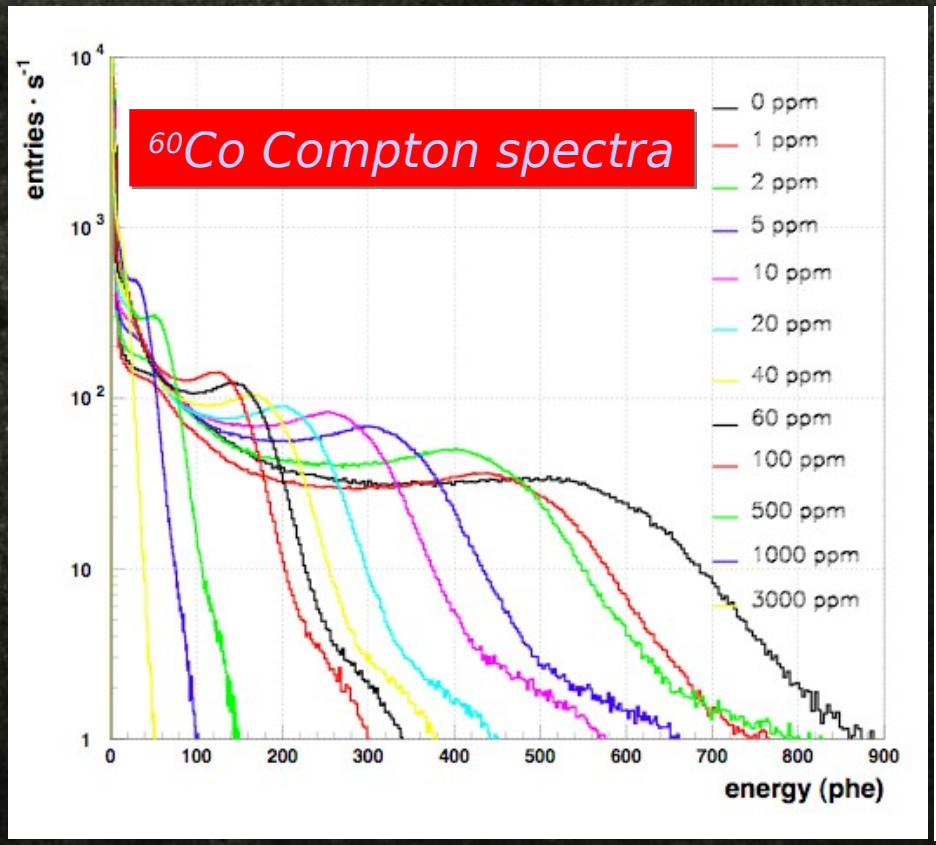

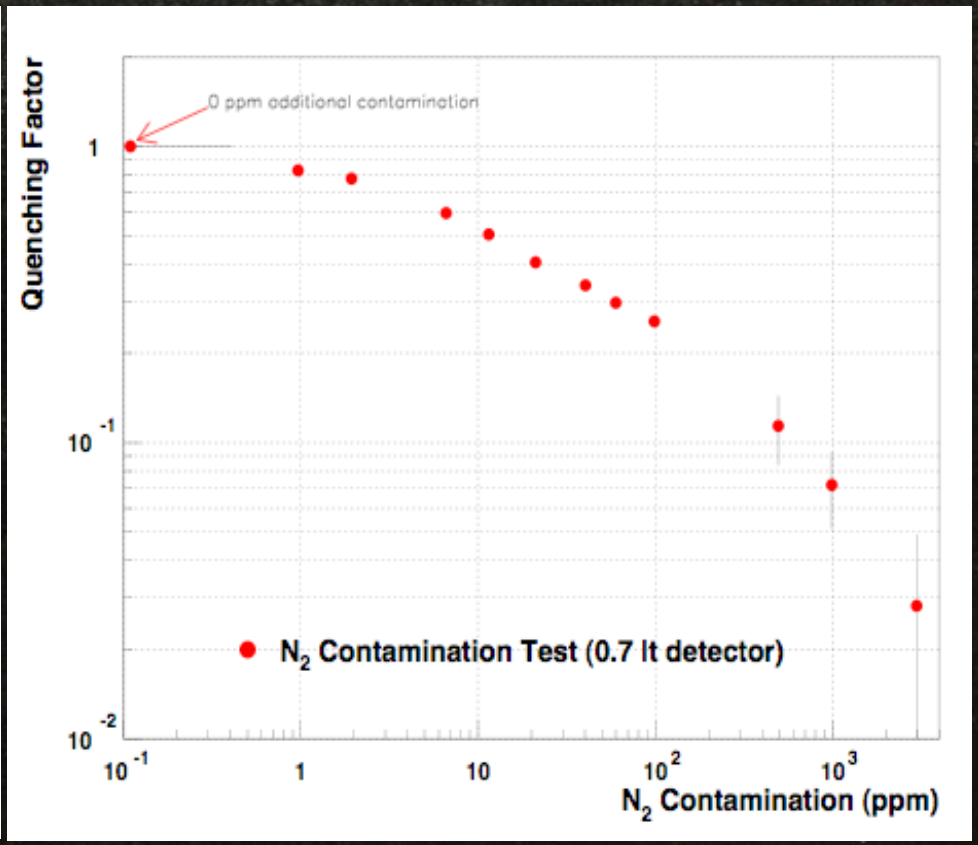

A dedicated procedure allows to fit the uncontaminated (0 ppm) spectrum to the N_2-contaminated spectra.

This allows to determine the overall Q_F as a function of $[N_2]$.

Film production

- Reflector layer is positioned inside the vacuum chamber (face-down on the top side of the chamber) together with two small reflector samples (diam. 7.5 cm), successively used for the conversion efficiency test.

- When vacuum pumping reaches the few x 10^{-5} mbar (30') and the TPB in the Knudsen cell reaches the melting temperature (240°C), the shutter of the cell is opened and the TPB evaporation starts.

- In about 20', the TPB film reaches the required thickness. Both the cell shutter and cell heater are switched off to stop the evaporation. Vacuum is broken by fluxing GAr in the chamber. Both the reflector foil and the test samples are then removed and stored in GAr atmosphere inside sealed plastic bags in a dark room.

✔ The procedure ensures an uniform distribution of TPB over both the reflector layer and test samples.

✔ Every evaporation cycle lasts about 2 hours.

✔ The presence of 2 crucibles allows for continuous operation of the system.

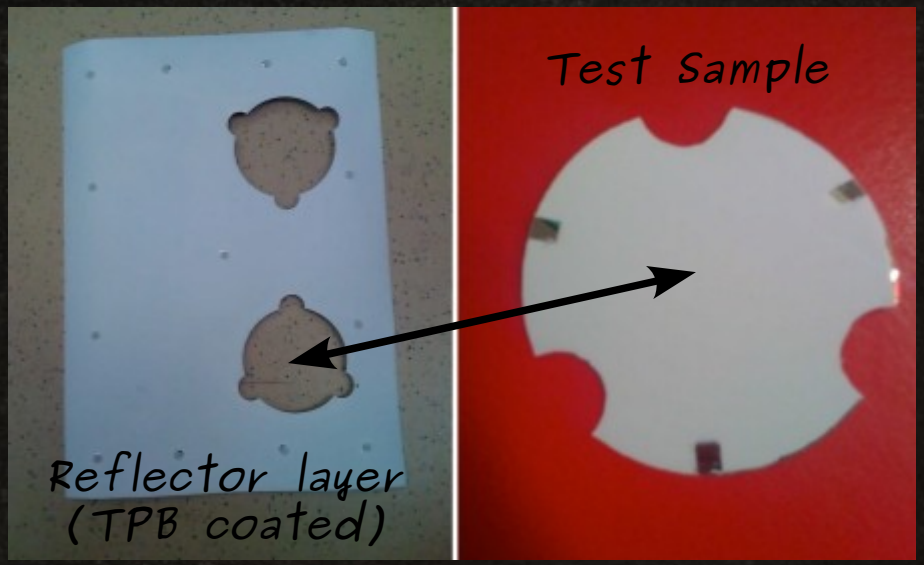

Expected α spectrum

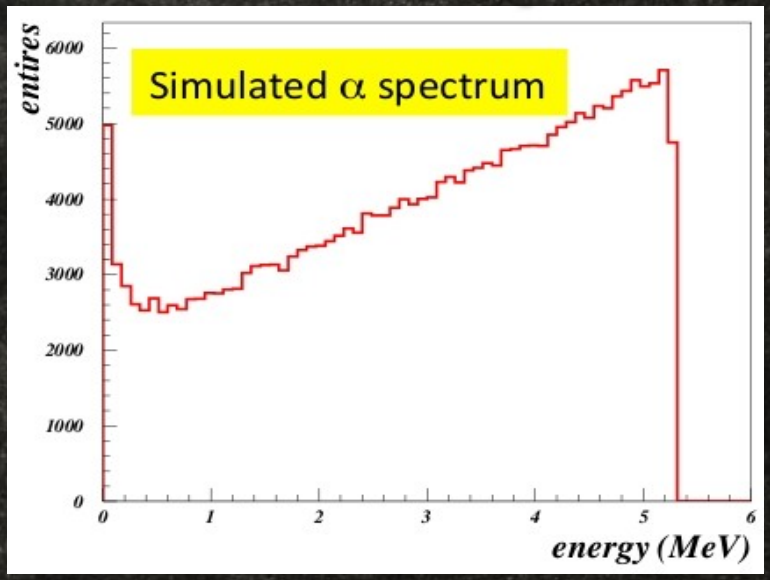

✔ Source: Aluminum alloy containing Uranium emitting ~ monochromatic α particles ($E_\alpha \simeq 5$ MeV).

✔ The energy spectrum of emerging α is continuous and linear increasing up to the max energy (~5 MeV) (MC simulation).

✔ The spectrum of photoelectrons collected by the PMT is little distorted by the fact that light is converted only on the sample surface and by the relative position of sample and source.

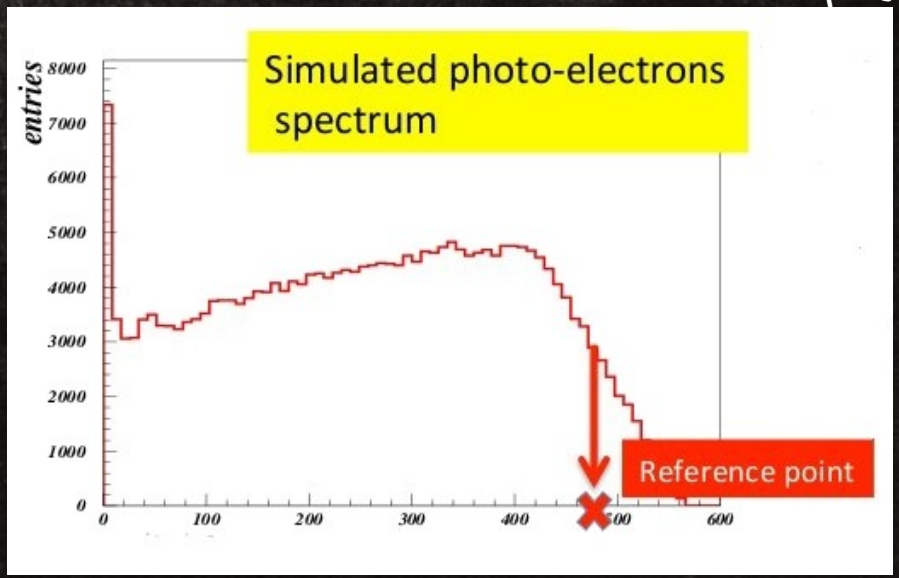

✔ The photoelectron spectrum increases linearly up to a maximum and then decrease linearly to zero.

✔ The reference point for the determination of the Light Yield (LY), and therefore of the conversion efficiency, is taken to be in the middle of the descending slope of the high energy part of the spectrum.

Testing procedure

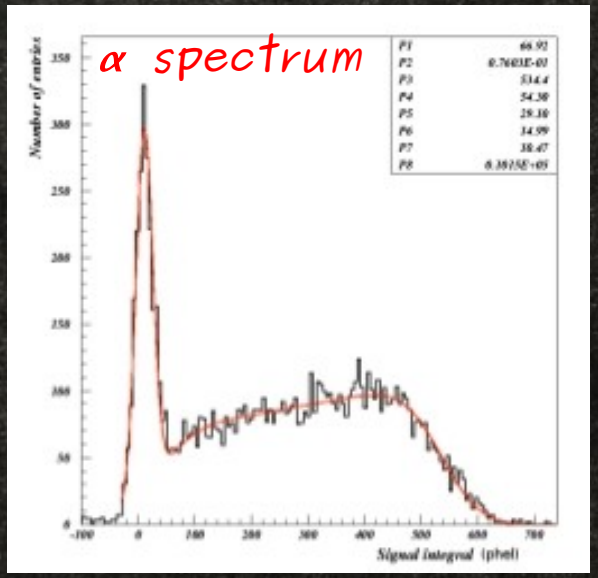

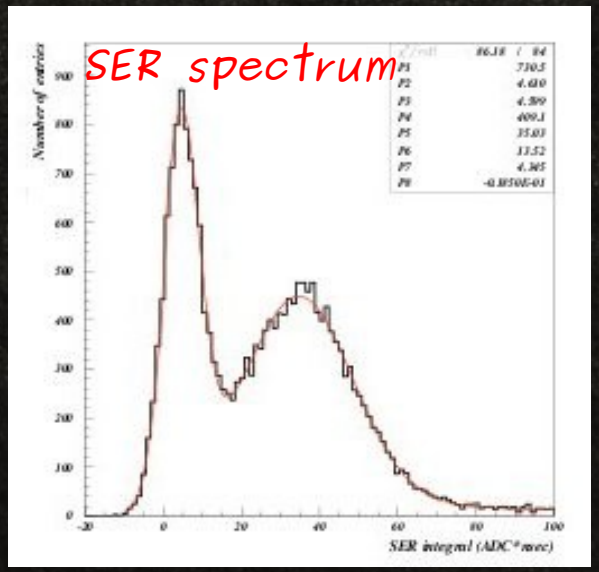

- WATER stainless steel chamber is pumped down to a pressure $<10^{-4}$ mbar.
- The chamber is flushed with 6.0 GAr – 2 bar pressure (range α ~3 cm) and 7 Nm^3/h flux.
- GAr scintillation waveforms are digitized with a PCI Aquiris board (DP235) @ 1 GHz.
- For each test sample 10000 waveforms are acquired, each waveform being constituted by 40 Ksamples (40 μsec interval time).
- Acquired waveforms are integrated over a time interval of 15 μsec from the onset.
- For each run a SER spectrum is constructed integrating single phes found in the tail of the waveforms (15 μsec – 40 μsec time window).
- The average SER value is then used for ADC-to-phe calibration and the α spectrum (waveform integrals distribution) expressed in phe is thus obtained.

Testing procedure

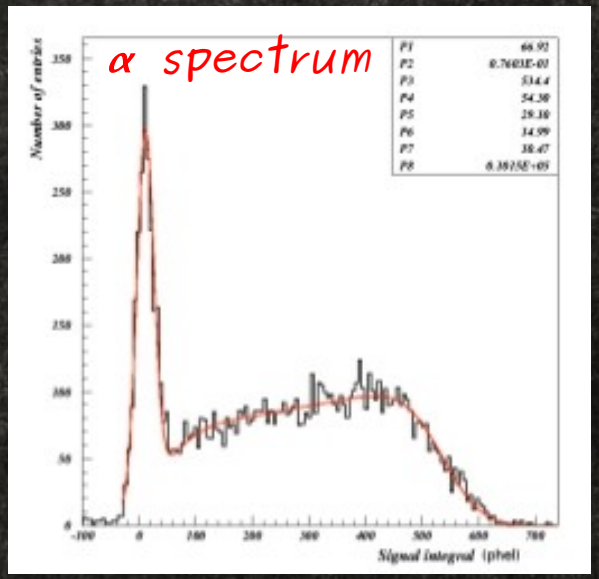

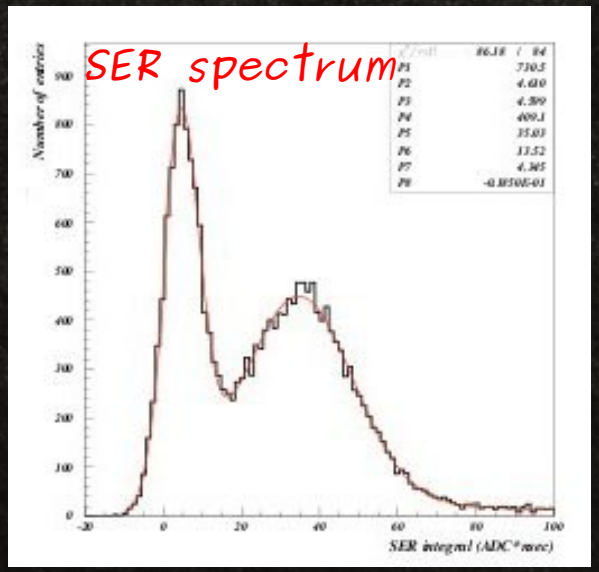

- The source consist of an aluminum alloy containing Uranium emitting ~ monochromatic α particles ($E_\alpha \simeq 5$ MeV).
- Due to energy degradation in the aluminum layer, the resulting α energy spectrum is continuous and linearly increasing up to the maximum energy.
- The spectrum of phes collected by the PMT is little distorted by the fact that light is converted only on the sample surface and by the relative position of sample and source.
- The spectrum is fitted with the convolution of an increasing linear function with a gaussian one + a gaussian function accounting for the electronic noise.
- LY, and therefore the conversion efficiency, is determined from the fit taking as reference point the shoulder at the end of the spectrum.
- An average wfm is calculated τ_{slow} and determined by fit.

Calibration

- The value of τ_{slow} is closely linked to the degree of purity of GAr in the chamber.
- GAr can be polluted by outgassing of the internal materials mainly with N_2, O_2 and H_2O, resulting in collisional quenching of the slow component of the scintillatin light. No photon absorption due to the GAr density and the small distances (~ 5cm).
- Different measures will in principle give different values of τ_{slow} (different outgassing of the sample, different level of vacuum). The Light Yield must therefore be referred to the same τ_{slow} for all the samples.

Need for a calibration

Calibration

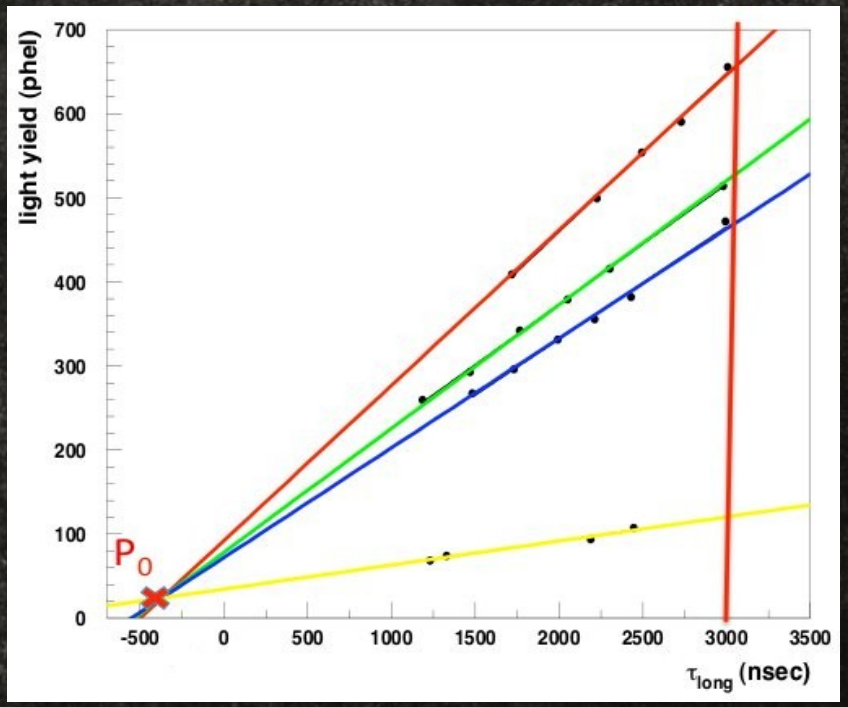

- Number of photons produced at any given energy: $N_{ph}=A+B\tau_{slow}/\tau_0$ (A e B constant).
- $LY=\epsilon_0\epsilon_{sample}(A+B\tau_{slow}/\tau_0)$ Sheaf of lines in the plane $\tau-LY$.
- Calibration procedure consist in determining the common midpoint $P_0(\tau=-A\tau_0/B, LY=0)$ of the sheaf of lines.
- The characteristic lines of few samples have been measured and simultaneously fitted requiring they have a common point (P_0).
- The knowledge of P_0 allows, once measured the (τ,LY) values for a sample, to draw the characteristic line for that sample and thus to extrapolate the LY value for pure Argon.
- The reference LY value for each sample is the one corresponding to $\tau_{slow}=3000$ ns.

TPB aging test: decay times

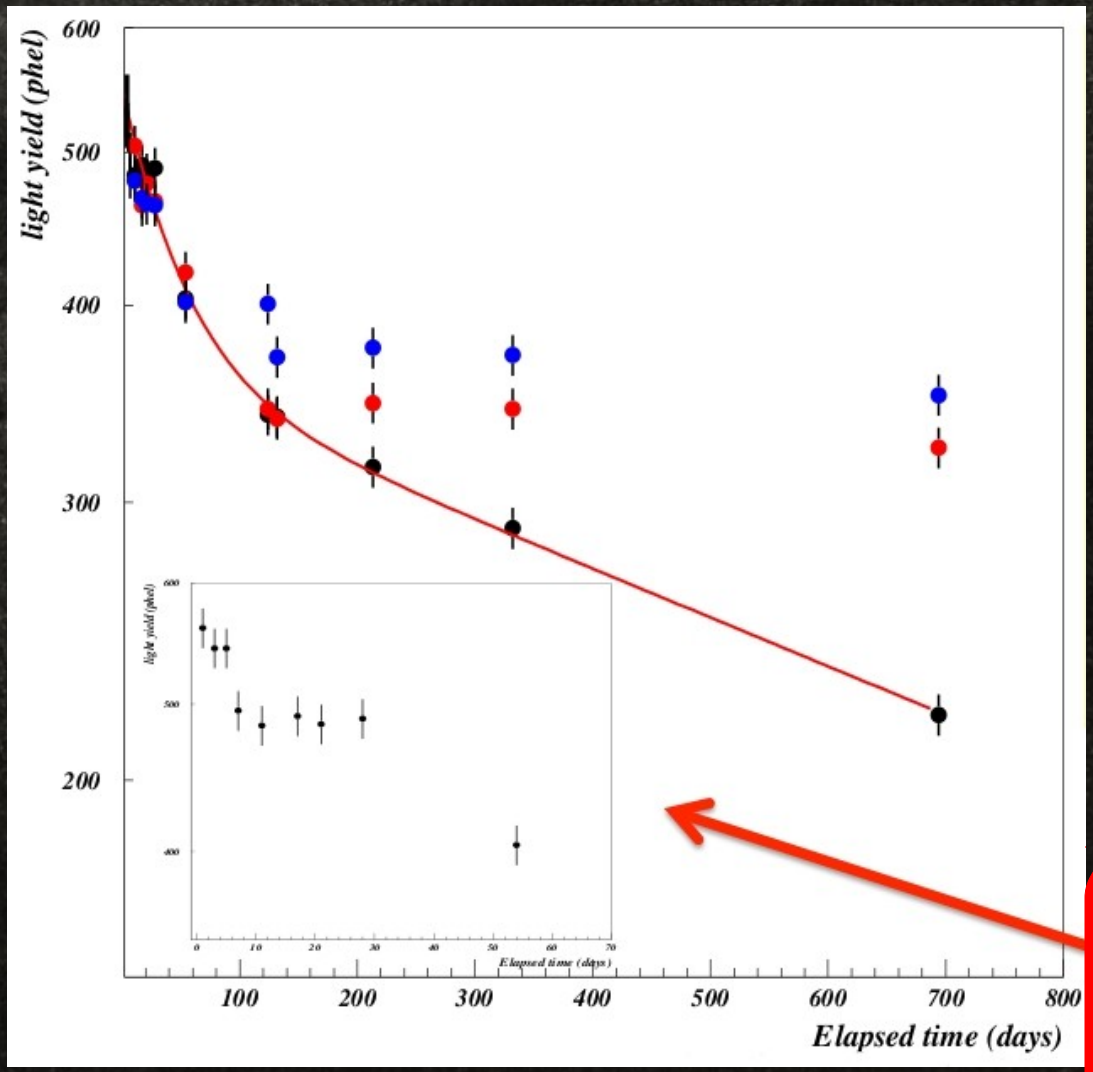

- ✔ Black points (sample exposed to light and air) have been fitted with a double exponential function.
- ✔ Two very different decay times have been found.
- ✔ A fast decay with τ_{fast} = 48 days.
- ✔ A fast decay with τ_{slow} = 1400 days.
- ✔ The ratio of the initial amplitude of the two components: Fast/Slow~0.9

Looking closer at the aging of the first 70 days the structure is more complicated than a single exponential. More decay components could be present.

High Quantum Efficiency Hamamatsu PMT

HAMAMATSU

PHOTOMULTIPLIER TUBE

TENTATIVE DATA SHEET

Sept. 2009

R11065

For Low Temperature Operation down to -186 deg. C
Special Bialkali Photocathode (Bialkali LT), Low Radioactivity
76 mm (3 Inch) Diameter, 12-stage, Head-on Type, Synthetic Silica

General

Parameter		Description / Value	Unit
Spectral response		160 to 650	nm
Wavelength of Maximum Response		420	nm
Window material		Synthetic silica	-
Photocathode	Material	Bialkali	-
	Minimum Effective Area	64	mm dia.
Dynode	Structure	Box & Linear-focused	-
	Number of Stages	12	-
Suitable Socket		E678-20A (supplied)	-
Operating Ambient Temperature		-186 to +50	deg. C
Storage Temperature		-186 to +50	deg. C

R11065 TEST DATA

January 12, 2010

	SERIAL NUMBER	SK [uA/lm]	SKB	SP [A/lm] 1500 V	IDB [nA] 1500V	QE [%] 420 nm
1	ZK4998	124.0	14.70	783	44.0	33.8
2	ZK4999	157.0	15.00	1040	56.0	35.4
3	ZK5001	136.0	14.50	1100	27.0	34.6
4	ZK5002	138.0	14.00	1010	15.0	33.9
5	ZK5006	137.0	13.10	1050	12.0	31.0
6	ZK5172	163.0	14.60	1170	34.0	33.3
7	ZK5173	143.0	14.10	808	32.0	32.5
8	ZK5175	114.0	12.00	777	12.0	29.8
9	ZK5176	110.0	11.20	897	30.0	27.8

- ✔ Box&Linear-focused 12 stage PMT
- ✔ Syntethic Silica 3" window (~160 nm cutoff)
- ✔ Working temp. down to −186°C
- ✔ QE>30% @ 420 nm
- ✔ High collection efficiency of photoelectrons at the first dynode (>95% with ΔV_{K-D1}=300V)
- ✔ Voltage divider custom made on a G10 printed circuit (according to Hamamatsu specifications)

PMT characteristics

Gain

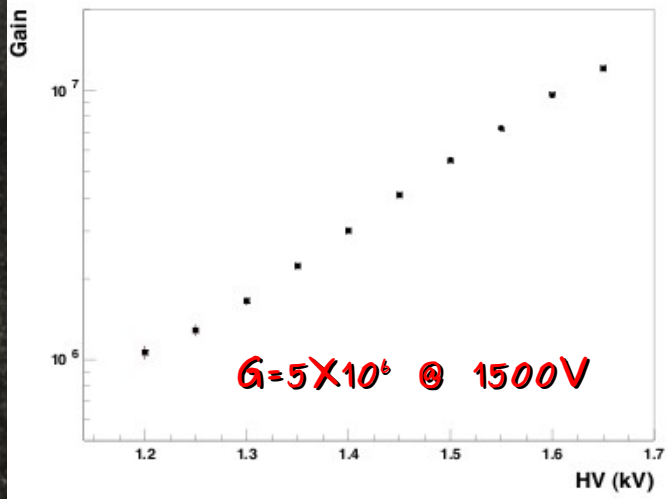

G=5X10⁶ @ 1500V

Peak to Valley

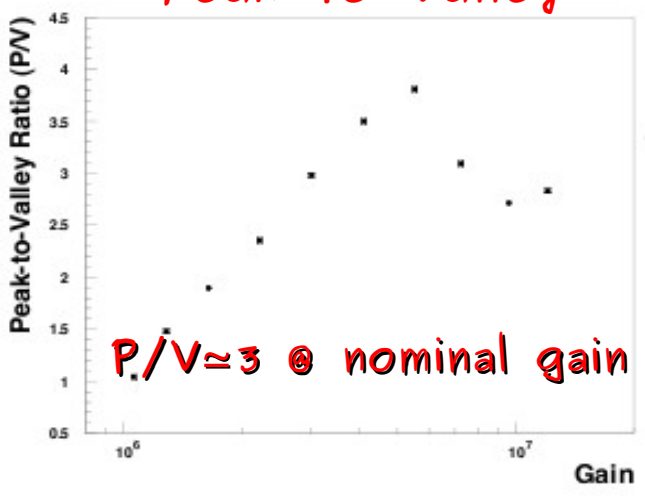

P/V≃3 @ nominal gain

SER Peak Resolution

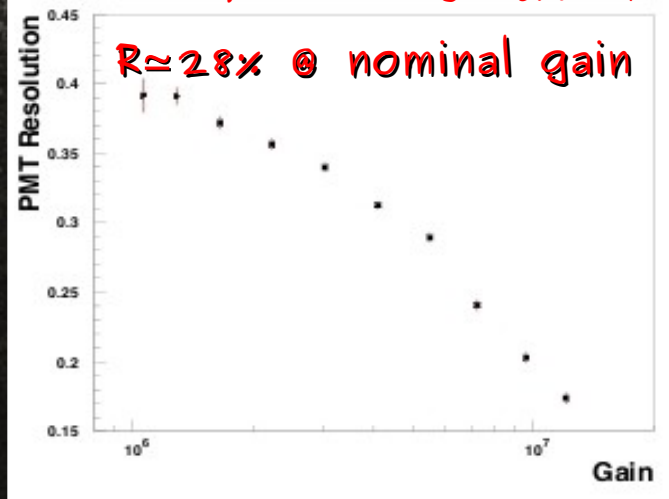

R≃28% @ nominal gain

SER stability

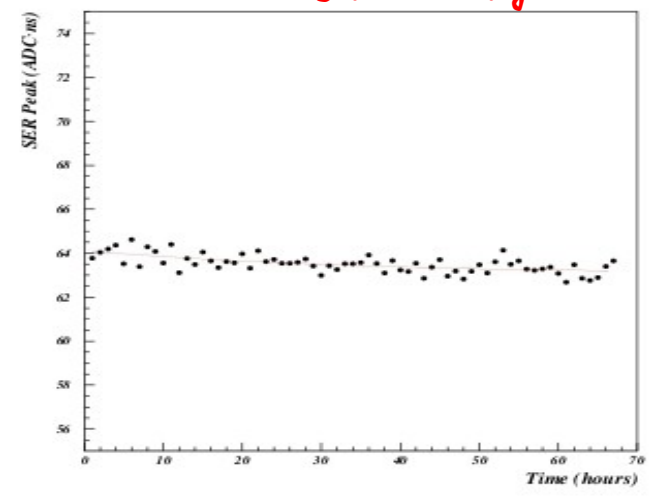

SER values shows a slightly decreasing exponential trend ($\tau \simeq 35$ h) attributed to residual effects of thermalization of the PMT at LAr temperatures.

DAQ and Calibration

- PMT anode current transmitted to a fast Waveform Recorder (Acqiris, DP235 Dual-Channel PCI Digitizer Card, 1 GS/s), 8 bit dynamic range). Signal waveform recorded with 1 ns sampling time over a full record length of 15 μs;

- The detector is exposed to a ^{241}Am source with monochromatic γ-emission at E_γ=59.54 keV;

- For each run single Photo-Electron Response (SER) spectrum is obtained.

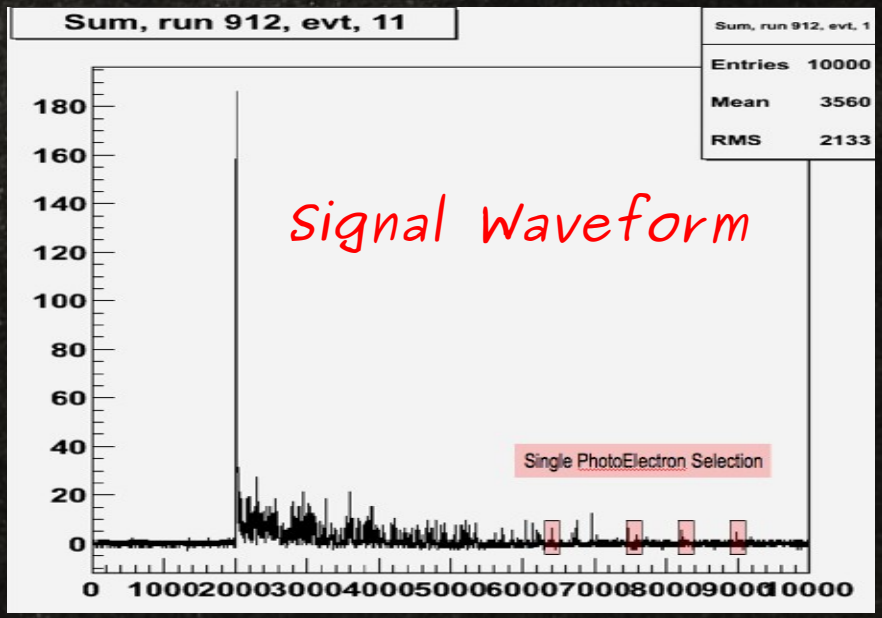

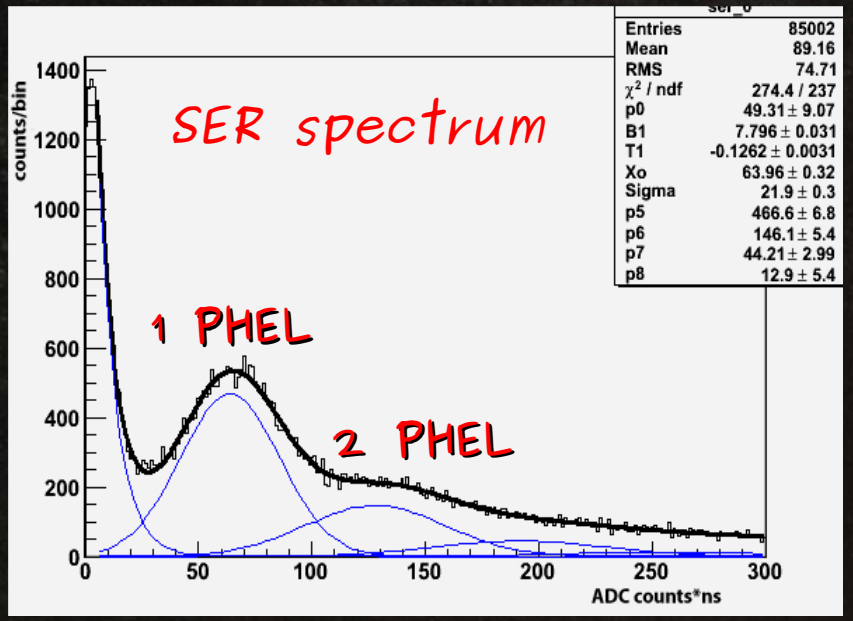

The mean value of 1 PHEL peak is proportional to the actual gain of the PMT and gives the calibration costant per single photo-electron.

ETL vs Hamamatsu: Single Electron Response

- ✔ Very similar pulse shapes for the single electron.
- ✔ The gain of the ETL PMT showed a steeper decreasing trend.
- ✔ The gain of the Hamamatsu PMT has a slightly decreas over the first day after activation and then stabilizes to a costant value.

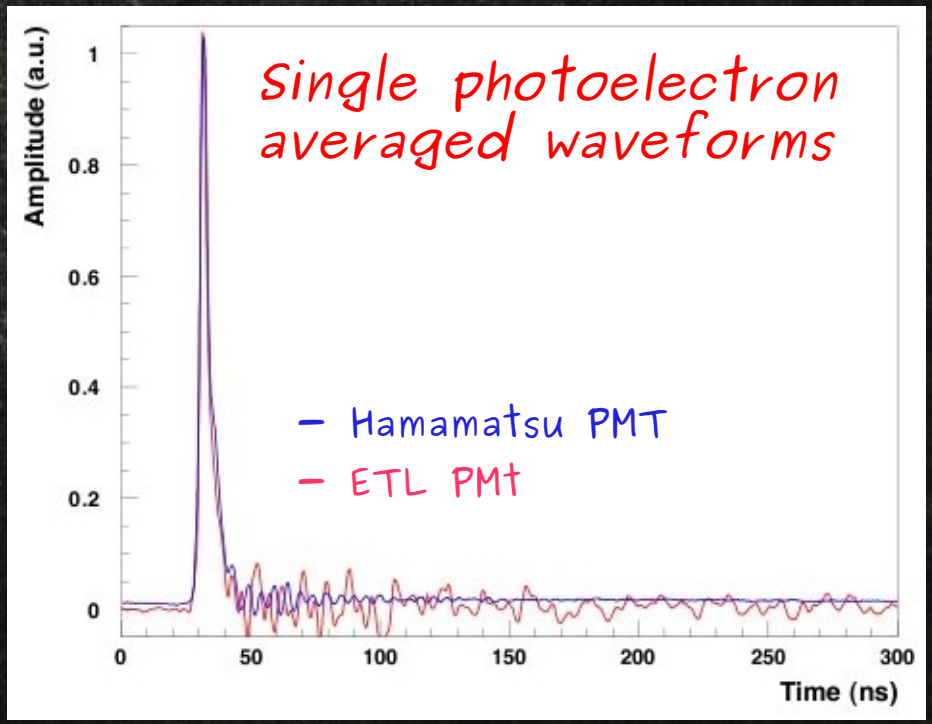

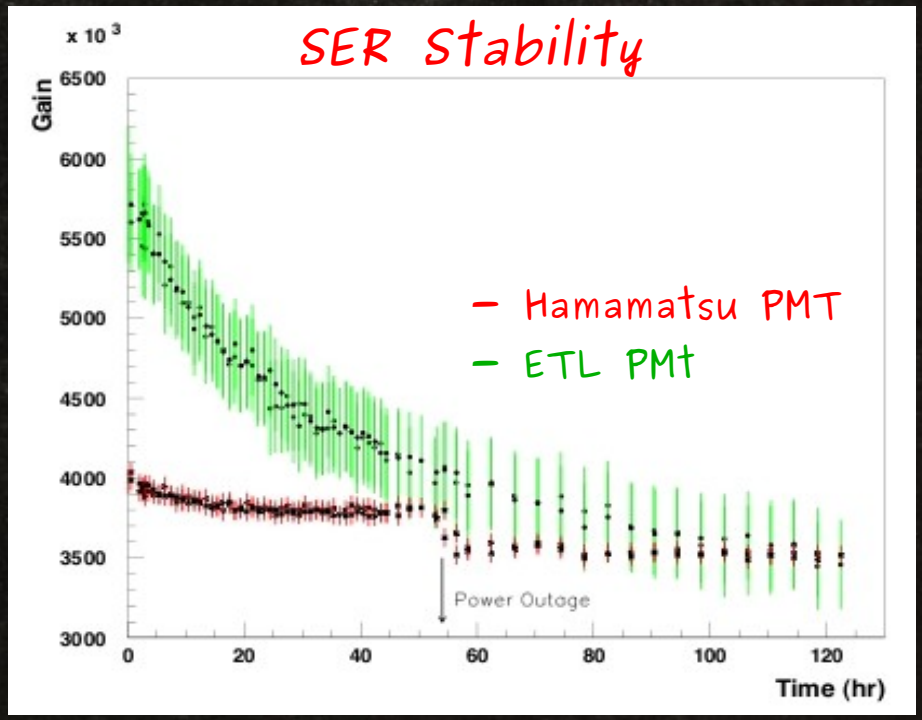

	Peak-to-Valley ratio	SER resolution
Hamamatsu R11065	3.5	32 %
ETL D750 (pre-series)	1.9	50 %

Peak to Valley Ratio @ 3.7 X 10^6 Gain

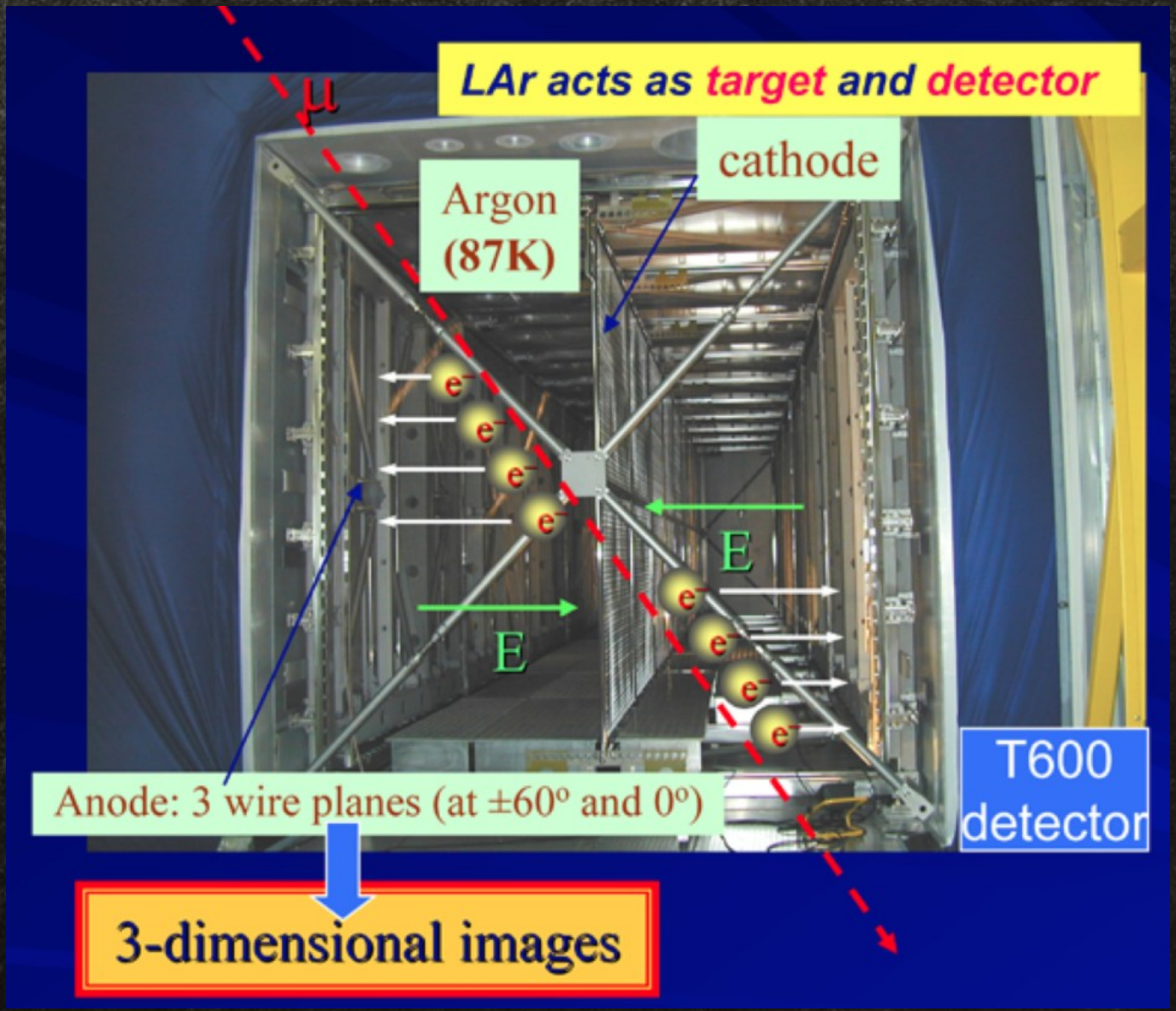
LAr acts as target and detector
μ
cathode
Argon
(87K)
e⁻
e⁻
e⁻
e⁻
E
E
e⁻
e⁻
e⁻
e⁻
T600
detector
Anode: 3 wire planes (at ±60° and 0°)
3-dimensional images

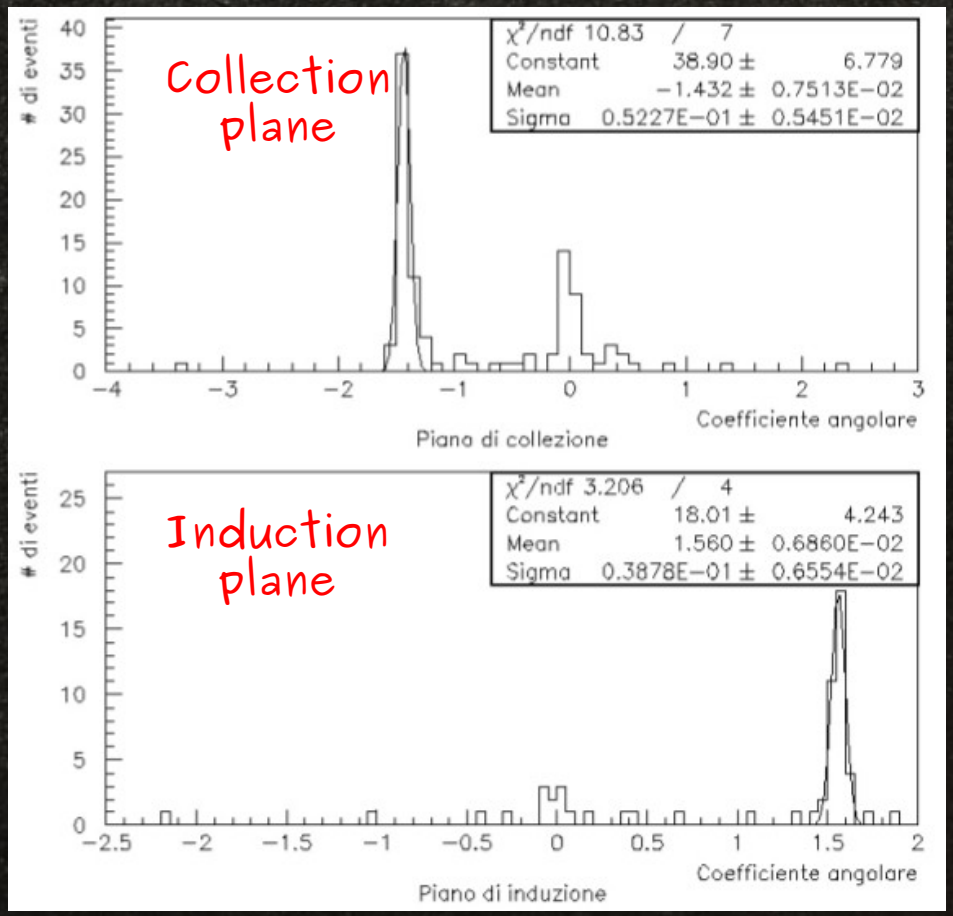
Collection plane
di eventi
χ²/ndf 10.83 / 7
Constant 38.90 ± 6.779
Mean −1.432 ± 0.7513E−02
Sigma 0.5227E−01 ± 0.5451E−02
Coefficiente angolare
Piano di collezione
Induction plane
di eventi
χ²/ndf 3.206 / 4
Constant 18.01 ± 4.243
Mean 1.560 ± 0.6860E−02
Sigma 0.3878E−01 ± 0.6554E−02
Coefficiente angolare
Piano di induzione

Test on TPB films conversion efficiency

✔ VUV photons emitted by LAr scintillation processes are not detected by standard PMTs (transmittance of PMT glass windows ~ 0 @ λ=128 nm).

✔ A good detection efficiency is reached down-shifting VUV light to longer wavelengths by using wavelength shifter materials (WLS).

✔ The most common WLS for LAr scintillation light is an aromatic hydrocarbon, *Tetraphenyl-Butadiene* (TPB). With an estimated wavelength-shifting efficiency $\geq$100% and an emission spectrum peaked around 440 nm and ranging from 390 nm to 520 nm, TPB is currently considered the best fluorescent wavelength converter (from VUV to blue-visible) available on the market.

✔ TPB is usually evaporated onto a reflective substrate (plastic mirror with high specular reflectivity). TPB films line internal surface of the sensitive volume of a detector, allowing for collection of shifted LAr photons at PMTs windows.

✔ *We realised a dedicated GAr set-up and developed a testing procedure for TPB films to determine their conversion efficiency, in order to check and ensure a constant high level of performance of the wavelength shifter.*

✔ *We determined the optimum TPB film thickness as well.*

Evaporation system

Evaporated films are produced with a custom evaporation system installed in the Mounting Hall facility of LNGS.

- ✔ The vacuum chamber is a stainless steel cylinder 60 cm diameter – 30 cm height.
- ✔ Two water cooled copper crucibles (Knudsen cell). Each one allows to load up to 4 gr of TPB.
- ✔ Quartz sensor to monitor the thickness of the film.
- ✔ Temperature controller to monitor and keep evaporation temperature stable.
- ✔ Turbo molecular pump for vacuum pumping.

GAr set-up

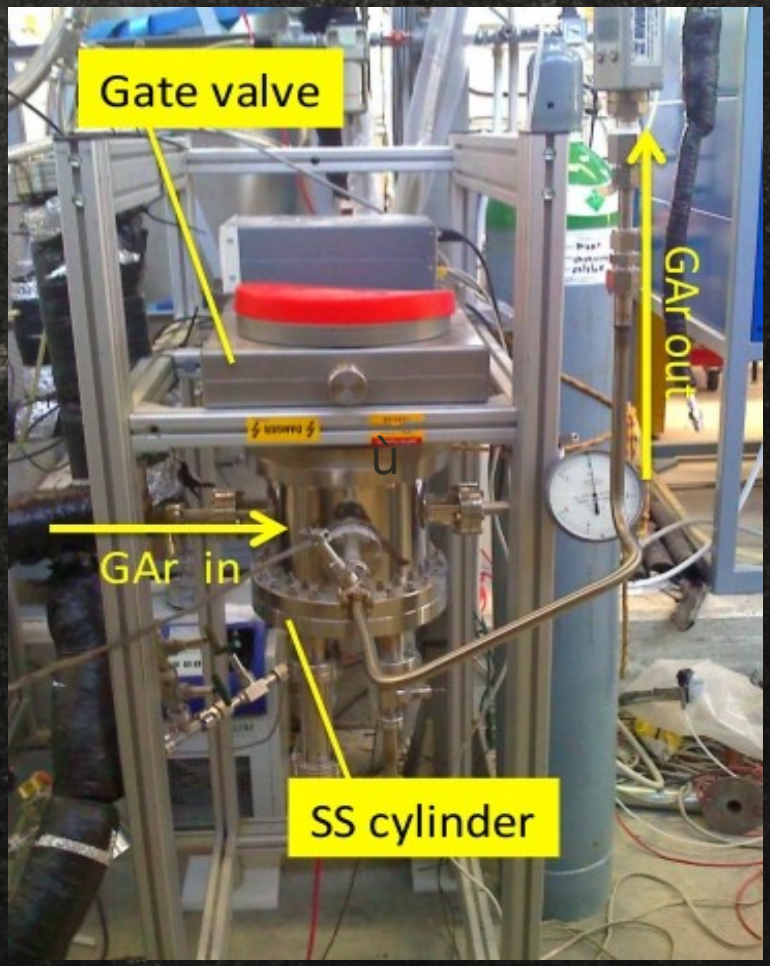

- ✔ Scintillation chamber is housed in a stainless steel vacuum tight cylinder.
- ✔ The cylinder is closed on the top by a gate valve (pneumatic) that allows *easy and fast* substitution of the sample to be analysed.

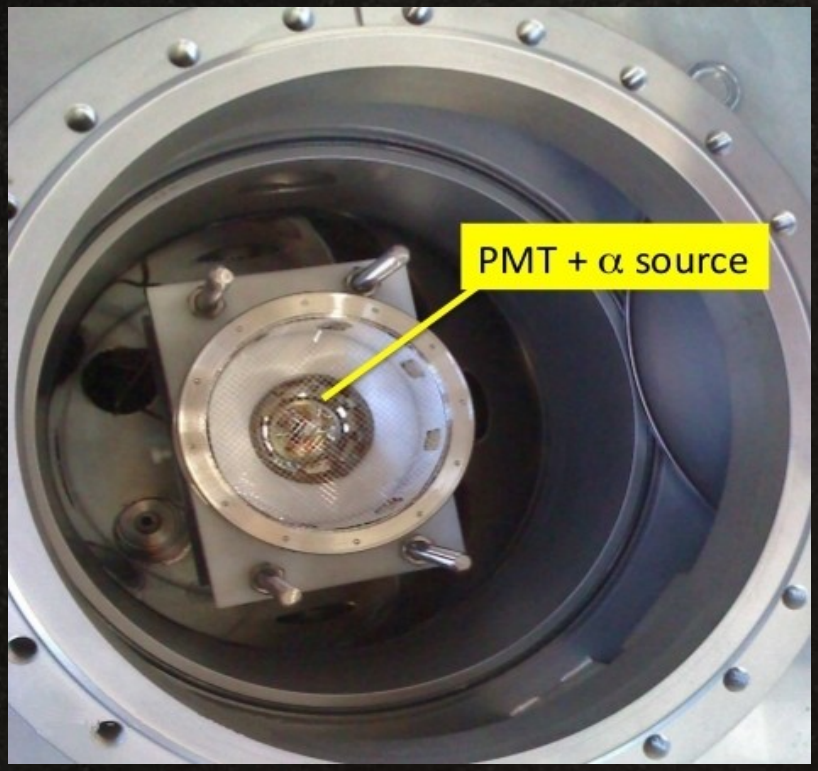

The choice of a GAr (rather than a LAr) detector ensures a *fast* testing procedure (no need of cooling down!).

GAr set-up

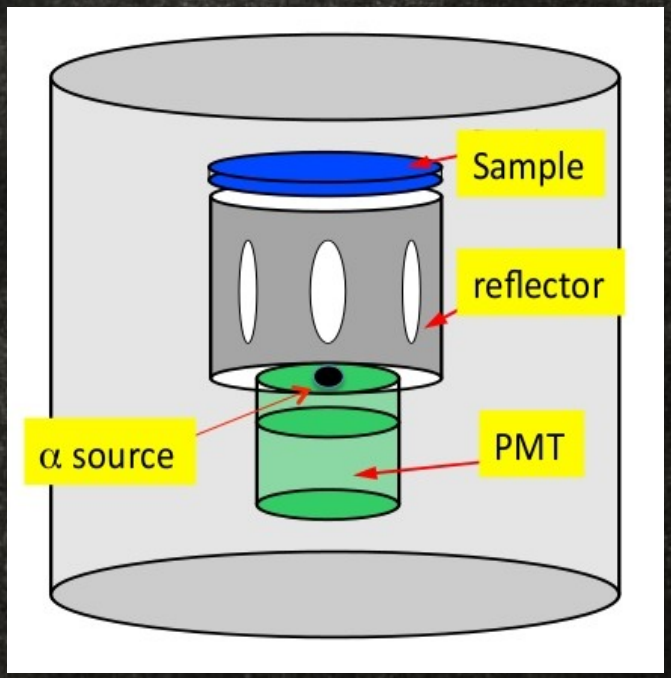

- Test chamber: cylindrical cell 8.0 cm diameter X 4.5 cm height.
- Film to be tested positioned at the top end.
- 2" PMT installed at the bottom end.
- Chamber lined up with a bare reflective foil.
- The chamber is flushed with high purity (6.0) GAr to limit the outgassing.
- Lateral surface of the cell perforated to allow the flow of GAr easily circulating inside it.

VUV scintillation light is produced by α particles emitted by an α source glued on the PMT window. VUV light is down-converted by the TPB film and detected by the PMT. Measuring the end point of the α energy spectrum (corresponding to $E_\alpha \simeq 5$ MeV) the GAr Light Yield, hence the conversion efficiency; characterizing the sample is determined.

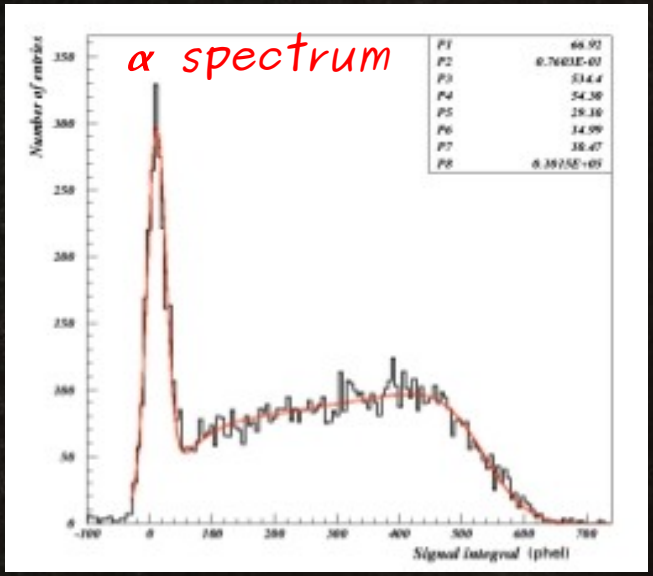

Efficiency vs Film thickness

A set of 7 films with thickness ranging from 50 μg/cm² to 1400 μg/cm² has been produced during the same evaporation with the same substrate.

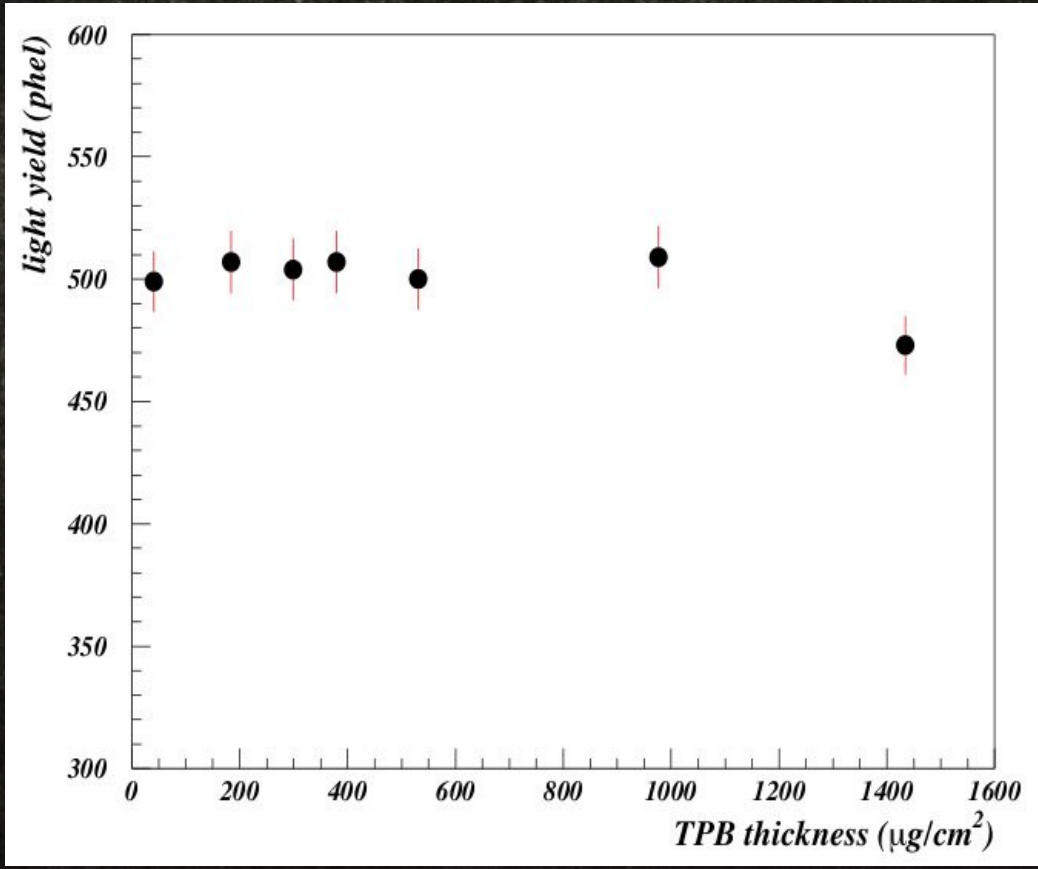

Light Yield is constant up to a thinkiness of 1000 μg/cm².

The conversion of 128 nm photons seems to be a "surface effect" for the thickness explored. The only difference is how easily the converted photon succeed in escaping the film.

A convenient choice of film thickness is ≃200 μg/cm² because:

- ✔ the film is uniform;
- ✔ minimizatoin of required TPB;
- ✔ the film is mechanically more robust (respect to higher densities) especially when bended at LAr temperatures.

LAr – GAr Light Yield correlation

To validate the testing procedure a direct correlation between the LY evaluation from the GAr test and the LY expectation value in LAr, when the TBP+reflector layer is operated in experimental conditions, must be proven.

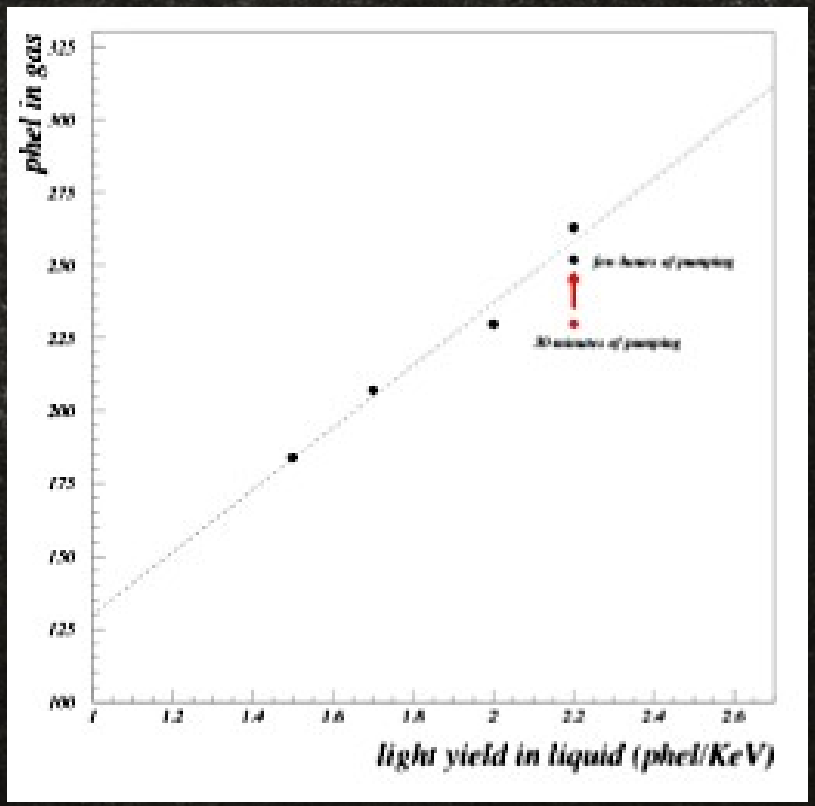

- ✔ 5 distinct evaporation sets have been produced.
- ✔ Each set has been used for two different measurements: one in GAr with this set-up, giving the Light Yield value in GAr (LY^{GAr}), and one in LAr with the 0.7 lt test chamber exposed to a gamma ray source, giving the Light Yield value in LAr (LY^{LAr}).
- ✔ The plot of LY^{GAr}.vs.LY^{LAr} values for the considered samples shows a strong linear correlation between the LY level determined with the GAr set-up and the LY value obtained in LAr experimental conditions.

Validation of the GAr testing procedure

TPB aging test

One aspect we explored is the effect that light and/or air can have on conversion efficiency of TPB films.

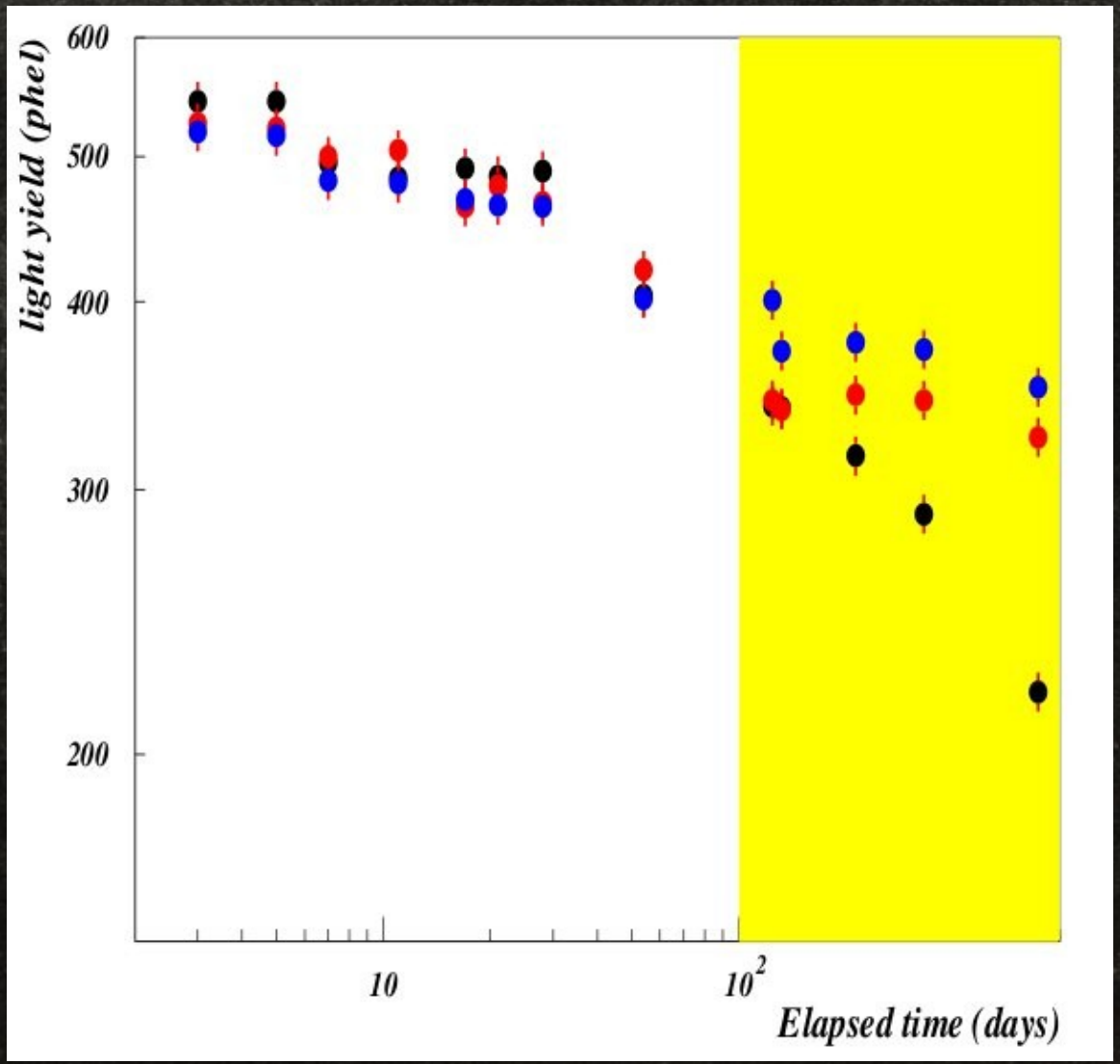

- ✔ Three TPB films indipendently evaporated on VM2000 foils (~200 $\mu g/cm^2$) have been exposed to diffuse light and atmosphere.
- ✔ Efficiency measurement performed for ~2 years.
- ✔ The 3 samples deteriorate in the same way up to day 100.
- ✔ In day 100 the "blue" sample is put in a dark vacuum chamber, the "red" sample in a dark chamber, the third one left to open air and ambient light.

TPB aging test

One aspect we explored is the effect that light and/or air can have on conversion efficiency of TPB films.

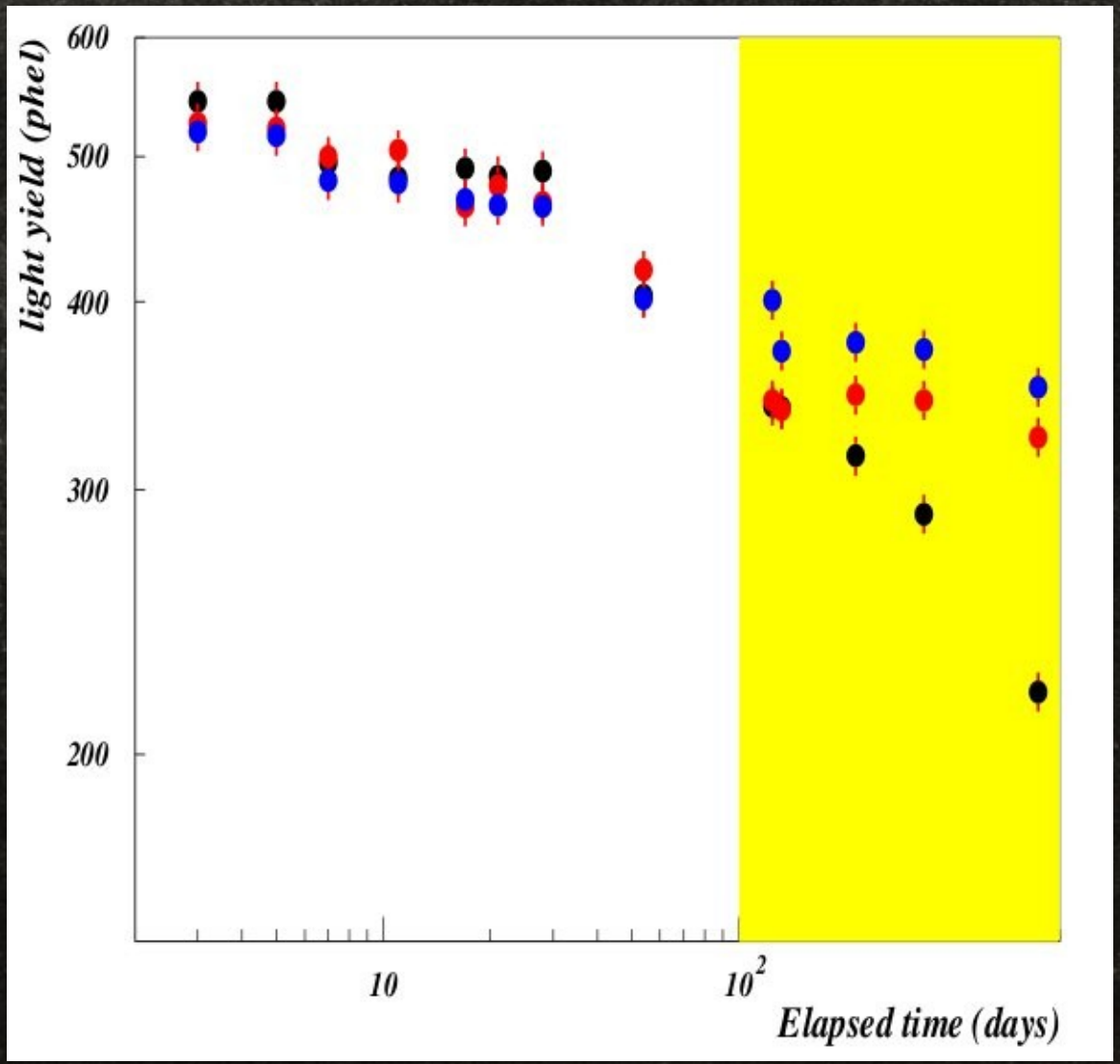

Samples kept in dark maintain unchanged their efficiency for more than one year and half

- The action of light and/or combination of light and air deteriorates the film shifting efficiency.
- Light exposition of the optical system during production, storage and detector mounting must be reduced to the lowest possible level.